ISSN 1028-8546

Azərbaycan Milli Elmlər Akademiyası
Fizika-Riyaziyyat və Texnika Elmləri Bölməsi
Fizika İnstitutu

1-2

Fizika

Cild

X

2004

Bakı ✵ Elm

THE MICROWAVE ABSORBENTS ON THE BASE OF THE HIGH-DISPERSE MATERIALS

S.T. AZIZOV, M.A. SADICHOV, E.R. KASIMOV, CH.O. KADJAR, R.M. KASIMOV
Institute of Physics of Azerbaycan Academy of Sciencies
370143, Baku, H. Javid ave.,33

The results of the investigations of the properties of the solid-state absorbents of microwaves, made on the base polyformaldegide and included in it the high-disperse absorbing fillers are presented.

Protection from the influence of the poison microwave radiation on the alive organisms is the one of the important ecological problems. The important role in its solving has the search of the high-effective wave absorbents on the base of the acceptable compositional materials and simple technology of its preparation. The investigation in this area are carried out in the industrially developed countries, but they are basically directed on the creation of the nonreflecting surfaces for the air and sea ships with the aim of the blanking of the probing radar signals. They didn't accept their usage for the protection of civil population from the microwave radiation action because of the difficulty and expensiveness of these works.

The existing microwave absorbents, as a rule, form on the base of the layer composition from the nonabsorbent matrix dielectric substance and thin-film or high-disperse metallic and ferromagnetic materials [1]. In such layer systems, situated on the metallic substrate, the radiation absorption creates because of the skin-effect in the surface layer of the filler, but carrying out of the selective absorption condition of the incident radiation in the wide band of frequency is achieved by the selection of the defined member and thicknesses of the compositional layers with the different content of the absorbing inclusions in them [2]. These absorbents well justify themselves in the long-wave region of the microwave band. The abilities to the selective absorption of these waves in the used compositional materials deeply decrease because of the increase of the skin-effect action with the increase of the incident radiation frequency. The attempts to compensate this natural effect by the increase of the absorbing fillers concentration in the compositional materials of the covering lead to the increase of the construction covering weight and decrease of its mechanic strength.

Moreover, the investigations of the reflected characteristics of the systems, consisting on the quarter-wavelength layer of the absorbing dielectric carried out on the metallic substrate, show the probability of the obtaining of the nonreflected wave absorption in them [3]. The nonreflected wave absorption is created because of the interference of waves, reflected from the boundaries of mediums division; moreover the demanded ratios of the amplitudes and phases of the reflected waves reach by the way of the selection of the corresponding values of dielectric constant ε', dielectric loss ε'' and thickness of the layer of the covering material. The reality of the existence of the nonreflected wave absorption phenomenon in the layer systems and in the double-layer system dielectric-metal, in particular, is proved theoretically and experimentally on the example of the investigations of the reflected characteristics of the polar molecular solutions in the microwave region [4]. The selective absorption in such systems is carrying out at the small thicknesses of the covering layer and can be realized in the more wide wave region, including the short-wave region of millimeter wave band. The character peculiarity of the selective wave absorption in the layer of polar dielectrics is existence of the frequency spectrum and, discrete thicknesses of the substance layer at which the conditions of the nonreflected (total) absorption of the incident radiation. They are individual for every substance and depend on their dielectric static and dynamic characteristics.

The access of the dielectric materials does their usage perspective at the creation of the cheep microwave absorption systems on their base with the use of the simple technology of their preparation. Moreover, they can be done from the solid-state matrix nonreflected dielectric material, including the high-disperse absorbing stolid or capsulated liquid dielectric materials, for the improvement of the mechanic strength of the solvents.

The experimental investigations of the solid-state solvents of the microwave radiation on the base of nonabsorping polyformaldegide and introduced in it high-disperse absorbing fillers from aluminium and polyamide with the particles size 30-50 [5], were carried out with the aim of the check of these positions. The choose of the aluminium and polyamide as fillers was sent for the necessity of the carrying out the comparable analysis of two types of the absorbents, differing by the nature of the creation of the appearing of the absorption of high-frequency radiation in them. If in the case of the aluminium absorption of incident radiation takes place in the metal surface layer because of the skin-effect, so in the polyamide case, having the wave dispersion in the super high-frequency region, the absorption of incident radiation is because of the volume hindered orientation of dipole groups in the direction of the applied field [6].

The measurements of characteristics of wave reflection absorbents were carried out at the wave length 1,5sm and temperature 20°C with the use of the experimental device, switched on throw waveguide tract to the panoramic standing-wave meter. The change of the value of wave reflection coefficient ρ and energy relative value E of reflected wave were carrying out in the dependence on the thickness of absorbent sample (fig.1), situated in the end of the cell on the metallic reflected substrate. As examples were used the pressed sets of disks of the different thicknesses with diameter 15mm at the pressure 10 atm. The disks were formed from the carefully mixed mixture of the powdery

polyformaldegide and polyamide or aluminium. The content of polyamide and aluminium in the samples was regulating in the limits of weight 1-25%.

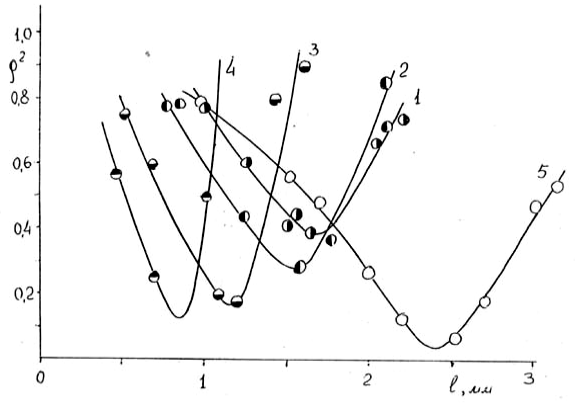

Fig. 1. The dependences between relative energy value of electromagnetic radiation *E*, reflected from the covering, and the thickness of covering l from polyformaldegide at temperature 20°C and wave length 1,5 sm. The high-disperse fillers of covering: aluminium 3(1), 5(2), 10(4) and polyamide 5(5) with weight content in percents.

The optimal values of samples thicknesses of covering of different compositions were defined by the results of the carried out experiments, at which the relative values of reflected energy *E* are minimal. From the dependences, given in the fig.1, it follows, that in the case of the usage of aluminium as a filler or polymeric covering the minimum of value *E* decreases with the increase of weight content формула of the filler in the covering material and achieves value 0,1 at φ=10%. The following increase of content φ of aluminium in the covering makes worth its mechanic strength and leads to the narrowing of the selective absorption band of radiation. The covering, made on the base of the mixture of polyamide and polyformaldegide were the most technological at the preparation, opposite to the aluminium coverings. Practically, total wave absorption (*E*=0,02) appeared at the polyamide content 5%. The obtained covering had the big thickness in the comparison with the coverings with the aluminium use, but had the better band of selective wave absorption.

The decrease of the thickness of the dielectric coverings can be achieved, if as fillers will be used the strongly absorbing materials, in particular, the liquid polar dielectrics, having dispersions in the SHF region. Their use especially prefers in the short-wave part of SHF region. Moreover, for the constructive solving of the problem of absorbents creation of the electromagnetic radiator the material of the absorbing covering should have the defined adhesive properties in respect to the metallic base. The elimination of these two contradictory demands to the absorbents material of the electromagnetic waves can be achieved by the use of the last by the composition from nonpolar solid dielectric with good adhesive properties to metals and uniformly distributed in its volume high-disperse inclusions from low-molecular polar liquids, having wave dispersions in SHF region.

[1] *Yu.K. Kovneristiy, Yu.I. Lazarev, A.A. Ravaev*. M., Nauka, 1982, 164 s. (in Russian)
[2] Preissner. NTZ Arch., 1969, v. 11, N4, p.175.
[3] *E.R.Kasimov, S.T.Azizov, R.M.Kasimov, Ch.O. Kadjar*. Izvestiya AN Azerb.m ser. Fiz-tech. i mat. nauk, 1995, t. 16, N5-6, s. 22-29. (in Russian)
[4] *R.M.Kasimov, M.A.Kalafi, E.R.Kasimov, Ch.O.Kadjar*. Injenerno-fizicheskiy jurnal, t. 71, N2, 1998, s.282-285. (in Russian)
[5] *S.T.Azizov*. Materiali Mejdunarodnoy konferencii "Aktualniye problemi tvyerdotelnoy elektroniki I mikroelektroniki", Taganrog, 1998, s. 115. (in Russian)
[6] *H. De Chanterac, P. Roduit, N. Beihadi-Jahar, A. Foirries-Lamer, Y. Dilgo, P.C. Lacaze*. Sunth Metala, 1992, N2, 52, p. 183-192.

S.T. Əzizov, M.A. Sadıxov, E.R. Qasımov, Ç.O. Qacar, R.M. Qasımov

YÜKSƏKDİSPERSİYALI MATERİALLAR ƏSASINDA MİKRODALĞALI UDUCULAR

Məqalədə poliformaldehid və yüksək dispersiyalı uducular daxil edilmiş poliformaldehid əsasında bərk mikrodalğalar uducularının xassələrinin tədqiqinin nəticələri verilmişdir.

С.Т. Азизов, М.А. Садыхов, Э.Р. Касимов, Ч.О. Каджар, Р.М. Касимов

МИКРОВОЛНОВЫЕ ПОГЛОТИТЕЛИ НА ОСНОВЕ ВЫСОКОДИСПЕРСНЫХ МАТЕРИАЛОВ

Приведены результаты исследования свойств твердотельных поглотителей микроволн, выполненные на основе полиформалдегида и внесенных в его высокодисперсных поглощающих наполнителей.

Received: 05.02.2004

THE ELECTRIC AND OPTICAL PROPERTIES OF THE LAYERED SEMICONDUCTOR $Ga_{0,5}Fe_{0,25}In_{1,25}S_3$

G.G. GUSEINOV, N.N. MUSAYEVA, I.B. ASADOVA
Institute of Physics of Azerbaycan Academy of Sciencies
370143, Baku, H.Javid ave.,33

The single crystals of the intermediate phase of system $(GaIn)_2S_3$-Fe4 of composition $Ga_{0,5}Fe_{0,25}In_{1,25}S_3$ have grown from the melt by Bridgemen method. The single crystals are layered, the symmetry is orthorombic, grating constants in the hexagonal device a=3,786·2, c=36, 606Å, sp.gr. R3m, z=16.

The edge of the optical absorption in the wide energy photon interval has been investigated and the forbidden band width E_g=1,843eV for $Ga_{0.5}Fe_{0.25}In_{1.25}S_3$ have been defined.

The structure In-$Ga_{0.5}Fe_{0.25}In_{1.25}S_3$-In has been prepared and its VAC and the temperature dependence in the temperature interval 100÷360K have been studied. The parameters of the given structure: 12.56 $cm^2/V\cdot$ sec, $n_k=1.55\cdot10^{10}$ cm^{-3}; $D_k^*=2\cdot10^{-2}$; $d_k=5.6\cdot10^{-9}$ cm; $\Delta\varepsilon$ =0.497eV have been calculated by the method of the differential analysis.

1. Introduction

The significance of the physical-chemical and structural study of substance with semiconductor properties is obvious. The synthesis and single crystals growth, the study of their physical-chemical and structural peculiarities, phase-formation regularities and the mechanism of structural phase transition have a great scientific –practical mean. In this aspect Ga_2S_3 – In_2S_3 system compounds are perspective objects for the solution of questions of the structurization, polymorphic, polytype, methods of the phase stabilization and the clarification of characteristics physical-chemical properties.

The phase equilibrium in Ga_2S_3 – In_2S_3 quasi-binary cut of the triple system Ga-In-S were for the first time studied by authors [1], where the formation of just one triple phase GaInS, melting uncongradually, was established. It should be noted that in these papers there is a visible discrepancy in the state diagram and values of hexagonal cell parameters. Neither was determined the crystal structure of the compound.

Judging from experimental facts on the presence of some polymorphy modifications in sesqui chalcogenide of A_2S_3 (A-Al,Ga,In) type, authors [2-6] investigated in details the phase –formation in the given system.

Applying the method of chemical transport reaction (CTR), the presence of polymorphy phases line, polytype forms and three independed compounds (table 1) was established. As result of *X*-ray analysis of crystals, obtained from before synthesized contents $Ga_{0.5}In_{1.5}S_3$ and $GaInS_3$ in various temperature gradients.

To reveal the influence of multivalent tetrahedral atoms on the stabilization of polymorphy modifications $(GaIn)_2S_3$, partially substituting tetrahedral placed atoms Ga and In by atoms Cu and Sn (conserving the total balance of the valence) by the method of direct synthesis, authors [7,8] realized 2H and 3R polytypes, having the layered structure of polytype line a=3.82Å, c=15Å·n (n=2,3) and a=6.52Å, c=18Å·n (n=2).

The present paper are dedicated to structural research, definition of nature of optical transitions and current – conduction mechanism of layered $Ga_{0.5}Fe_{0.25}In_{1.25}S_3$ single crystals in a wide temperature range (100÷360K).

Table 1
Crystallographic data of polymorphic phases and polytype forms of compounds of $(GaIn)_2S_3$

The content of the phase	Sp.gr.	a, Å	b, Å	c, Å	Z
$GaInS_3$	P3m1	3.81		18.19	2
$GaInS_3$	P3m1	3.81		54.61	6
$GaInS_3$	$P6_1$	6.65		17.92	6
$GaInS_3$	$P6_3mc$	3.81		30.62	10/3
$GaInS_3$	P3m	3.81		45.89	5
$GaInS_3$	$Bb2_1m$	19.06	6.19	3.81	4
$Ga_{0.5}In_{1.5}S_3$	P3m1	3.84		12.33	1
$Ga_{0.5}In_{1.5}S_3$	R3m	3.81		100.04	11
$Ga_{0.67}In_{1.33}S_3$	2H	7.64		74.00	8
$GaInS_3$	R3m	3.82		63.41	6
$Ga_{0.25}In_{1.75}S_3$	C2/m	6.55	3.72	12.62 $\beta=100^0$	4
$GaInS_3$	Shpinell Str.type	10.79			8

The present paper is devoted to the structural investigation of the layered single crystals $Ga_{0.5}Fe_{0.25}In_{1.25}S_3$, definition of the character of the optical transitions and conduction current mechanism in the wide temperature interval (100÷360K).

2. Experimental results and discussion

2.1. The single crystals growth.

The crystallization from the melt by Bridgemen method of $Ga_{0.5}Fe_{0.25}In_{1.25}S_3$ has been carried out in the following mode and constants: the quantity of the beforehand synthesized substance ~5,6gr, the melt high is 30mm, the diameter of the container from the quartz is 8mm, the initial temperature is ~1273K, the cooling velocity is ~290K/h, the annealing band is 673K, the annealing time is 30 hours. The experiment result was successful. The all mass of the sample was crystallized in the form of the disoriented crystal blocks, which have absolute cleavage and easily crush on the thin layers of the needed forms and sizes. About the quality of the

grown single crystals can see on the given Laue photograph (fig.1).

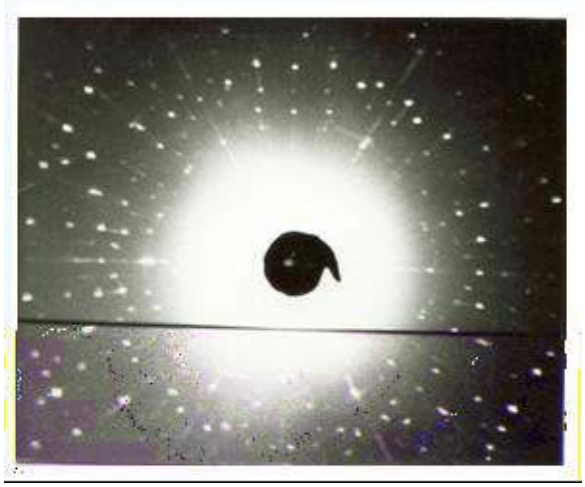

Fig.1. Laue X-ray diffraction for $Ga_{0.5}Fe_{0.25}In_{1.25}S_3$

2.2. X-ray investigations.

For the definition of the crystal lattice parameters, symmetry and the structural type were obtained. The following roenthgenodifractional experiments: 1) by Laue methods and pumping were adjusted the crystalographical directions and defined their values: 2) the roenthgenoflections fro the plane-parallel planes for the definition of the character of the diffraction type ool were obtained; 3) powder diffractogram (DRON-20; N_i is filter, limit is $0,5^\circ<2\theta<70^\circ$).

On the base of the calculations and analysis of the obtained results it was established, that single crystals $Ga_{0,5}Fe_{0,25}In_{1,25}S_3$ are crystallised in the rombohedral lattice with periods, in the hexagonal device a=3.786·2Å, c=36.606Å; sp. gr. R3m, z=16, V=1817.57Å, V_s = 37.86Å^3.

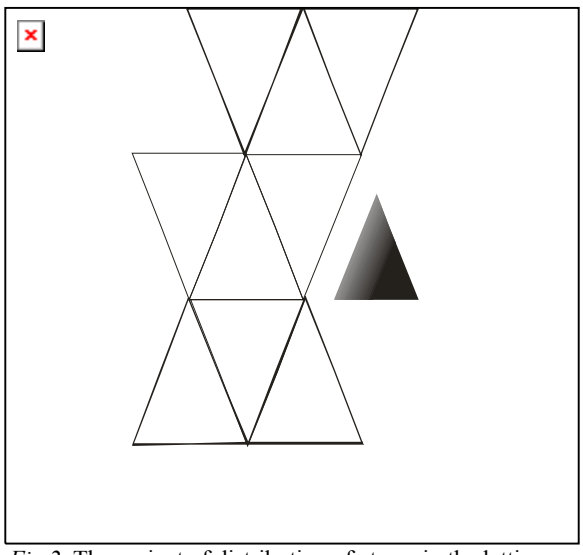

Fig.2. The variant of distribution of atoms in the lattice of $Ga_{0.5}Fe_{0.25}In_{1.25}S_3$

By the crystalochemical analysis it is established that investigated single crystals are triple-packet polytype of the set c=12·nÅ and its structure is polytype on the base of $Ga_{0,5}Fe_{1,5}S_3$ structure in the ordered variant. The variant of atom distribution in the lattice is given on the fig.2. As it is seen from the figure, the layer consequence is correspond to the variant -$c$kk$c$- and the "a" period of the lattice is total because of the statistical filling of the octahedron empties. It is need to note, that in the difference from the changing atoms of Cu and Sn, the iron atoms stabilize the formation of the another kind of polytype, but not one- and divalent cations.

2.3. Optical properties.

For the definition of the electron effect mechanisms in the single crystals $Ga_{0,5}Fe_{0,25}In_{1,25}S_3$ the optical investigations in the wide interval of photon energy were carried out.

On the device, constructed on the base of the monochrometer MDR-12, the transmitted spectrums T of single crystals $Ga_{0,5}Fe_{0,25}In_{1,25}S_3$ at the wave length 400-800nm were obtained. The different single crystal samples by the thickness 10÷40mkm were investigated.

The optical absorption coefficient α has calculated from the experimental values of T, using the formulae [9]

$$T = (1 - R)^2 \exp(-kd), \qquad (1)$$

here R is the reflection coefficient, d is the sample thickness. The spectral dependence of optical absorption coefficient $\alpha(h\nu)$ for the samples from $Ga_{0,5}Fe_{0,25}InS_3$ is given on the fig.3a.

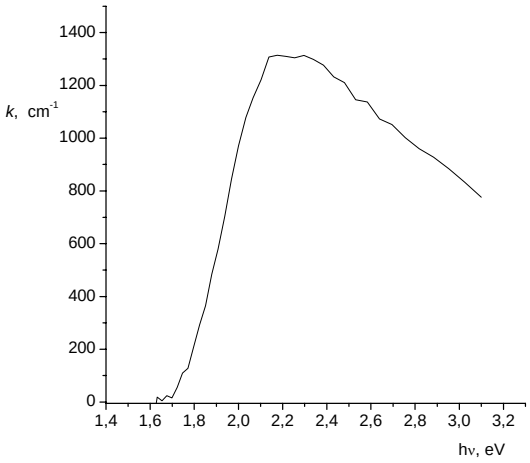

Fig.3 a. Spectral dependence of $k(h\nu)$ for $Ga_{0.5}Fe_{0.25}In_{1.25}S_3$

As it is seen from the figure, at the absorption energy $h\nu \sim\sim Eg$, k strongly increases and achieves the value 10^3sm^{-1}, and in the big energy region its slowly decrease is observed.

The theory of the interband optical transitions [10] shows, that k in the dependence on the photon energy $h\nu$ changes according to the expression:

$$k(h\nu) = A(h\nu - E_g)^r \qquad (2)$$

where h is Plank constant, ν is frequency, A is constant, r is quantity, having values 2,3,1/2, 3/2 in the dependence on the optical transition nature. The obtained results have been analyzed on the base of the theory of the direct transition [9].

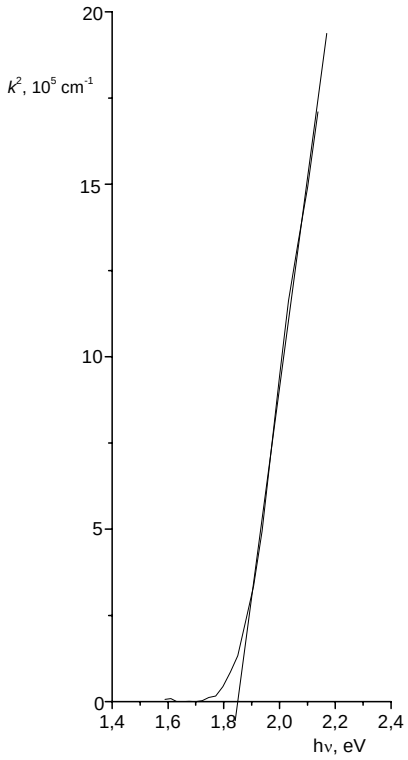

Fig.3 b. Spectral dependence of $k^2(h\nu)$ for $Ga_{0.5}Fe_{0.25}In_{1.25}S_3$

In the region of the longwave absorption edge, the experimental data were given in the coordinates $k^2 \sim h\nu (r=1/2)$ (fig.3,b). It is seen that at the energies $h\nu \geq 1{,}85$eV the k values are well laid on the line in the coordinates $k^2=f(h\nu)$. The line dependence k^2 on $h\nu$ is the evidence that intrinsic absorption edge in the single crystals $Ga_{0,5}Fe_{0,25}In_{1,25}S_3$ forms by the direct allowed optical transitions.

The values of the forbidden band width for the direct allowed transition, which are 1,843eV are obtained by the extrapolation of the lines $k^2=f(h\nu)$ to the value k=0.

2.4. Electric properties.

The injection effects have been studied by the way of the investigation of volt-ampere characteristics (VAC) of structures In-$Ga_{0,5}Fe_{0,25}In_{1,25}S_3$ –In (in the sandviche form) in the electric fields till $3 \cdot 10^5$ V/cm in the temperature interval 100÷360K with the aim of the revealing of the charge transition mechanism, definition current carrier movement and their concentrations, trap parameters (activation energy, concentration and e.t.c.) in the single crystals $Ga_{0,5}Fe_{0,25}In_{1,25}S_3$.

The typical VAC for the investigated samples are presented on the fig.4. With the increase of the electric field from $5 \cdot 10^2$ till $3 \cdot 10^5$V/sm, the current changes in the wide interval ($10^{-4} \div 4 \cdot 10^4$A). It is especially seen, that in spite of the big change of the electric field, the ohmity destroys after the 10^5V/sm. Starting from 10^5V/smthe current increases faster and on the VAC line the quarter region is observed.

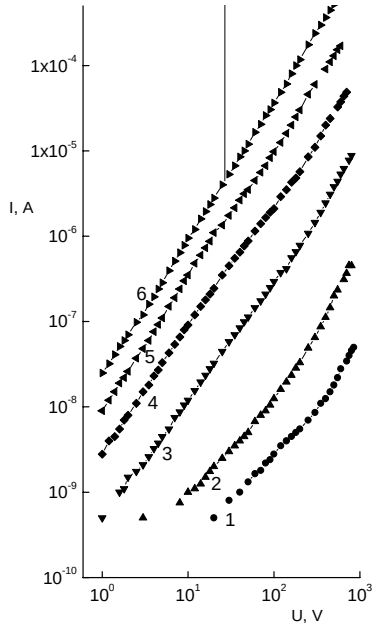

Fig.4. Volt-ampere characteristic of $Ga_{0.5}Fe_{0.25}In_{1.25}S_3$ single crystal at temperatures: 1-131K; 2-236K; 3-270K; 4-300K;5-317K;6-340K.

This fact is proved in the graphics of the temperature dependence of the current at the different electric fields (fig.5), including the region of the carrying out of Ohm law and nonlinear region of VAC. It is seen that inclination of the curves 1-3 is the same, but inclination of the curve 4 is slowly decreases.

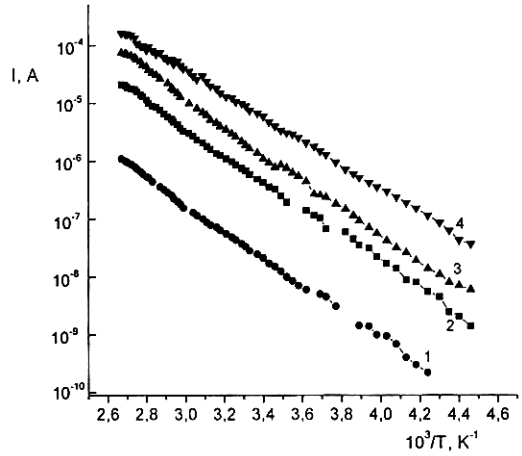

Fig.5. The dependence of $\alpha \sim U$ at T=300 K.

For the clarifying of the current change mechanism in the single crystals $Ga_{0,5}Fe_{0,25}In_{1,25}S_3$ in the dependence on the electric current and the temperature, the obtained results were analyzed on the base of the method of injective spectroscopy [11], i.e. power current I dependence on voltage $U(I \sim U^{\alpha})$.

$$\alpha = \frac{d \lg I}{d \lg U} = \frac{U}{I} \frac{dI}{dU} . \qquad (3)$$

Such approach allows to more clearly realize the VAC structure, to fix its special points and to border the injection mode [12-14].

The dependence $\alpha(U,I)$ at the temperature 300K has the one experimental point (α_{min}=0,677 at U_{min}=180V(I_{min}=4,65.10^{-6}A) (fig.6).

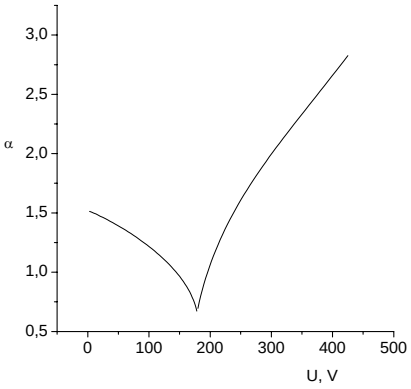

Fig.6

The local levels in the forbidden band (E_t=0,52eV), trapping the injected charge carriers, in the result of which the slow current increase takes place, are defined by the formulae

$$E_t = kT \ln\left[2\left(\frac{2\pi m^* kT}{h^2}\right)^{3/2} \frac{3(1+\alpha_m)e\mu SU_m}{2\alpha_m^2(5-8\alpha_m^2)LI_m}\right] \quad (4)$$

where

$$2\left(\frac{2\pi m^* kT}{h^2}\right) \approx 10^{19} - \text{“}^{-3}\left(\frac{m^*}{m}\frac{T}{300K}\right)^{3/2} = N_c$$

is the effective state density in the conductivity band, m_n=0,4m_e is the effective mass, h is Plank constant, k is Bolzman constant, T is Kelvin temperature, L is samples thickness, S is contact area.

The definitions of the main carrier movement by formulae (1) (μ=12,56sm^2/V·sec) give the possibility to estimate the initial (I=0) contact concentration of these carriers by the formulae

$$n_{k0} = \frac{\exp\left\{\sqrt{1-\alpha_{\min}}\left(\sqrt{1-\alpha_{\min}}-1\right)\right\}}{1-\sqrt{1-\alpha_{\min}}} \frac{I_{\min}L}{e\mu SU_{\min}} \quad (5)$$

According to [11] VAC approximation

$$V >> |V_k| = \frac{2\pi|\rho_k|L^2}{\varepsilon} \quad (6)$$

(here $|\rho_k| = en_k$ -) is the density module of the space charge of the cathode, V_k is the cathode strength), when the applied shifting is in many times more than volume back strength, caused by the charge(or recombination) barrier in the semiconductor, the approximation Mott-Gerni takes place

$$j = \frac{e\mu n_{k0}}{L}V >> \frac{8\pi e^2 \mu n_{k0}^2 L}{\varepsilon}$$

which is the result of the noncreation of the space charge because of the high value of the field.

In fact, the condition (3) is also the criteria of strength constant of the electric field in the structure. That's why the existence of the sublinear region on the VAC of structure In-$Ga_{0,5}Fe_{0,25}In_{1,25}S_3$-In with 0<$\alpha_{min}$<1 degree, characterises the constant field mode on the intercontact layer, which allows to estimate also the transparency of the contact landing barrier Dk*, its thickness d_k [11-15] and effective high $\Delta\varepsilon = kT\ln\frac{N_c}{n_{k0}}$.

Corresponding to the given formulae, the VAC processing gives the following parameters: n_k=1.55·10^{10}cm^{-3}; D_k^* =2·10^{-2}; d_k=5.6·10^{-9}cm; $\Delta\varepsilon$=0.497eV.

Conclusion.

In conclusion, we note that at the interaction in the system $(GaIn)_{2-x}S_3$-Fe_{1-x} in the difference from the edge consisting phases $GaFeS_3$ and $InFeS_3$, the intermediate phases of the layered structure of polytypes of trigonal modification of $Ga_{0,5}In_{1.5}S_3$ with lattice periods a=3,796, c=12,210A.

The single crystals of the composition $Fa_{0,5}Fe_{0,25}In_{1,25}S_3$ have been grown and it has established that its structure consist on the 3 packets with 3R symmetry with sera atom - ггкк*г*. In the result of the statistical occupation of the tetrahedron and octahedron positions, the identification period of the lattice "a" increases in two times and become a=3,786.2, c=36,606Å.

By the crystal analysis it is established, that partial permutation of In and Ga atoms by the trivalent Fe atom, causes the stabilization of the polytype modification form c=12·nÅ. Besides the changes of Fe atom quantity in the composition give the possibility to control the forbidden band width, as with the increase of Fe atom quantity, the forbidden band width decreases (E_g for $Ga_{0.5}Fe_{0.5}InS_3$ - 1.885eV, where z=5.33 and for $Ga_{0.5}Fe_{0.25}In_{1.25}S_3$ -1.843eV, where z=16) in the comparison with the matrix modifications of $GaInS_3$ [16], the forbidden band width of which changes from 2,40 till 2,60eV.

[1] *M.I. Zargarova,R.S. Gamid.,* Inorganic materials, 5 (5), 1969, 371-374.

[2] *I.R. Amiraslanov, G.G. Guseinov, H.S. Mamedov, A.S.Guliyev.* Crystallography, 33 (3), 1988, 767-768.

[3] *G.G.Guseinov, I.R. Amiraslanov, A.S.Guliyev, H.S.Mamedov*. Inorganic materials, 23 (5), 1987, 854-856.
[4] *G.G.Guseinov, I.R. Amiraslanov, A.S. Guliyev, H.S.Mamedov*, Crystallography, 32 (1), 1987, 243-244.
[5] *I.R.Amiraslanov, Y.G.Asadov, P.A.Maximov, V.N.Molchanov*. Crystallography, 36 (2), 1981, 332-335.
[6] *M.G.Kazimov, G.G.Guseinov, AB.Magerramov, I.G.Aliyev*. Fizika, NAS Azerbaijan, 5 (1), 1999,18-19.
[7] *M.G.Kazimov, G.G.Guseinov, G.S.Mekhtiyev, E.A.Isayeva.* Izvestiya NAS Azerbaijan, 2, 2002, 78-83.
[8] *G.G.Guseinov, V.A.Gasimov, F.G.Magerramova.* Fizika, NAS of Azerbaijan, 8 (2), 2002, 33-35.
[9] *J.I.Pankove.* Optical processes in Semiconductors, Moscow , Mir, 1973.
[10] *E.I. Johnson*. Semiconductors and semimetals, New York, 3, 1967.
[11] *A.N.Zyuganov, S.V.Svechnikov*. The injection-contact phenomena in semiconductors. Kiev, Nauk. Dumka, 1981.
[12] *B.G.Tagiev, O.B.Tagiev, N.N.Musayev.* Semiconductors, 29 (8) 1995.
[13] *B.G.Tagiev, N.N.Musayeva, R.B.Jabbarov.* Semiconductors, 36 (2) 2002.
[14] *B.G.Tagiev, U.F.Kasumov, N.N.Musayeva, R.B.Jabbarov*. Physica of solid state, 43 (3), 2003, 403-408
[15] *V.Berishvili, A.N.Zyuganov, S.V.Svechnikov, P.S.Smertenko.* Poluprovodnikovaya texnika i mikroelectronika, 28, 1978, 23-31
[16] *I.R. Amiraslanov, T.X. Azizov, G.G. Huseynov, A.S.Guliyev*. Inorganic materials, 24 (5), 1988, 723-726.

Q.H.HÜSEYNOV, N.N. MUSAYEVA, İ.B.ƏSƏDOVA

$Ga_{0.5}Fe_{0.25}In_{1.25}S_3$ LAYLI YARIMKEÇİRİJİNİN ELEKTRİK VƏ OPTİK XASSƏLƏRİ

Brijman metodu ilə $(GaIn)_2S_3$–Fe sisteminin aralıq fazası olan $Ga_{0.5}Fe_{0.25}In_{1.25}S_3$ monokristalı yetişdirilmişdir. Monokristallar rombogdrik simmetriyalı təbəqəli quruluşa malikdir və qəfəsin periodu a=3.786x2, s=36.606 E, pr.qr. R3m, z=16.
Fotonların geniş intervalı üçün optik udulmanın kənarı tədqiq olunmuş və $Ga_{0.5}Fe_{0.25}In_{1.25}S_3$ üçün qadağan olunmuş zolağın eni təyin olunmuşdur.
In- $Ga_{0.5}Fe_{0.25}In_{1.25}S_3$-In strukturu düzəldilmiş və onun volt-amper xarakteristikası və 100÷360K temperatur intervalında temperatur asılılığı öyrənilmişdir. Differensial analiz metodu ilə göstərilən strukturun parametrləri təyin olunmuşdur: μ=12.56 sm^2/V sek, n_k=1.55 10^{10} cm^{-3}; D_k^* =2 10^{-2}; d_k =5.6 10^{-9} sm; $\Delta\varepsilon$=0.497 gV.

О.Н. Гусейнов, Н.Н. Мусаева, И.В. Асадова

ЭЛЕКТРИЧЕСКИЕ И ОПТИЧЕСКИЕ СВОЙСТВА СЛОИСТОГО ПОЛУПРОВОДНИКА $Ga_{0.5}Fe_{0.25}In_{1.25}S_3$

Методом Бриджмена из расплава выращены монокристаллы промежуточной фазы системы $(GaIn)_2S_3$–Fe состава $Ga_{0.5}Fe_{0.25}In_{1.25}S_3$. монокристаллы слоистые, симметрия ромбоэдрическая, периоды решетки в гексагональной установке a=3.786x2, c=36.606 Å, пр.гр. R3m, z=16.

Исследован край оптического поглощения в широком интервале энергии фотонов и определены ширины запрещенной зоны E_g =1.843 эВ для $Ga_{0.5}Fe_{0.25}In_{1.25}S_3$.

Изготовлено структура In- $Ga_{0.5}Fe_{0.25}In_{1.25}S_3$-In и изучено его ВАХ и температурный зависимость в интервале температур 100÷360К. Методом дифференциального анализа вычислены параметры указанной структуры: μ=12.56 $см^2$/В сек, n_k=1.55 10^{10} $см^{-3}$; D_k^* =2 10^{-2}; d_k=5.6 10^{-9} см; $\Delta\varepsilon$=0.497 эВ.

Received:18.11.03

THE TRANSIENT RADIATION OF NONINVARIANT SOURCE IN THE PLANE-LAYERED MEDIUM II.

I.M. ABUTALIBOV, M.B. ASADOVA, I.G. JAFAROV
The Azerbaycan State Pedagogic University
370000, Baku, Uz. Hajibekov str., 34

The process of the transient radiation of noninvariant source, particularly, the magnetic moment in the plane-layered medium is considered. The eigen field and radiation field are calculated with the help of Hertzian vectors.

In the previous ref [1] the expressions for Hertzian vectors, which are the initial functions for the calculation of the field, had been obtained by us.

The field of the magnetic moment in the plane-layered medium in the first approximation has the form:

$$\vec{E}=\vec{E}^{\,0}+\delta\vec{E},\ \vec{B}=\vec{B}^{\,0}+\delta\vec{B}, \tag{1}$$

where $\vec{E}^{0}$ and $\vec{B}^{0}$ are field's vectors in the homogeneous medium, $\delta\vec{E}$ and $\delta\vec{B}$ are deposits in the first approximation to the electric and magnetic fields. It is noticed, that any of electromagnetic field sources, moving in the homogeneous medium with the constant velocity, which is less, than phase radiation velocity, don't radiate. Therefore, the complete eigen field is defined by the expressions:

$$\vec{E}^{s}=\vec{E}^{0}+\delta\vec{E}^{s},\qquad \vec{B}^{s}=\vec{B}^{0}+\delta\vec{B}^{s}, \tag{2}$$

and radiation field is as follows

$$\vec{E}^{r}=\delta\vec{E}^{r},\ \vec{B}^{r}=\delta\vec{B}^{r}. \tag{3}$$

Moreover, the field's vectors $\vec{E}^{0}$ and $\vec{B}^{0}$ are expressed by Hertzian vectors by the following formulae:

$$\vec{E}^{0}=-\frac{4\pi\vec{P}}{\varepsilon^{0}}+\frac{1}{\varepsilon^{0}}\,rot\left(rot\vec{\Pi}^{0}_{e}-\frac{\varepsilon^{0}}{c}\frac{\partial\vec{\Pi}^{0}_{m}}{\partial t}\right) \tag{4}$$

$$\vec{B}^{0}=rotrot\vec{\Pi}^{0}_{m}+\frac{1}{c}\frac{\partial}{\partial t}\left(rot\vec{\Pi}^{0}_{e}\right), \tag{5}$$

Fourier-images of which are equal to:

$$\vec{E}^{0}_{\omega\vec{\chi}}(z)=-\frac{4\pi\vec{P}_{\omega\vec{\chi}}}{\varepsilon^{0}}-\frac{1}{\varepsilon^{0}}\left[\vec{k}_{s}\left[\vec{k}_{s}\vec{\Pi}^{0}_{e\omega\vec{\chi}}\right]\right]-\frac{\omega}{c}\left[\vec{k}_{s}\vec{\Pi}^{0}_{m\omega\vec{\chi}}\right], \tag{6}$$

$$\vec{B}^{0}_{\omega\vec{\chi}}(z)=-\left[\vec{k}_{s}\left[\vec{k}_{s}\vec{\Pi}^{0}_{m\omega\vec{\chi}}\right]\right]+\frac{\omega}{c}\left[\vec{k}_{s}\vec{\Pi}^{0}_{e\omega\vec{\chi}}\right] \tag{7}$$

where $\vec{k}_{s}=\vec{\chi}+\vec{\upsilon}\omega/\upsilon^{2}$ is the wave vector of the eigen field.

The vectors $\vec{E}^{0}_{\omega\vec{\chi}}$ and $\vec{B}^{0}_{\omega\vec{\chi}}$ describe the eigen field of the magnetic moment in the homogeneous isotropic nonmagnetic medium [2]. The eigen field is defined by the residue of the integrands in the pole $\xi=\omega/\upsilon$ and radiation field - in the poles $\xi=\xi_1$ and $\xi=\xi_2$. Moreover, the general expressions are for the addition to the field's vectors:

$$\delta\vec{E}^{s,r}_{\omega\vec{\chi}}(z)=\frac{Res\,\delta\varepsilon_{\xi}}{(\varepsilon^{0})^{2}}\cdot\left\{4\pi\vec{P}_{\omega\vec{\chi}}+[\vec{\kappa}_{s}[\vec{\kappa}_{s}\vec{\Pi}^{0}_{e\omega\vec{\chi}}]]\right\}-\frac{1}{\varepsilon^{0}}\left\{[\vec{\kappa}_{s,r}[\vec{\kappa}_{s,r}\delta\vec{\Pi}^{s,r}_{e\omega\vec{\chi}}]]+\frac{\omega\varepsilon^{0}}{c}\left[\vec{k}_{s,r}\delta\vec{\Pi}^{s,r}_{m\omega\vec{\chi}}\right]\right\} \tag{8}$$

$$\delta\vec{B}^{s,r}_{\omega\vec{\chi}}(z)=-\left[\vec{k}_{s,r}\left[\vec{k}_{s,r}\delta\vec{\Pi}^{s,r}_{m\omega\vec{\chi}}\right]\right]+\frac{\omega}{c}\left[\vec{k}_{s,r}\delta\vec{\Pi}^{s,r}_{e\omega\vec{\chi}}\right], \tag{9}$$

It is noticed, that $Res\,\delta\varepsilon_{\xi}$ in the poles $\xi=\xi_1$ and $\xi=\xi_2$ is equal to 0 (zero) (the first figured bracket in (7) disappears), and in the pole $\xi=\omega/\upsilon$ for the chosen concrete expressions (see (23)-(25) in ref [1]) gives the same result:

$$\mathrm{Res}\left[\delta\varepsilon_{\xi}\right]_{\xi=\omega/\upsilon}=\Delta\varepsilon/2\pi i \tag{10}$$

Based on the expressions, obtained in ref [1] from formulae (6)-(8), we obtain the following final expressions for the change of the eigen field:

$$\delta\vec{B}^{s}_{\omega\vec{\chi}}(z) = \frac{z}{|z|}\frac{\Delta\varepsilon c^2\ exp(i\omega z/\upsilon)}{(2\pi)^2\upsilon\omega^2}\left(\varepsilon^0 - c^2/\upsilon^2 - \chi^2c^2/\omega^2\right)^{-2}\times$$
$$\times\left\{\vec{e}_3\chi^2\left(m_z - \frac{\omega\gamma^{-2}}{\upsilon\chi^2}\vec{m}\vec{\chi}\right) - \vec{\chi}\left(m_z\omega/\upsilon + \vec{m}\vec{\chi}\right) + \vec{m}_\perp\left(\chi^2 + \frac{\omega^2\gamma^{-2}}{\upsilon^2}\right)\right\}, \qquad (11)$$

$$\delta\vec{E}^{s}_{\omega\vec{\chi}}(z) = \frac{z}{|z|}\frac{\Delta\varepsilon c^2\ exp(i\omega z/\upsilon)}{(2\pi)^2\upsilon\omega^2\left(\varepsilon^0\right)^2}\left(\varepsilon^0 - c^2/\upsilon^2 - \chi^2c^2/\omega^2\right)^{-2}\times$$
$$\times\left\{\left(\vec{e}_3\frac{\omega}{\upsilon} + \vec{\chi}\right)[\vec{\chi}\vec{m}]_z\frac{\upsilon}{c}\left(2\varepsilon^0 - c^2/\upsilon^2 - \chi^2c^2/\omega^2\right) - \frac{\omega\left(\varepsilon^0\right)^2}{c}[\vec{\chi}\vec{m}] + \frac{\left(\varepsilon^0\right)^2\omega^2\gamma^{-2}}{\upsilon^2}[\vec{m}\vec{\beta}]\right\}, \qquad (12)$$

and for the radiation field we have:

$$\delta\vec{B}^{r1,2}_{\omega\vec{\chi}}(z) = \mp\frac{ic}{2\pi\upsilon\omega}\delta\varepsilon_{\xi_{1,2}}\frac{\left(\varepsilon^0 - c^2/\upsilon^2 - \chi^2c^2/\omega^2\right)^{-1}}{\sqrt{\varepsilon^0 - \chi^2c^2/\omega^2}}exp\left(\pm i\omega z\sqrt{\varepsilon^0 - \chi^2c^2/\omega^2}/c\right)\times$$
$$\times\left\{\vec{e}_3\chi^2\left(m_z - \frac{\omega\gamma^{-2}}{\upsilon\chi^2}\vec{m}\vec{\chi}\right) - \vec{\chi}\left(\vec{m}\vec{\chi} \pm m_z\frac{\omega}{c}\sqrt{\varepsilon^0 - \chi^2c^2/\omega^2}\right) + \right. \qquad (13)$$
$$\left. + \vec{m}_\perp\left(\chi^2 \pm \frac{\omega\gamma^{-2}}{\upsilon^2}\cdot\frac{\upsilon}{c}\sqrt{\varepsilon^0 - \chi^2c^2/\omega^2} + \frac{1}{\varepsilon^0}[\vec{\chi}\vec{e}_3][\vec{\chi}\vec{m}]_z\left(1 \mp \frac{\upsilon}{c}\sqrt{\varepsilon^0 - \chi^2c^2/\omega^2}\right)\right)\right\},$$

$$\delta\vec{E}^{r1,2}_{\omega\vec{\chi}}(z) = \mp\frac{i}{2\pi\upsilon(\varepsilon^0)^2}\delta\varepsilon_{\xi_{1,2}}\frac{\left(\varepsilon^0 - c^2/\upsilon^2 - \chi^2c^2/\omega^2\right)^{-1}}{\sqrt{\varepsilon^0 - \chi^2c^2/\omega^2}}exp\left(\pm i\omega z\sqrt{\varepsilon^0 - \chi^2c^2/\omega^2}/c\right)\times$$
$$\times\left\{\vec{e}_3[\vec{\chi}\vec{m}]_z\left[-\left(\varepsilon^0 - 1\right)\frac{\chi^2c^2}{\omega^2} \mp \frac{c}{\upsilon}\sqrt{\varepsilon^0 - \chi^2c^2/\omega^2}\left(\varepsilon^0\gamma^{-2} + \frac{\chi^2\upsilon^2}{\omega^2}\right)\right] + \vec{\chi}\frac{c}{\omega}[\vec{\chi}\vec{m}]_z\times\right. \qquad (14)$$
$$\left.\times\left[\frac{\upsilon\varepsilon^0}{c} + \left(-\frac{c}{\upsilon} \pm \sqrt{\varepsilon^0 - \chi^2c^2/\omega^2}\right)\left(\varepsilon^0 \pm \frac{\upsilon}{c}\sqrt{\varepsilon^0 - \chi^2c^2/\omega^2}\right)\right] - \left(\varepsilon^0\right)^2[\vec{\chi}\vec{m}]_\perp + \frac{\left(\varepsilon^0\right)^2\omega\gamma^{-2}}{\upsilon}[\vec{m}\vec{e}_3]\right\}.$$

In the formulae (10)-(14) the longitudinal and transversal parts are divided, moreover the expressions of the unit vector $\vec{e}_3 = \vec{\upsilon}/\upsilon$ are the longitudinal part of the field, and all rest are transversal part of the field.

The formulae (13) and (14), describing the transient radiation of the magnetic moment in the plane-layered nonmagnetic medium become simpler strong enough at the meaning on all possible directions of vector $\vec{\chi}$:

$$\delta\vec{\vec{E}}^{r1,2}_{\omega} = \mp\frac{ic[\vec{m}_\perp\vec{e}_3]}{2\pi\upsilon\omega\left(\varepsilon^0\right)^{5/2}}\delta\varepsilon_{\xi_{1,2}}\left(\varepsilon^0 - c^2/\upsilon^2\right)^{-1}\times$$
$$\times\left\{\frac{\chi^2}{2}\left[\frac{\upsilon\varepsilon^0}{c} + \left(-\frac{c}{\upsilon} \pm \sqrt{\varepsilon^0}\right)\left(\varepsilon^0 \pm \frac{\upsilon}{c}\sqrt{\varepsilon^0}\right)\right] + \frac{\left(\varepsilon^0\right)^2\omega^2\gamma^{-2}}{c\upsilon}\right\}exp\left(\pm i\omega z\sqrt{\varepsilon^0}/c\right), \qquad (15)$$

$$\delta\vec{\vec{H}}^{r1,2}_{\omega} = \mp\frac{c\vec{m}_\perp}{2\pi\upsilon\omega}\delta\varepsilon_{\xi_{1,2}}\left(\varepsilon^0 - c^2/\upsilon^2\right)^{-1}\left\{\chi^2 - \frac{1}{2\varepsilon^0}\chi^2\left(1 \mp \frac{\upsilon}{c}\sqrt{\varepsilon^0}\right) \pm \frac{\omega^2\gamma^{-2}}{c\upsilon}\sqrt{\varepsilon^0}\right\}\times \qquad (16)$$
$$\times exp\left(\pm i\omega z\sqrt{\varepsilon^0}/c\right),$$

From above formulae we obtain the simple relation for the radiation field lengthways (against) on the source moving direction (θ=0, π, χ=0):

$$\delta\vec{\vec{H}}_{\omega}^{r1,2} = \mp\sqrt{\varepsilon^0}\left[\vec{e}_3\delta\vec{\vec{E}}_{\omega}^{r1,2}\right] = \frac{i\vec{m}_{\perp}\omega}{2\pi c^2}\,\delta\varepsilon_{\xi_{1,2}}\,\frac{1-\upsilon^2/c^2}{1-\varepsilon^0\upsilon^2/c^2}\,exp\left(\pm\, i\,\frac{\omega\sqrt{\varepsilon^0}}{c}\,z\right). \qquad (17)$$

From (16) it is seen, that at the ultrarelativistic velocities the radiation field in the direction of magnetic moment moving, is plane wave with the wave vector $\vec{k}_{\prime\prime}=\left(\omega\sqrt{\varepsilon^0}/c\right)\vec{e}_3$, that we can't say about other directions ($\theta\neq$0).

The sign "±" of the vector $\delta\vec{\vec{E}}_{\omega}^{r1,2}$ is caused by that at the wave propagation against the moving direction, vector $\delta\vec{\vec{E}}_{\omega}^{r1,2}$ as polar one changes the direction on the opposite direction in the way, that vectors $\delta\vec{\vec{E}}_{\omega}^{r1,2}$, $\delta\vec{\vec{H}}_{\omega}^{r1,2}$, $-\vec{e}_3$ constitute the rightsrew orthogonal system.

Analogically, in the ultrarelativistic approximation, for the eigen field of the magnetic moment, moving in the plane-layered nonmagnetic medium, mean on all possible directions of vector $\vec{\chi}$ in plane, which is perpendicular to its velocity and oriented lengthways its direction, we obtain:

$$\vec{\vec{H}}_{\omega}^{s} = \vec{\vec{H}}_{\omega}^{0} + \delta\vec{\vec{H}}_{\omega}^{s} = \frac{\vec{m}_{\perp}}{2\pi^2\upsilon}\,\frac{1-\upsilon^2/c^2}{1-\varepsilon^0\upsilon^2/c^2}\left[1+\frac{z}{|z|}\,\frac{\Delta\varepsilon}{2}\,\frac{\upsilon^2}{c^2}\,\frac{1}{1-\varepsilon^0\upsilon^2/c^2}\right]exp(i\omega z), \qquad (18)$$

$$\vec{\vec{E}}_{\omega}^{s} = \vec{\vec{E}}_{\omega}^{0} + \delta\vec{\vec{E}}_{\omega}^{s} = \left[\vec{\vec{H}}_{\omega}^{s}\vec{\beta}\right], \qquad (19)$$

From formulae (18), (19) it is seen, that change of the eigen fields depends on the velocity and inhomogeneous of the dielectric constant, moreover this change increases in the source moving direction ($z>0$), and decreases in the opposite direction($z<0$).

As it is known, the field of the ultrarelativistic source on its properties is close to the one of the light wave field. Moreover, the condition $\vec{\chi}<<\omega/c$ should be carried out and projection of the magnetic moment in moving direction $m_z\cong 0$, i.e. the radiation field is defined by the transverse component $\vec{m}_{\perp}$:

$$\sqrt{\varepsilon^0}\,\delta\vec{E}_{\omega}^{r1,2} = \left[\delta\vec{H}_{\omega}^{r1,2}\vec{n}\right] = \pm\,\frac{i\omega}{2\pi c^2}\,\delta\varepsilon_{\xi_{1,2}}\,\frac{1-\upsilon^2/c^2}{1-\varepsilon^0\upsilon^2/c^2}\left[\vec{m}_{\perp}\vec{n}\right]exp\left(\pm\, i\,\frac{\omega\sqrt{\varepsilon^0}}{c}\,z\right). \qquad (20)$$

Moreover, the deposit to the eigen field becomes the transversal wave:

$$\delta\vec{E}_{\omega}^{s}(z) = \left[\delta\vec{B}_{\omega}^{s}(z)\vec{\beta}\right] = \frac{z}{|z|}\,\frac{\Delta\varepsilon\upsilon}{(2\pi c)^2}\,\frac{1-\upsilon^2/c^2}{\left(1-\varepsilon^0\upsilon^2/c^2\right)^2}\left[\vec{m}_{\perp}\vec{\beta}\right]exp(i\omega z/\upsilon). \qquad (21)$$

From formulae (21) it follows, that $\delta\vec{E}_{\omega}^{s}(-\upsilon) = \delta\vec{E}_{\omega}^{s}(\upsilon)$ is even function, and $\delta\vec{H}_{\omega}^{s}(-\upsilon) = -\delta\vec{H}_{\omega}^{s}(\upsilon)$ is odd function of source velocity. The value of field's vectors of the radiation field is even velocity function: $\delta\vec{E}_{\omega}^{r1,2}(-\upsilon) = \delta\vec{E}_{\omega}^{r1,2}(\upsilon)$, $\delta\vec{H}_{\omega}^{r1,2}(-\upsilon) = \delta\vec{H}_{\omega}^{r1,2}(\upsilon)$.

Because of that in ultrarelativistic case $\delta\varepsilon_{\xi_1} >> \delta\varepsilon_{\xi_2}$, the relation of the values of field's vectors can express in the form of the function:

$$f(\upsilon) = \frac{\delta\vec{E}_{\omega}^{r1}}{\delta\vec{E}_{\omega}^{r2}} = \frac{\delta\vec{H}_{\omega}^{r1}}{\delta\vec{H}_{\omega}^{r2}} = \frac{\delta\varepsilon_{\xi_1}}{\delta\varepsilon_{\xi_2}} >> 1\,, \qquad (22)$$

it means that radiation forward is stronger, than radiation back. For the function (22) at the different distributions of the inhomogeneous of the dielectric constant (see (16)-(18) ref [1]), accordingly, we have:

$$f_1^{(n)}(\upsilon) = \frac{exp\left(\pi^2 n\sqrt{\varepsilon^0}\right)}{\frac{2\pi^2}{\beta}\,n(1-\beta\sqrt{\varepsilon^0})}\,, \qquad (23)$$

$$f_2^{(n)}(\upsilon)=\frac{1+\beta\sqrt{\varepsilon^0}}{1-\beta\sqrt{\varepsilon^0}}\,exp\left(4\pi n\sqrt{\varepsilon^0}\right), \qquad (24)$$

$$f_3^{(n)}(\upsilon)=\frac{1+\beta\sqrt{\varepsilon^0}}{1-\beta\sqrt{\varepsilon^0}}\,exp\left\{\left(\frac{2\pi}{\beta}\right)^2\cdot n^2\beta\sqrt{\varepsilon^0}\right\}. \qquad (25)$$

On the fig.1 the graphics of these functions for the case, when $n=\Delta z/\lambda=1$ are presented.

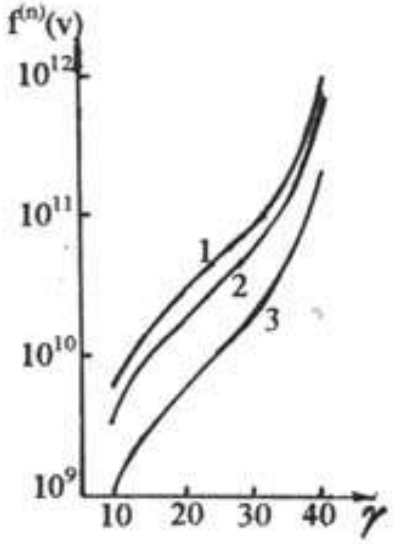

Fig.1. The dependence of function $f^{(n)}(\upsilon)$ on $\gamma=(1-\beta^2)^{-1/2}$.
1 - function $f_1^{(n)}(\upsilon)$;
2 - function $f_2^{(n)}(\upsilon)\cdot 10$;
3 - function $f_3^{(n)}(\upsilon)\cdot 10^{-10}$.

From fig.1it is seen, that radiation forward is stronger, than radiation back, moreover it increases with the velocity increase, that is corresponds to ultrarelativistic case ($\gamma>>1$), when transversal radiation is almost caused by radiation forward.

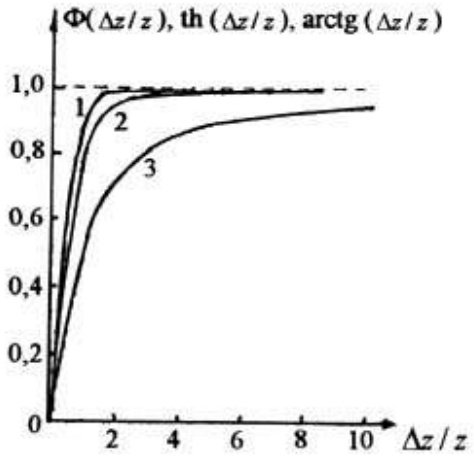

Fig.2. The dependence of functions (see(23)-(25) ref [1] on Δz/z.
1- function *Φ(Δz/z);*
2 - function *th (Δz/z)*;
3 - function *arctg (Δz/z)*.

Morewover, the radiation forward has the main part of the energy. In the fig.2. the graphics of functions ref [3], expressing the nonhomogeneous of dielectric constant from which it is seen, that graphic 1 of probability integral function achieves the maximal value, are given, that causes the increase of function 3 with the comparison of the functions 1 and 2.

[1] *I.M.Abutalibov, M.B.Asadova, I.G.Jafarov*.J. «Fizika», vol.9,number2,2003,p.34-38
[2] *I.G. Jafarov, I.M. Abutalibov, M.B. Asadova*. «Izvestiya» NAN, Ser. Fizika, matematika I tekhnika, №5(1), 2003, s. 104-109.(in Russian).
[3] Spravochnik po specialnim funkciyam. Pod. red. *M. Abramovica i I. Sigan*, Moskva, «Nauka»,1979. (in Russian).
[4] *A.R. Yanpolskiy*. Giperbolicheskiye funkcii, GIFML, Moskva, 1960. (in Russian).

İ.M. Abutalıbov, M.B. Asadova, İ.H. Cəfərov

QEYRİ-İNVARİANT MƏNBƏNİN MÜSTƏVİ TƏBƏQƏLİ MÜHİTDƏ KEÇİD ŞÜALANMASI II

Qeyri-invarian mənbənin, maqnit momentinin, müstəvi-təbəqəli mühitdə keçid şüalanmasına baxılmışdır. Hers vektorları vasitəsilə məxsusi sahə və şüalanma sahəsi hesablanmışdır.

И.М. Абуталыбов, М.Б. Асадова, И.Г. Джафаров

ПЕРЕХОДНОЕ ИЗЛУЧЕНИЕ НЕИНВАРИАНТНОГО ИСТОЧНИКА В ПЛОСКОСЛОИСТОЙ СРЕДЕ II

Рассмотрен процесс переходного излучения неинвариантного источника, в частности, магнитного момента, в плоскослоистой среде. С помощью векторов Герца вычислены собственное поле и поле излучения.

Received: 25.03.04

SIMULATIONS OF RELAXATION PROPERTIES OF FERROELECTRIC LIQUID CRYSTALS

A.R. IMAMALIYEV
Baku State University,
Z. Khalilov str., Baku, 370145

The numerical analysis of relaxation properties of ferroelectric liquid crystal (FLC) in the case of one-dimensional model is made. The dependence of uniform state relaxation time both on material parameters of FLC and surface conditions is considered. At some value of dispersion part of anchoring energy the relaxation time rises abruptly i.e. a memory effect is obtained.

The linear electrooptic effect in ferroelectric liquid crystals (FLC) occurs with memory (bistability) under some circumstances [1,2], that allows essentially to simplify the addressing scheme of FLC display. In spite of this we do not see the mass production of FLC displays today so it is not possible to obtain the reproducible bistable switching of FLC. From this point of view there is some necessity for theoretical and experimental investigation of this phenomenon in order to correct the condition of bistability for FLC cell. The investigation of relaxation process of after switching of an electric field would be help us to understand the reason of bistability. In this paper on the base of one-dimensional model the dependence of relaxation time on various material parameters of FLC and surface conditions has been studied.

The FLC cell geometry is shown in fig.1. $\vec{n}\ (\sin\theta\cos\phi, \sin\theta\sin\phi, \cos\phi)$ and $\vec{P}_S$ are the director and the spontaneous polarization respectively. The tilt angle θ mainly depends on temperature and usually far from smectic *A* - smectic *C** phase transition temperature its value gets nearly constantly. So at low temperatures the space-time distribution of director $\vec{n}(\vec{r}, t)$ can be replaced by azimuthal angle distribution $\phi(\vec{r}, t)$. For monodomain samples this angle changes only in the direction normally to sample plane that allows us to suggest $\phi(\vec{r}, t) = \phi(x, t)$. The latter can be determined from balance toque equation [3]

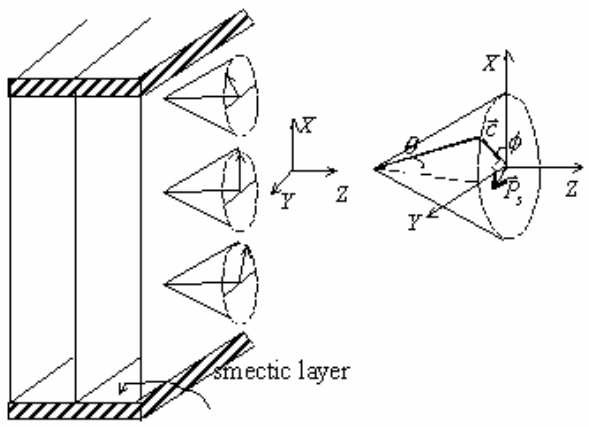

Fig.1.

$$\gamma\theta^2\frac{\partial\phi}{\partial t} = G\theta^2\frac{\partial^2\phi}{\partial x^2} + P_S E\cos\phi + \left(\frac{P_S^2}{2\chi_\perp\varepsilon_0} + \frac{\Delta\varepsilon\varepsilon_0\theta^2E^2}{2}\right)\sin 2\phi \qquad (1)$$

with boundary conditions

$$G\frac{d\phi}{dx}\Big|_{\pm d/2} = \left(W_1\cos\phi \pm W_2\sin 2\phi\right)_{\pm d/2} \qquad (2)$$

$$0\le x\le d/2, \quad -\pi/2\le\phi\le\pi/2$$

The following notations are used: G is an elastic constant, P_S is a spontaneous polarization, E is an electric field strength, $\Delta\varepsilon = \varepsilon_{||} - \varepsilon_\perp$ is an anisotropy of dielectric permittivity, $\chi_\perp$ is a transversal component of the dielectric susceptibility, $\varepsilon_0 = 8{,}85\ pF/m$ is electric constant.

The first term in the right hand side of equation (3) expresses the polar interaction of molecules with the substrate surface. The polar interaction tends to orient the spontaneous polarization toward, or out of the surface. It is equivalent to a condition $\phi(d/2) = -\phi(-d/2) = \pi/2$ for given geometry. The second term is a dispersive part of the surface energy: the dispersion interaction is responsible for planar orientation of molecules and required $\phi(d/2) = \phi(-d/2) = \pi/2$. The appropriate anchoring energies are denoted by W_1 and W_2. The signs «-» and « +» concern to top and bottom surfaces respectively.

The equation (3) is a nonlinear diffusion equation with boundary conditions (2) of general form and can't be solved analytically. We have solved it numerically by using the sweep method [4] and MATHCAD 2001 calculating program.

As an initial solution we take the twist state ($\phi(x,0) = \frac{x}{d}\cdot\pi$). After applying the voltage exceeding the threshold this state switches to uniform state ($\phi(x) = \frac{\pi}{2}$). Then we remove this voltage and this state relaxes to twist state. It is seen clearly from the time dependence of light transmittance of the cell (fig. 2). As a relaxation time it has taken the time during witch the light transmittance decreases from I_{max} to $0.1(I_{max}-I_{min})$. As mentioned above the dependence of this time from the material parameters of FLC and surface parameters help us to understand the reason of memory.

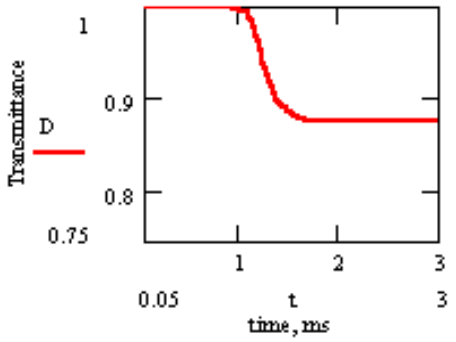

Fig.2.

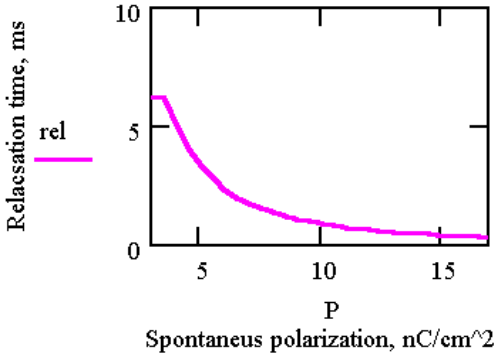

Fig. 3.

The relaxation time strongly decreases with increasing of spontaneous polarization (fig. 3). We connect it with influence of polarization charges field. In uniform state the spontaneous polarization is oriented uniformly as well as the director that creates the excess of free energy density $\frac{P_S^2}{2\varepsilon_0\chi_\perp}$. This factor plays a destabilizing role and the uniform state quickly relaxes to uniform state.

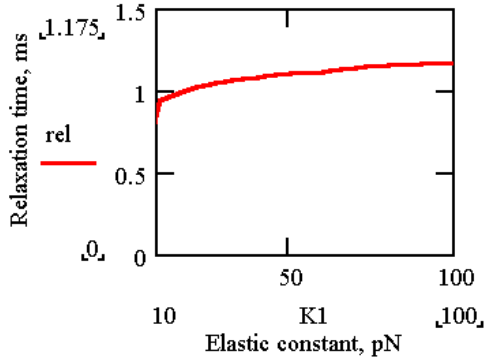

Fig. 4.

The increasing of elastic constant causes the slow increasing of the relaxation time (fig. 4). The relaxation of the uniform state leads to excess of elastic free energy $\frac{1}{2}G\theta^2\left(\frac{\pi}{d}\right)^2$. This energy increases with increasing of the elastic constant and the relaxation process becomes difficult.

With increasing of the polar anchoring energy the relaxation time decreases almost linearly (fig. 5). For uniform state the polar anchoring creates the destabilizing excess energy $\frac{W_1}{d}$ for one of substrates that causes the relaxation of the uniform state.

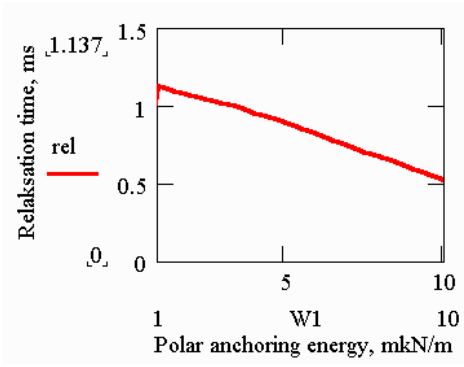

Fig. 5.

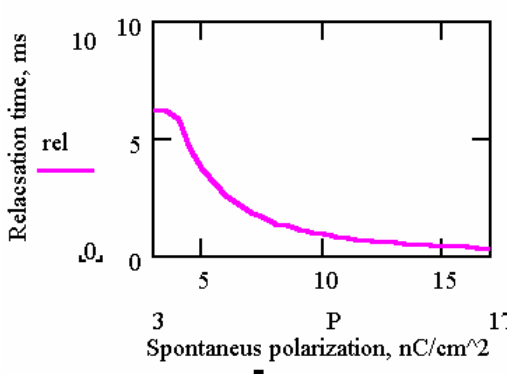

Fig. 6.

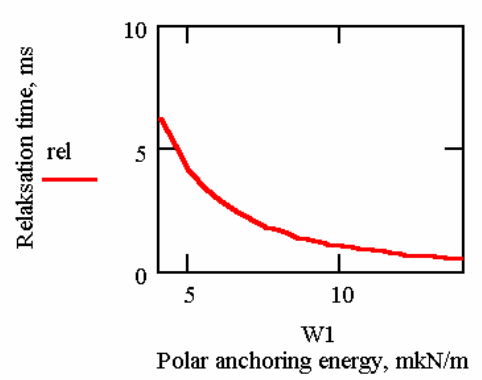

Fig. 7.

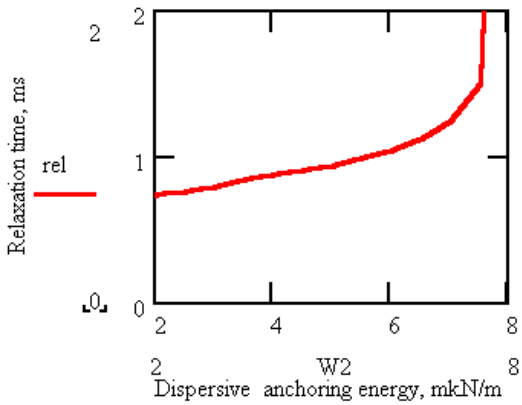

Fig.8.

For most cases one assumed that the polar anchoring energy linearly depends on the spontaneous polarization:

$$W_1 = W_1 + \alpha P_S \qquad (3)$$

By taking into account this expression in our calculation the dependence $\tau_{rel}(P_S)$ remains almost unchanged whilst the dependence $\tau_{rel}(W_1)$ takes qualitatively different form (fig.6,7).

As expected the dependence of relaxation time on dispersion anchoring energy have the form of monotonically increasing function (fig.8). This part of anchoring energy plays a stabilizing role both for upper and lower surfaces and tends to hinder the relaxation of uniform states. At the some value of dispersion anchoring energy the relaxation time approaches infinity i.e. the uniform state do not relaxes and a memory effect is obtained.

All of these results are well-known facts and confirmed by experiments.

[1] *N.A. Clark, S.T. Lagerwall.* Mol.Cryst.&Liq.Cryst., 1983, v. 93, p. 213.

[2] *Y. Ouchi , H. Takezoe , A. Fukuda.* Jap. J. Appl. Phys, 1987, v. 26, p. 1.

[3] *H.E. Abbasov, A.R. Imamaliyev*. Journal "Fizika" of Azerbaijan National Academy of Science, 2003, v. 9, №1, p. 6.

[4] *A.A. Samarskiy, A.B. Gulin*. Chislenniye metodi. M.: Nauka, 1987, 427s. (in Russian).

A.R. İmaməliyev

SEQNETOELEKTRİK MAYE KRİSTALLARIN RELAKSASİON XÜSUSİYYƏTLƏRİNİN MODELLƏŞDİRİLMƏSİ

Birölçülü hal üçün seqnetoelektrik maye kristalın (SMK) relaksasiya xassələri ədədi üsulla analiz olunmuşdur. Bircins halın relaksasiya müddətinin həm SMK-nın maddi parametrlərindən, həm də səth şəraitindən asılılığına baxılmışdır. İlişmə enerjisinin dispersion hissəsinin müəyyən qiymətində sıçrayışla artır, yəni yaddaşlı keçid alınır.

А.Р. Имамалиев

МОДЕЛИРОВАНИЕ РЕЛАКСАЦИОННЫХ СВОЙСТВ СЕГНЕТОЭЛЕКТРИЧЕСКИХ ЖИДКИХ КРИСТАЛЛОВ

Проведен численный анализ релаксационных свойств сегнетоэлектрического кристалла (СЖК). Рассмотрена зависимость времени релаксации от материальных параметров СЖК и поверхностных условий. При некотором значении дисперсионной части энергии сцепления время релаксации растет скачком, т.е. получается переключение с памятью.

Received: 05.02.04

THE UNSTABLE THERMOMAGNETIC WAVE IN THE ANISOTROPIC SOLIDS

E.R. GASANOV
Baku State University
Az-1148, Baku, Z. Khalilov str., 23

It is shown, that in the anisotropic crystals the unstable thermomagnetic wave propagates. The frequencies and increase increment have been calculated. The directions of wave propagations are defined. It is proved, that in the anisotropic crystals it is possible the simultaneous propagation of several increasing waves.

In the ref [1] it is shown, that hydrodynamic motions in the nonequillibrium plasma, which has the temperature gradient ∇T, lead to the magnetic fields appearing. Plasma with the temperature gradient ∇T has vibrational properties, which are strongly differ from usual plasma properties. In such plasma in the absence of external magnetic field the transversal ($\vec{k}\perp\nabla\vec{T}$) thermomagnetic waves are possible, in which the oscillation of only magnetic field takes place. If there is the constant external magnetic field $\vec{H}_0$, so the wave vector of thermomagnetic waves should be perpendicular to it and lay in the plane ($\vec{H}_0$, $\nabla\vec{T}$). The homogeneous magnetic field in such plasma rotates in the temperature gradient direction. In plasma $\Omega_e\tau>>1$ (Ω_e is Larmor electron frequency, τ is frequency of their collisions) the thermomagnetic wave increases with the increment $\gamma\sim\Omega_e\tau\Lambda(\vec{H}\nabla\vec{T})|\vec{K}|$.

In the solid-state there is the electron flux and that's why is possible the thermomagnetic wave appearance at the existence of ∇T in the absence of external magnetic field. The probability of excitation of thermomagnetic waves in the isotropic solid-state was investigated in the ref [2]. In this work we will investigate the thermomagnetic waves appearance in the anisotropic solid-states and conditions of the increase of these waves, i.e. the instability of the thermomagnetic waves in the anisotropic solid-states without external magnetic field.

The electric current density in the isotropic current solid-states at the presence of the electric field $\vec{E}$, temperature gradient ∇T, electron concentration gradient ∇n, and hydrodynamic motions with velocity $\vec{v}(r, t)$, has the form:

$$\vec{j}=\sigma\vec{E}^*+\vec{\sigma}^1\left[\vec{E}^*\vec{H}\right]-\alpha\nabla\vec{T}-\alpha^1\left[\nabla\vec{T},\vec{H}\right] \qquad (1)$$

$$\vec{E}^*=\vec{E}+\frac{[\vec{v}\vec{H}]}{c}+\frac{T}{e}\frac{\nabla\vec{n}}{n},\ (e>0) \qquad (2)$$

The definition of $\vec{E}$ from formulae (1), taking into consideration the formulae (2), lead to solution of vector equation:

$$\vec{x} = \vec{a} + [\vec{b}, \vec{x}] \qquad (3)$$

in respect of the unknown vector $\vec{x}$.

From formulae (3) we obtain

$$\vec{b}\vec{x}=\vec{a}\vec{b}+[\vec{b}, \vec{x}]=[\vec{b}\vec{a}]+[\vec{b}[\vec{b}\vec{x}]] \qquad (4)$$

Substituting the formulae (4) in formulae (3), we obtain

$$\vec{x} = \frac{\vec{a} + [\vec{b}\vec{a}] + (\vec{a}\vec{b})\vec{b}}{1 + b^2} \qquad (5)$$

Using Maxwell equations $rot\vec{H} = \frac{1\pi}{c}\vec{j}$, taking into consideration the formulae (1,2,5), we obtain the complete electric field at the existence of the external magnetic field and temperature gradient in the isotropic solid-state

$$\vec{E} = \eta\vec{j} + \eta^1[\vec{j}\vec{H}] + \eta^{11}(\vec{j}\vec{H})\vec{H} + \Lambda\nabla\vec{T} + \Lambda^1[\nabla\vec{T}\vec{H}] + \Lambda^{11}(\nabla\vec{T}\vec{H})\vec{H} \qquad (6)$$

Here η is the opposite value of ohmic resistance, Λ is the differential thermoelectromotive force, $\Lambda^1$is the Nernst-Ettingshausen effect.

In the anisotropic solid-state all coefficients in the equation (6) are tensors. Then the equation (6) for the anisotropic solid-state will have the form:

$$E_i = \eta_{ik}j_k + \eta^1_{ik}[\vec{j}\vec{H}]_k + \eta^{11}_{ik}(\vec{j}\vec{H})H_k + \Lambda_{ik}\nabla_k\vec{T} + \Lambda^1_{ik}[\nabla\vec{T}\vec{H}]_k + \Lambda^{11}_{ik}(\nabla\vec{T}\vec{H})H_k \qquad (7).$$

We consider the case, when the external magnetic field $\vec{H}_0=0$. Then in the equation (7), the members, having η^1, η^{11}, Λ^{11} are equal to zero. Added to the equation (7) Maxwell equations, we obtain the following system of equations:

$$\begin{cases} E_i^1 = \eta_{ik} j_k^1 + \Lambda_{ik}^1 [\nabla \vec{T} \vec{H}]_k \\ rot\vec{E}^1 = -\dfrac{1}{c}\dfrac{\partial \vec{H}^1}{\partial t} \\ rot\vec{H}^1 = \dfrac{4\pi}{c}\vec{j}_1 + \dfrac{1}{c}\dfrac{\partial \vec{H}^1}{\partial t} \end{cases} \quad (8)$$

We propose, that all variable values have the plane monochromatic wave character.

Then from formulae (8) we obtain

$$E_i^1 = \left[A\eta_{ik} K_e K_k + B\eta_{ik} + \frac{c\Lambda_{ik}^1}{\omega} K_e \nabla_k T \right] E_k^1 = Z_{ik} E_k^1 \quad (9)$$

$$A = \frac{ic^2}{4\pi\omega}, B = i\frac{\omega^2 - c^2k^2}{4\pi\omega};$$

$$E_i^1 = \delta_{ik} E_k, \delta_{ik} = \begin{matrix} 1, i=k \\ 0, i\neq k \end{matrix}$$

the solution of the equation (9) in respect of the frequency ω is very difficult. That's why we consider the thermomagnetic wave propagation in the transversal ($\vec{k} \perp \nabla \vec{T}$) and longitudinal ($\vec{k} \| \nabla \vec{T}$) directions.

Waves at $\vec{k} \perp \nabla \vec{T}$.

The dispersion equation $|Z_{ik}-1|=0$ after writing on components has the form:

$$(Z_{11}-1)(Z_{22}-1)(Z_{33}-1) + Z_{31}Z_{21}Z_{23} + Z_{21}Z_{32}Z_{13} - Z_{31}Z_{13}(Z_{22}-1) - Z_{32}Z_{23}(Z_{11}-1) - Z_{21}Z_{12}(Z_{33}-1) = 0 \quad (10).$$

Substituting values Z_{ik} from formulae (9) in the formulae (10) for the definition of the frequency ω, we obtain the equation of the form

$$\sum \varphi_i \omega^i = 0, \text{ where } i=0, 1, 2, 3, 4, 5 \quad (11)$$

The values of all φ can be obtained easily from the equation (9). It is impossible to solve the equation (11) in the common case and that is why we will consider the crystals with the concrete symmetry properties in respect of the conductivity σ_{ik} and - λ'_{ik} – Nernst-Ettingshausen effect.

In the crystal $\sigma_{ik}=\sigma_{ki}=\sigma$ and $\lambda'_{21}=\lambda'_{31}$ from the formula (11) at $\vec{k} \perp \nabla \vec{T}$ we obtain:

$$i\frac{48}{\sigma}\omega^2 + \left(i\frac{16\pi^2}{\sigma}\omega_{11}^T - 64\pi^3 \right)\omega - i32\pi^2 \frac{c^2k^2}{\sigma} + 64\pi^3\omega_{21}^T = 0 \quad (12)$$

$$\omega_{11}^T = \Lambda_{11} c k_1 \nabla T, \ \omega_{21}^T = \Lambda_{21} \nabla_2 T \cdot c k, \ k=k_1, \ k_2=k_3=0$$

From the formula (12) after the simple algebra, we obtain

$$\omega_{1,2} = -\frac{1}{3}\left(\frac{\omega_{11}}{2} + i2\rho\sigma \right) \pm (x+iy) = i\omega_0 \pm i\left(\frac{1}{\sqrt{2}} y - 2\pi\sigma \right) \quad (13)$$

$$x = \frac{1}{\sqrt{2}} = \frac{1}{\sqrt{2}} \sqrt{u + \frac{2c^2k^2}{3}};$$

$$y = \frac{1}{\sqrt{2}} \sqrt{u - \frac{2c^2k^2}{3}};$$

$$u = \left[\left(\frac{2c^2k^2}{3} \right)^2 + \left(4\pi\sigma\omega_{21} + \frac{\omega_{11}^2}{18} \right)^2 \right]^{1/2}$$

From the formulae (13) it is seen, that for the increase of waves with the frequency ω_0 the following condition is needed:

$$\frac{1}{\sqrt{2}} y > 2\pi\sigma \quad (14)$$

The inequality (14) executes at any ratio $\frac{\omega_{21}}{\omega_{11}}$ in the crystals

$$\sigma = \frac{\omega_{11}}{4\pi} \quad (15)$$

and needs the execution of the following inequality.

$$16\left[1 + 18\left(\frac{\omega_{21}}{\omega_{11}} \right)^2 \right] > 1 \quad (16)$$

We can to simplify the frequencies of the thermomagnetic wave, taking into consideration the formulae (14-16), and obtain the equation for the real part of the frequency

$$\omega_0 = -\frac{\omega_{11}}{6} + \left(\frac{\omega_{11}\omega_{21}}{2}\right)^{1/2} \qquad (17)$$

As it is seen from the formula (17), the frequency ω_0 is high and changes in the region $\omega_0 > ck$.

Waves at $\vec{k} \| \nabla\vec{T}$.

Substituting the values of Z_{ik} for the longitudinal thermomagnetic waves in the formulae (10) from formula (9) we obtain the equation:

$$\sum F_i \omega^i = 0\,,\ i=0, 1, 2, 3, 4, 5. \qquad (18)$$

However, the values $F_i\left(\omega_{11}^T, \sigma\right)$ is obtained very difficult, that's why we will analyze the existence and conditions of instability of the longitudinal thermomagnetic waves for the crystals, which were investigated in the case $\vec{k} \perp \nabla\vec{T}$.

In the crystals η_{ik}-$\eta_{ki}=\sigma$ and $\Lambda^1_{ik} = \Lambda^1_{ki}$ from the formulae (18), we obtain the dispersion equation:

$$\omega^2 + i\left(\frac{\omega_T}{24} + \frac{4\pi^3\sigma}{3}\right)\omega - \frac{2c^2k^2}{3} = 0, \quad \omega_T = ck\Lambda^1\nabla_1 T \qquad (19)$$

$$\omega_{1,2} = -i\left(\frac{\omega_T}{48} + \frac{4\pi^{33}\sigma}{3}\right) \pm \sqrt{\frac{2}{3}}ck\left[1 + \frac{3}{4c^2k^2}\left(\frac{\omega_T}{48} + \frac{2\pi^3\sigma}{3}\right)^2\right]^{1/2} \qquad (20)$$

It is seen easily from the formulae (20), that waves with the frequencies ω_1 and ω_2 are damped. At $\sigma \approx \frac{ck}{4\pi^3}$ the wave has thermomagnetic character with the frequency

$$\omega_0 \approx 96\omega_T \ . \qquad (21)$$

As it is seen from the formulae (20), thermomagnetic wave with the frequency ω_0 damps very quickly with the increment $\omega_1 \approx \frac{\omega_T}{48}$.

If we consider the thermomagnetic wave propagation in the crystals $\eta_{ik}=\eta_{ki}=\sigma$ and $\Lambda_{23}=\Lambda_{22}$, $\Lambda_{32}=\omega_{33}$, then we obtain the dispersion equation.

$$\omega^2 - \frac{i}{48}\left(\omega_T - 64\pi^3\sigma\right) + \frac{\pi^2}{3}\left(\omega_{12} - \omega_{31}\right)\left(\omega_{22} - \omega_{33}\right) - \frac{2c^2k^2}{3} + i\,\frac{4\pi^3\sigma}{3}\left(\omega_{22} - \omega_{33}\right) = 0 \qquad (22)$$

From formula (22) for the crystals with $\sigma = \frac{\omega_T}{64\pi^3}$ формула we obtain the following expressions

$$\omega_{1,2} = \pm\sqrt{2}\left[\left(R^2 + r^2\right)^{1/2} + i\left(R^2 - r^2\right)^{1/2}\right]^{1/2} \qquad (23)$$

$$R^2 = \left(\Omega^4 + \omega_c^4 + \omega_\eta^4 + \frac{\omega_c^2\Omega^2}{2}\right)^{1/2},$$

$$r^2 = \omega_c^2 + \Omega_1^2\,,\ \Omega^2 = \frac{\pi^2}{3}\left(\omega_{31} - \omega_{12}\right)\left(\omega_{22} - \omega_{33}\right)$$

$$\omega_c^2 = \frac{2c^2k^2}{3}\,,\ \omega_\eta^2 = \frac{4\pi^2\sigma}{3}\left(\omega_{22} - \omega_{33}\right),$$

$\omega_T = \omega_{33}$-ω_{22}-ω_{13}-ω_{21} .

From formulae (23), it is seen, that wave with the increments $\omega_T = \sqrt{2}\left(R^2 - r^2\right)^{1/4}$ increases.

The ratio $\frac{\omega_1}{\omega_0} = \frac{R^2 - r^2}{R^2 + r^2} < 1$ that was needed for the obtaining of the dispersion equation (22). The analysis shows, that wave with the frequency $\omega_0 = \frac{1}{\sqrt{2}}\left(R^2 + r^2\right)^{1/4}$ has the pure thermomagnetic character at $\omega_T \geq ck$. At $\omega_T = ck$ the mixed wave and at $\omega_T < ck$ the electromagnetic wave can be unstable.

For the obtaining of the frequency numerical value of these waves it is needed (in the different crystals) it is needed to know ∇T and Λ^1. In the crystals $\nabla T\Lambda \sim 1$ $\omega_o \sim ck \sim 10^{10}$Herz. It is known, that Gunn semiconductor devices, prepared from the compound GaAs work in the frequency intervals $\omega \sim 10^9 \div 10^{11}$Herz. If we prepare the crystal technologically with data $\nabla T\Lambda^1 \sim 1$, then prepared device on the base of this crystal can change Gunn devices, that is more benefit.

[1] *L.E. Gurevich*. JETF, 1963, 44. (in Russian)

[2] *E.R. Gasimov*. AMEA, Xabarlar, c.XXIII, N5, s.6.

[3] *L.R. Landau i E.M. Lifshits*. "Mechanika sploshnikh sred", M., 1954. (in Russian)

[4] *L.R. Landau i E.M. Lifshits*. "Elektrodinamika sploshnikh sred", M., 1959. (in Russian)

E.R. Həsənov

AİİZOTROP KRİSTALLARDA DAYANIQSIZ TERMOMAQNİT DALĞALARI

Anizotrop kristallarda dayanıqsız termomaqnit dalğaların yayılmvası isbat edtlmişdir. Termomaqnit dalğalarının artma inkrementi hesablanmışdır. Dalğaların yayılma istiqamətləri təyin edilmişdir. Kristallarda bir neçə artan termomaqnit dalğalarının yayılması isbat edilmişdir.

Э.Р. Гасанов

НЕУСТОЙЧИВАЯ ТЕРМОМАГНИТНАЯ ВОЛНА В АНИЗОТРОПНЫХ ТВЕРДЫХ ТЕЛАХ

Показано, что в анизотропных кристаллах распространяется неустойчивая термомагнитная волна. Вычислена частота и инкремент нарастания. Определены направления распространения волн. Доказано, что в анизотропных кристаллах одновременно возможно распространение нескольких нарастающих волн.

Received: 05.04.04

THE NONREFLECTION ABSORPTION OF THE MICROWAVES IN THE SOLUTIONS OF THE ACETONITRIL IN BENZOL

S.T. AZIZOV, M.A. SADICHOV, E.R. KASIMOV, CH.O. KADJAR, R.M. KASIMOV

Institute of Physics of Azerbaijan National Academy of Sciences
Baku, Az-1143, H. Javid ave. 33.

The conditions of nonreflected resonance absorption for the polar dielectric materials with the regular layer thickness are given.

The obtaining and investigation of the materials, absorbing the electromagnetic radiation without its noticed reflection represent the scientific and especially practical interest. The all possible compositional materials, the technology of the obtaining of which is the comparable simple are the most perspective in this connection.

In the ref [1,2] it was shown, that under the certain conditions in the polar dielectrics, having the wave dispersion and carried out on the metallic substrate, the full blanking of the going through electromagnetic radiation, and its reflection from the conducting surface, can take place. However, the experimental discovering of this effect by the direct investigation of the reflected characteristics in the wide frequency band is troubled by the specifications.

Moreover, the probability of the observing the effect of the full absorption of the electromagnetic radiation was proved by the investigations of the dielectric properties and reflection characteristics of the binary solutions of the polar liquids in the unpolar solvents in the band of the centimeter waves [3,4]. It was established, that the full nonreflection wave absorption appears at the defined layer thicknesses and compositions of the solutions at the given incident radiation frequency and solution temperature. As the revealing of the given effect is possible in the solutions, the polar components of which have the dispersion in the microwave wave region, so the carried out its studying as an example binary solutions, which are different on its dielectric properties of the polar liquids in the same unpolar solvent. They could be used for the working on of the technique of the effect observing of the full wave absorption in the polar solutions on its reflection characteristics on the first steps of these investigations. Taking into consideration, that earlier have been investigated the properties of the aceton-benzol solutions, the solutions of the polar acetonitril in the unpolar benzol, dielectric properties of which have been studied enough in the range of the SHF had been chosen as an object.

The investigations were carried out at the wave length λ=1.5 and temperature 20°C, taking into consideration that dispersion region of acetonitril lies in the region of the centimeter and millimeter waves.

The measurements of the reflecting characteristics of the given solutions were carrying out with the use of the panoramic standing-wave meter P2-66 and I2P-67 and short-circuit measured waveguide cell on the end, connected with it. This cell had been thermostating and had the device for the graded regulation of the thickness of the solution layer. The minimum R_{min} were defining in the cell and investigating their dependences on the concentration of the polar component in the solution on the experimentally taken dependences of the wave reflection coefficient R module on the solution layer thickness l in the cell. The quantitative estimation of the dielectric properties of the investigated solutions was carrying out parallelly with the use of the mentioned in the ref [5] the measurement method. This method is based on the definition of the dielectric constant ε' and dielectric loss $\varepsilon''$of the solution on the data of the measurement of the standing-wave ratio and solution layer thickness l in the point of the first minimum of the dependences R on l. The acetonitril and benzol by the kind ХЧА were using as the components of the investigated solutions.

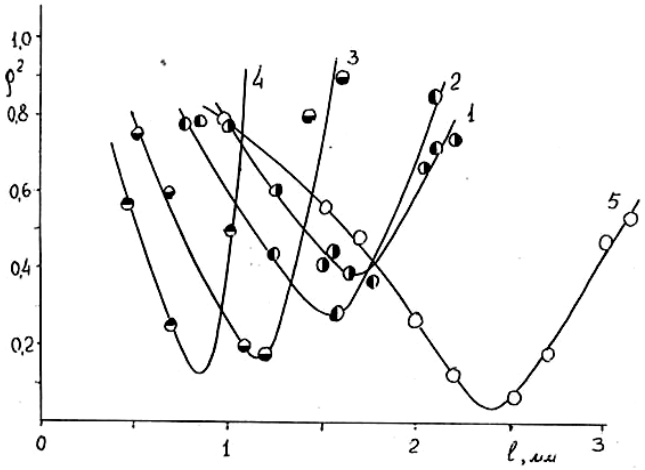

Fig.1. The dependences of the module of reflection wave coefficient R the molecular concentration for the acetonitril-benzol solution at the temperature T=20°C and wave length λ=1,5 cm.

The typical family of the dependences of obtained concentration R_{min} on l for the solutions acetonitril-benzol, obtained at λ=1.5 is given on the fig1. The concentration dependences R of the given solutions have the clear marked zero minimums R_{min}, according to defined values of benzol concentration irrespective of choose of number N of function minimum $R_{min}(l)$. The zero minimum R_{min} of the concentration dependences shifts to the side of the low concentrations of polar component of the solution with N increase. Moreover, the distance between nearest minimums R_{min} decrease and leads to the zero values at big N. At the later increase of benzol concentration in the investigated solution conditions for the appearing of the nonreflected absorption of the electromagnetic waves and at the high values N of function minimums $R_{min}(l)$ will be generating.

Obtained experimental values of the chosen concentrations of acetonitril in benzol are given in the table 1. The selective values φ, obtained by the calculated way with the use of measurement data ε' and ε'' solutions were given also.

The following technique was working for their location. According to the ref [6] the selective values ε' and ε'', at which the full wave absorption in the substance layer takes place, are defined from the following equations:

$$(1+y^2)\cdot\lambda_b/\lambda_g = tg\,(2\pi yx) - y\,tg\,(2\pi x)$$
$$y\cdot sh\,(4\pi yx) + sin\,(4\pi x) = 0, \qquad (1)$$

where $x=l_0/\lambda_g$, $y= tg\Delta/2$; $\Delta= arc\ tg\ \varepsilon''/(\varepsilon'-p)$; $p = (\lambda/\lambda_k)^2$; $\lambda_b=\lambda/\sqrt{(1-p)}$ $\lambda_b = \lambda/\sqrt{(1-p)}$, λ_g, is the length of the electromagnetic wave in the waveguide system, null and fill up by the dielectric correspondingly; λ_k is the critical wavelength of the waveguide; l_0 is the thickness of the substance layer, at which the reflection is absent.

The value l_0, including (1), closes to $(2n-1)\lambda_g/4$ and differs from the last on the small value, depending on the substance properties and number N of dependence minimum R_{min} on l.

As

$$\varepsilon'=p+(\lambda/\lambda_g)^2\cdot(1-y^2);\ \varepsilon''=2y(\lambda/\lambda_g)^2, \qquad (2)$$

so dependences between selective values ε', ε'', $l_0/\lambda g$ have the given type in the coordinate plane [ε', ε''] on the fig.2. The dependence ε'' on ε' increases monotonely with the increase of ε' and at the big values N reaches to the abscissa. The inverse dependence is observed for the functions l_0/λ_g ε' and ε''.

The values ε' and ε'' of the solutions at the different benzol concentrations, obtained in the experiment were using for the construction of the values dependences ε' on ε'' of the corresponding solutions in the same coordinate plane. The coordinates of points of intersection of the experimental and theoretical dependences fig.2 were discovered by the graphical way by their compatibility with the family of the curves selective values ε', ε'', calculated on the equations (1)-(2), and later the corresponding resonance values of benzol concentrations in the solution were observed on them.

As it follows from the table 1 the calculated values of φ are close enough to the experimental ones. The calculated and experimental values of φ for the aceton-benzol solutions, given in the ref [4] are also in the table. They prove the defined influence of the solvent on the effect of the full wave absorption appearance in such solutions.

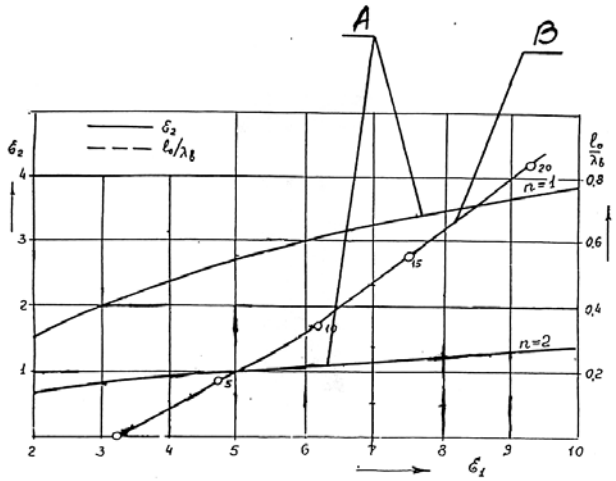

Fig.2. The dependences between values of the dielectric constant ε' and dielectric loss ε'', corresponding to the nonreflected absorption condition of the electromagnetic radiation in the polar substances (A); and obtained experimentally (B) for the acetonitril solution in benzol at temperature T=20°C and wave length λ=1,5cm. The molar concentrations of the polar components of solution in percents.

The studied effect of the selective nonreflected absorption of the electromagnetic waves in the solutions has the common character and can be discovered at the defined selection of the measurement frequency, temperature and composition of the investigated solution.

Table 1

Experimental x and calculated x_p values of resonance polar concentrations of the polar component of solutions of acetonitril and anizol in benzol at temperature 20°C and wave length 1,5 sm.

Solutions ε_0 , τ	acetonitril-benzol		anizol-benzol	
	36,8	3,3	4,39	12,3
	X_P	X	X_P	X
number of zero minimums N	19,4	19,4	-	-
1	7,4	6,6	65,0	63,5
2	4,8	4,6	37,2	34,6
3	3,6	3,4	26,0	24,5
4				

[1] *I. Preissner*. NTZ Arch., 1989, 4, p. 175.

[2] *R.M. Kasimov*. Izmeritelnaya Technika, 1970 , 10, s. 48. (in Russian)

[3] *R.M. Kasimov, M.A. Kalafi, E.R. Kasimov, Ch.O. Kadjar, E.Yu. Salayev*. JETF, t. 66, №5, 1996, s. 167-171. (in Russian)

[4] *E.R. Kasimov, M.A. Kalafi, Ch.O. Kadjar*. Fizika, t. 1, №2, 1995, s. 37-44. (in Russian).

[5] *R.M. Касимов*. Metrologiya, 1987, 7, 45. (in Russian)

[6] *R.M. Kasimov*. Injenerno-fizicheskiy jurnal, 1994, №5-6, t. 67, s 489. (in Russian).

S.T. Əzizov, M.A. Sadıxov, S.R. Qasımova, Ç.O. Qacar, R.M. Qasımov

ASETON BENZOL MƏHLULLARINDA MİKRODALĞALARIN ƏKSOLUNMAYAN UDULMASI

Məqalədə qalinliği tənzim olunan polyar dielektrik materiallar üçün əksolunmayan rezonans udulma şərtləri verilir.

С.Т. Азизов, М.А. Садыхов, С.Р. Касимова, Ч.О. Каджар, Р.М. Касимов

БЕЗОТРАЖАТЕЛЬНОЕ ПОГЛОЩЕНИЕ МИКРОВОЛН В РАСТВОРАХ АЦЕТОНИТРИЛА В БЕНЗОЛЕ

Показаны условия безотражательного резонансного поглощения для полярных диэлектрических материалов с регулируемой толщиной слоя.

Received:

CHARACTER OF DISTRIBUTION OF LOCAL LEVELS IN THE QUASI-FORBIDDEN BAND OF POLYMER PHASE OF POLYMER-PIEZOELECTRIC COMPOSITE

M.A. KURBANOV, S.N. MUSAEVA, E.A. KERIMOV
Institute of Physics of Azerbaijan National Academy of Sciences
Baku, Az-1143, H. Javid ave. 33.

On the basis of the analysis of temperature dependences of electrical conductivity, values of activation energy it is found, that electrothermopolarization results in change of a position of Fermi level in the quasi-forbidden band of a polymer phase of a polymer-piezoelectric composite. Dynamical position of Fermi level, related in it a decrease of an activation energy testify for the benefit of a monotonic distribution of local levels on energy in the quasi-forbidden band of polymer. It is considered, that in process of filling traps Fermi level rises and gets in region of local levels with a smaller activation energy.

The effect of deduction of charges inside volume of a polymer phase at electrothermopolarization of a polymer-piezoceramic composite is caused by presence in energy structure of polymer of set of the located levels being traps of injected charges. Infringements of structure of a polymer phase, conformation of macromolecules, connected with their inevitable deviation from a correct linear arrangement at dispersion polymer by piezoelectric particles are the precondition to this. Really, for a linear polymer circuit it is shown [1], that defect of it, depending on a sign on potential energy, causes eliminating a level from a strip of the allowed states of electron, or from its bottom, or the top edge, in immediate proximity from its space arrangement. Presence of such states in energy structure of polymer causes downturn of potential energy of the entrapped electron (carrier) and, as consequence, its fastening in one of low possible energy states and localization in spatial area which sizes correspond to extent of infringement of potential energy generated this state. Movement of the carrier is probably only by or tunnel jump on other located state with suitable energy, or its activation in area of located states. That the interval of the forbidden energies in polymer is very wide (E~10 eV), both opportunities do not result in the appreciable contribution to mobility of carriers. In immediate proximity from the occupied level there can be a free level with suitable energy, presence of such level far from occupied inefficiently as overlapping of wave functions of such states is not enough and probability of tunnel transition decreases. Activation in area of located states demands rather high energy, approximately 0,5E. To have such energy action with phonons or an electric field practically it is not possible.

Features of distribution of energy levels in the quasi-forbidden band and localization of charges in them, and also the effects connected to them (the piezo-, piroelectric effects) are an object of research of given article. Interest to studying questions touched in the given article is dictated first of all by the purpose of perfection of piezo-, piroelectric properties and an ensure of their stability at various mechanisms of ageing in that physical and chemical conditions which corresponds to conditions of their work.

Composites on the basis of polyvinylidenftoride (PVDF), polypropylene (PP) and piezoceramics of lead-zirconate-titanate families (PZT) such as PCR were investigated. Composites are received by the hot pressing method at temperature 493K and pressure 30 MPa. Composite samples were polarized at the temperature T_p=393K, the electric field intensity E_p=*1÷3MV/m* and time of polarization t_p=0,5 hour.

Let's note, that though in polymer there are carriers of a charge, but it remains good dielectric and the relaxation of charges in it demands big enough time. Consideration of electrothermopolarization process demands composites to understand character of change stationary electrical conductivity of phases by action of a polarizing strong field E_p and the high polarizing temperature T_p, working simultaneously. There are certificates of an opportunity of the electronic mechanism of conductivity of polymer in case of injection of carriers from electrodes and orientation of dipoles under action E_p and T_p [2-4]. By virtue of specificity of the conditions realized at electrothermopolarization of a composite, it is possible to count, that electronic conductivity is inherent in the character of this process. The conditions accompanying of piezo-, piroelectric states of a composite with the generated volume charges are the base of above mentioned. Formation of volume charges is connected to development of the following processes: injection of electrons and their transport to the phase boundary under action E_p; stabilization of electrons at local levels of the quasi-forbidden band of a polymer phase; occurrence of the strong local field acting on piezoparticles. Only injection of electrons, their transport to the phase boundary and the orientation of domains connected to these phenomena in piezophase it is possible to explain formation of high piezo- and piroelectric effects in composites [5-7] (fig. 1 and fig. 2).

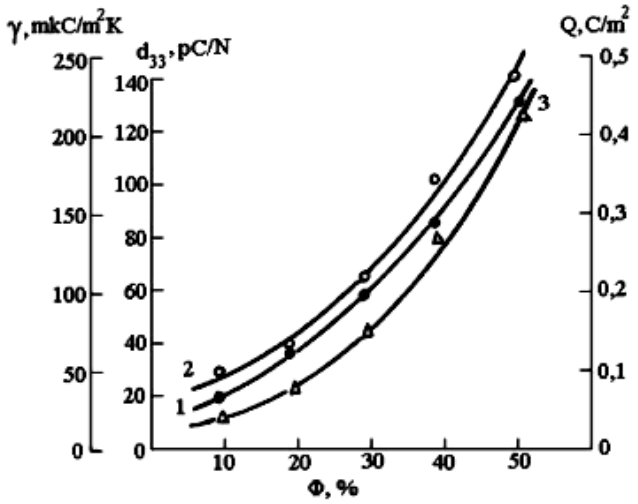

Fig. 1. Dependences of piezomodule d_{33} (1), pyrocoefficient γ (2) and electric charge Q (3) on volume contents Φ of piezoceramics in the composite PVDF+PCR-3M.

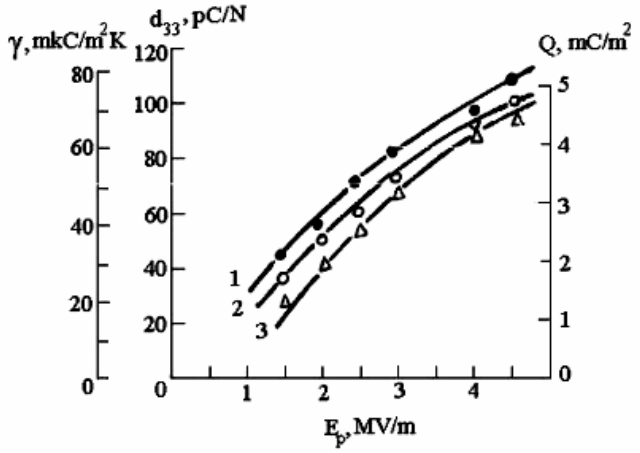

Fig. 2. Dependences of piezomodule d_{33} (1), pyrocoefficient γ (2) and electric charge Q (3) on polarization electric field intensity E_p for the composite PVDF+PCR-3M.

In table 1 values of activation energy W_A, calculated from the temperature dependence of electrical conductivity of the composite PVDF+PCR-3M are presented. It is experimentally found, that at a constancy of time and temperatures of polarization with increase of polarization electric intensity the activation energy decreases (fig. 3). It is possible to believe, that such change W_A is connected to change of Fermi level in the quasi-forbidden band of a polymer phase in process of filling local levels at electrothermopolarization.

Table 1.

Composites	Polarization voltage, V	Activation energy, eV	Piezomodule d_{33}, 10^{-12} C/N
PVDF+PCR-3M	50	0,69	18
	200	0,63	32
	400	0,57	56
	600	0,47	106
PP+PCR-3M	50	0,72	12
	200	0,68	28
	400	0,63	59
	600	0,45	120
PP+PZT-19	50	0,68	10
	400	0,64	48
	600	0,59	66

Let's consider the possible mechanism of this effect. For the disorder structures two models of density of states are known. It is model CFO (Cohen - Fritzshe-Owshinsky) and model Mott [8,9]. In both models there are tails of density of states of conduction and valence bands, coming into the forbidden zone. In model CFO tails of bands can be blocked without qualitative change of the general form of density of states in the field of overlapping. In model Mott tails of bands can not penetrate into the forbidden zone very deeply, however, in this area the peak of density of states to which Fermi level is adhered is formed. At a choice of model for composites at which the polymer phase is disorder, it is possible to use the model CFO. However, in this case it is necessary stability of Fermi level in an interval of energy where tails of bands are blocked also. Thus, in case of model Mott and areas of overlapping of tails of bands enable to allow presence of peak of density, that during polarization where there is a strong injection of carriers of charges, Fermi level should not change. The results of research resulted in the table 1, and also change of values of the injected charges (fig.2) and the activation energy (fig.3) at polarization show, that Fermi level changes after electrothermopolarization. Dynamism of Fermi level testifies that at polarization in a polymer phase charges are stabilized and in process of filling local levels of the quasi-forbidden band of this phase Fermi level rises and gets in area of local levels with rather smaller activation energy. Such it is possible if to assume, that distribution of local levels on energy in the quasi-forbidden band of a polymer phase is monotonous. If to consider models Mott or CFO appreciable change of activation energy and the big accumulation of charges in the quasi-forbidden band of a polymer phase was impossible. Appreciable change of activation energy, and also formation of high piezo-, piroelectric effects and electret states in composites testify for the benefit of monotony of distribution of local levels on energy in the quasi-forbidden band of polymer.

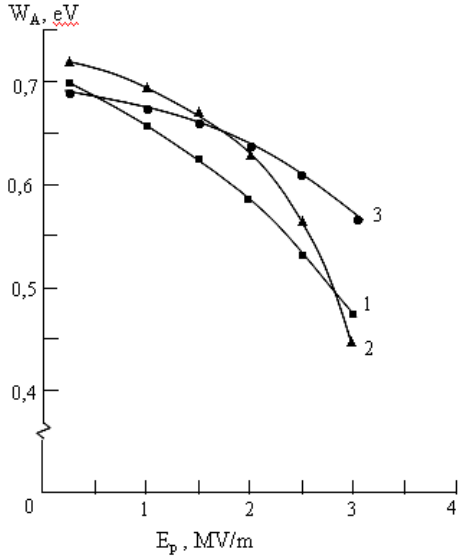

Fig. 3. The dependence of the activation energy on polarization electric field intensity. 1- PVDF+PCR-3M; 2 - PP+PCR-3M; 3 - PP+PZT-19.

Temperature dependences electrical conductivity on the basis of which the activation energy is determined (table 1) and experimental results on piezo-, piroelectric properties of composites (fig. 1, 2) show, that more comprehensible model for polymer - piezoelectric composites is monotonous distribution of local energy levels in the quasi-forbidden band. Really, to growth of concentration of the traps of charge carriers a seized at levels there is a rise of Fermi level and its approach a level of course. In process of rise of Fermi level there is its hit in area of local levels of the big density, but to smaller activation energy of charges in it. Only such distribution of local states on energy will allow the big accumulation of charges on the phase boundary that experimentally proves. All this allows to suppose, that the density of states in the quasi-forbidden band of a polymer phase monotonously falls down from edge of mobility deep into the quasi-forbidden band.

[1] *B. Koiller, H.S. Brandi*. Theoret. Chem. Acta, 1981, v.60, №1, p.11-17.
[2] Electrets. By *G. Sesler's* edition. Moscow, Mir, 1983, 486 p.
[3] *M.E. Borisova, S.N. Koykov*. Physics of dielectrics. Leningrad: LSU, 1979, 240 p.
[4] *M.G. Shaktakhtinsky, M.A. Kurbanov, S.N. Musaeva*. Physics of active composite materials. Materials of the scientific conference, devoted to the 80 anniversary of the president of the Azerbaijan Republic of H.A.Aliyev, IPh ANAS, Baku, 2003, p.155-167.
[5] *M.G. Shakhtakhtinsky, M.A. Kurbanov, A.I. Mamedov, S.N. Musaeva, I.A. Faradzhzade.* The role of the interphase interaction in formation of the properties of polymer-piezoelectric composites. News of ANAS, a series of physical-technical and mathematical sciences, 1999, v. XIX, №6, p, 178-182.
[6] *M.A. Kurbanov, S.N. Musaeva, I.A. Farajzade, R.I. Najafov.* On the role of interphase space charges and their related effects in polymer-piezoelectric composites. Fizika, 2001, v.4, №2, p.71-73.
[7] *M.A. Kurbanov, A.O. Orudzhev, S.N. Musaeva, R.I. Najafov.* On interphase space charges and their related effects in active dielectric composites. Works of the Third International conference «Electrical isolation - 2002», June 18-21 2002, Sankt- Peterburg, p. 78-81.
[8] *N.F. Mott, E.A. Devis*. Electronic processes in non-crystal substances. Moskow: Mir, 1982, 603 p.
[9] *D.S. Sanditov, G.M. Bartenev.* Physical properties of the disorder structures. Novosibirsk: Science, 1982, 368p.

M.Ə. Qurbanov, S.N. Musayeva, E.A. Kərimov

POLİMER-PYEZOELEKTRİK KOMPOZİTDƏ POLİMER FAZANIN KVAZİQADAĞAN OLUNMUŞ ZONASINDA LOKAL SƏVİYYƏLƏRİN PAYLANMA XARAKTERİ

Polimer-pyezoelektrik kompozitlərdə elektrikkeçiriciliyinin temperatur asılılığına və aktivləşmə enerjisinin araşdırılmasına əsasən müəyyən edilmişdir ki, kompozitin elektrotermopolyarizasiyası polimer fazanın kvaziqadağan olunmuş zonasında Fermi səviyyəsinin vəziyyətinin dəyişməsinə səbəb olur. Fermi səviyyəsinin dinamikliyi və onunla əlaqədar olaraq aktivləşmə enerjisinin azalması polimerin kvaziqadağan olunmuş zonasında lokal səviyyələrin enerjiyə görə monoton paylanmasının göstərir. Fərz edilir ki, lokal səviyyələr dolduqca, Fermi səviyyəsi yuxarı qalxır və daha az aktivləşmə enerjisinə malik lokal səviyyələr oblastına düşür.

М.А. Курбанов, С.Н. Мусаева, Э.А. Керимов

ХАРАКТЕР РАСПРЕДЕЛЕНИЯ ЛОКАЛЬНЫХ УРОВНЕЙ КВАЗИЗАПРЕЩЕННОЙ ЗОНЫ ПОЛИМЕРНОЙ ФАЗЫ В КОМПОЗИТЕ ПОЛИМЕР-ПЬЕЗОЭЛЕКТРИК

На основании анализа температурной зависимости электропроводности и значений энергии активации найдено, что электротермополяризация приводит к изменению положения уровня Ферми в квазизапрещенной зоне полимерной фазы композита полимер-пьезоэлектрик. Динамичность положения уровня Ферми и связанное с ней уменьшение энергии активации свидетельствуют в пользу монотонности распределения локальных уровней по энергии в квазизапрещенной зоне полимера. Считается, что по мере заполнения ловушек уровень Ферми поднимается и попадает в область локальных уровней с меньшей энергией активации.

Received: 20.05.04

GÜNƏŞ KONSENTRATORLARININ NORMAL İŞ MÜDDƏTİNİN HESABLANMASI

S. M. MƏMMƏDOV, G. S. QƏMBƏROVA
Azərbaycan MEA Naxçıvan Bölməsi Təbii Ehtiyatlar İnstitutu fiziki tədqiqatlar laboratoriyası
Naxçıvan MR, Naxçıvan şəhəri, Babək küç 10

Günəş şüalarını toplayaraq kiçik ölçülü nümunələri yüksək temperatura qədər qızdırmaq üçün istifadə olunan günəş konsentratorları ancaq müəyyən müddət normal iş qabiliyyətini saxlayır. Məqalədə bu müddətin müxtəlif materiallardan hazırlanmış konsentratorlar üçün hesablanması meodikası verilir.

Çox illər ərzində aparılan hesablamalara görə məlumdur ki, Yer kürəsi il ərzində

Günəşdən orta hesabla $1{,}5\cdot10^{24}$ C enerji alır. [1] Bu o deməkdir ki, planetin sət-hinin hər kvadrat metrinə bir saniyədə təqribən $\sigma_0=150$ C enerji düşür. Bu enerjini sferik güzgüyə əsaslanan xüsusi qurğunun – konsentratorun köməyi ilə toplayıb kiçik ölçülü nümunələri yüksək temperatura qədər qızdırmaq olar. Bu zaman ancaq tədqiq olunan nümunə deyil, həm də konsentratorun özü qızır. Nəticədə müəyyən müddətdən sonra müxəlif termik əmsallara malik olan qayta-rıcı səth və altlıq təbəqənin fərqli genişlənmələri konsentratorun qaytarma əmsalını kəskin aşağı salır. Məsələn, altlıq təbəqənin misdən, qaytarıcı səthin isə alüminiumdan hazırlanması zamanı konsentratorun qaytarma əmsalı yüz saat ərzində doxsan faizlik sabit qiymətini saxlaya bilmişdir. [2] Sonra alüminium təbəqənin əriməsi konsenratorun işini dayandırmışdır. Çox saylı belə faktlar konsentratorun işində hansı metal cütünün daha uzunmüddətli normal işə malik olacağını bilmək zərurətini yaratdı.

Əyrilik radiusu R, diametri d, dərinliyi α olan sferik güzgüdən ibarət konsentratorun normal iş müddətini τ aşağıdakı kimi hesablamaq olar.(şəkil 1)

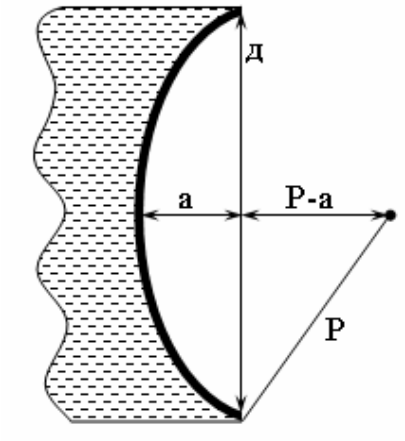

Şəkil 1. Günəş konsentratoru.

Günəş enerjisinin konsentrator tərəfindən qəbul olunan miqdarı

$$Q_1 = \sigma_0 \cdot S_o \cdot \tau \qquad (1)$$

Burada $S_0=\pi d^2/4$ konsentratorun günəş şüalarını qəbul edən kəsiyinin sahəsidir. Qaytarıcı səthdə şüaların udulma əmsalını k ilə işarə etsək, konsentratorda udulan enerji $Q_2=kQ_1$ olar. Udulan enerjinin həm altlıq təbəqə-nin, həm də qaytarıcı səthin qızmasına və nəhayət əriməsinə sərf olunduğunu qə-bul etsək

$$Q_2=c_1m_1(\theta-t)+c_2m_2(\theta-t)+\lambda m_2 \qquad (2)$$

olar.Burada c_1 və c_2 uyğun olaraq altlıq təbəqənin və qaytarıcı səthin xüsusi isti-lik tutumları, m_1 və m_2 isə həmin təbəqələrin kütləleridir; t – konsentratorun ilk temperaturu, θ - son temperaturudur, λ- qaytarıcı səthin materialının xüsusi ərimə istiliyidir. İstilik balansı tənliyində $t = 0$, $c_1m_1 >> s_2m_2$ nəzərə alsaq

$$k\sigma_0S_0\tau = c_1m_1\theta + \lambda m_2 \qquad (3)$$

Burada $k\sigma=\lambda m_2/S$ kəmiyyəti τ müddətində qaytarıcı səthin, $\sigma=c_1m_1\theta/S$ isə altlıq təbəqənin vahid səthinin aldığı enerjini göstərərsə

$$k\sigma_0S_0\tau = (k\sigma + \sigma)S$$

$$\tau = \frac{\sigma(k+1)\cdot S}{k\sigma_0S_0} \qquad (4)$$

olar. Burada S – konsentratorun səthinin sahəsidir. Məlumdur ki, sferik güzgünün baş simmetriya oxunun ən kənar radius ilə əmələ gətirdiyi bucaq φ olarsa

$$S = 2\pi R^2(1-\cos\varphi) = 2\pi R^2\left(1-\frac{R-a}{R}\right) = 2\pi R^2\,\frac{a}{R} = 2\pi aR$$

$$\frac{S}{S_0} = \frac{2\pi aR}{\pi d^2 / 4} = \frac{8aR}{d^2} \qquad (5)$$

olar. Bu ifadələri (4) – də nəzərə alsaq

$$\tau = \frac{8\sigma(k+1)aR}{k\sigma_0 d^2} \qquad (6)$$

Vahid səthə düşən enerjinin σ təyinindən göründüyü kimi

$$k\cdot\frac{c_1 m_1\theta}{S}=\frac{\lambda m_2}{S}; \quad k=\frac{\lambda m_2}{c_1 m_1\theta} \qquad (7)$$

Nəzərə alsaq ki, $m_2=\rho_2 v_2=\rho_2 x_2 S$ və $m_1=\rho_1 v_1=\rho_1 x_1 S$

$$k = \frac{\lambda\rho_2 x_2}{c_1\rho_1 x_1\theta} \qquad (8)$$

olar. Burada x_1 – altlıq təbəqənin, x_2 – isə qaytarıcı səthin qalınlığıdır. göründüyü kimi $x_1 >> x_2$ olduğundan $k<<1$ olur. ona görə də (6) ifadəsini

$$\tau = \frac{8\sigma aR}{k\sigma_0 d^2} \qquad (9)$$

kimi yazmaq olar. Verilmiş konsentrator üçün α, R və d – ni xətti ölçmələr vasi-təsilə σ - nı isə

$$\sigma = \frac{c_1 m_1\theta}{S} = c_1\rho_1 x_1\theta \qquad (10)$$

ifadəsindən təyin etməklə iki növ materialdan hazırlanmış konsentatorun minimal normal iş müddətini hesablamaq olar.

Nəzəri və eksperimental nəticələrin nə dərəcədə uzlaşmasını görmək üçün təklif olunan metodika ilə mis və alüminiumdan ibarət olan konsentratorun normal iş müddətini hesablayaq.

Bu zaman konsentratorun konveksion soyumasını nəzərə almayacağıq. Çünki soyuma prosesi normal iş müddətini ancaq artıra bilər. Cədvəl məlu-matlarına görə

$$\lambda = 3{,}9\cdot 10^5 c/kq,$$
$$\rho_2 = 2{,}7\cdot 10^3 kq/m^3,$$
$$\rho_1 = 8{,}9\cdot 10^3 kq/m^3,$$
$$c_1 = 380\, c/kq\cdot K,$$
$$\theta = 650^0 S,$$

konsentratorda aparılan xətti ölçmələrə görə

$$a=3\cdot 10^{-3} m,\quad R=2\cdot 10^{-2} m,\quad d=3\cdot 10^{-2} m,$$
$$x_1=3\cdot 10^{-3} m,\quad x_2=2\cdot 10^{-4} m$$

(8), (9) və (10) düsturlarında bu qiymətləri nəzərə alsaq $\tau\approx 250$ (saat) olar.

Əgər konsentratorun normal işində soyuma prosesinin iki dəfə müddəti ar-tırdığını qəbul etsək, onda təcrübi və nəzəri nəticələrin uzlaşdığını görərik. Soyuma və qızma proseslərinin bərabər ehtimallı olması bu nəticəni çıxarmağa imkan verir.

.

[1] Gnerqetiçeskaə proqramma SSSR, izd. «Znanie», Moskva 1986

[2] İspolğzovanie solnüa i druqix istoçnikov luçistoy gnerqii v materialo-vedenii. Kiev, naukovaə dumka, 1983.

С. М. Мамедов, Г. С. Гамбаров

ВЫЧИСЛЕНИЕ ВРЕМЕНИ НОРМАЛЬНОЙ РАБОТЫ СОЛНЕЧНЫХ КОНЦЕНТРАТОРОВ

В статье объясняется уменьшение коэффициента отражения солнечных лучей при нагреве солнцем самого концентратора. Дается методика вычисления времени нормальной работы концентратора, если заранее известно из каких материалов он состоит.

S.M. Mamedov, G.S. Gambarova

CALCULATION THE TIME OF NORMAL WORK OF THE SUN CONSENTRATORS

In this paper the increase of the coefficient of the reflection of sunrays by heat of own concentrator of sun is explained. The technique of the calculation of normal work time of sun concentrator, if its composition is known, is given.

Received: 05.02.04

ELECTRON DIFFRACTION INVESTIGATION OF PHASE TRANSITIONS IN $A^3B^3C_2^6$ COMPOUNDS

D.I. ISMAILOV
Institute of Physics, Academy of Sciences of Azerbaijan
Az-1143, H. Javid av., 33, Baku.

By electron diffraction investigations peculiarities of film formation of $A^3B^3C_2^6$ group compounds have been established. It is shown that the interval of amorphous film compositions obtained at room temperature is much higher than the interval in massive samples. There have been determined kinetic parameters of phase transformations in amorphous films $TLInSe_2$, $TLGaSe_2$ and $TLInS_2$ obtained under the usual conditions and the influence of external field. There have been established 3 superstructural phases of $TLGaSe_2$ and $TLInTe_2$ compounds, two of them are formed as a result of epytaxial growth of $TLGaSe_2$ for NaCl and one of $TLInTe_2$ compound for KCl.

In $A^3B^3C_2^6$ system there have been formed a number of ternary compounds $TlInSe_2$, $TlInS_2$, $TlInTe_2$, $TlGaSe_2$, $TlGaS_2$, $TlGaTe_2$ having special physical properties which are the results of strong anisotropy of bond forces between atom groups [1]. Structural characteristics of bulk samples concerning the group of semiconductor materials with the common formula $A^3B^3C_2^6$ are given in table 1. There are a great number of works dedicated to different properties of these compounds. On the basis of the mentioned semiconductor materials there have been created sensitive elements of photodetectors, detectors of optic radiation, strain gauges and etc.

It is known that physical properties and in some cases the structure of semiconductor films obtained by vacuum evaporation differ from the properties of the single crystals of the corresponding composition .Many problems related to the diagram of state and phase equilibrium of $A^3B^3C_2^6$ system compounds are unsolved so far. Therefore, the investigation of phase formation, phase transformations and features of thin films substructures of abovementioned compounds obtained by vacuum condensation are of high-priority.

I Phase composition of Tl-In-Se system.

According to data [12-13] in Tl-In-Se system at TlSe-InSe in the 1:1 ratio there have been found $Tl\ InSe_2$ compound. *X* – ray data [14-17] of some phases formed in TlSe-InSe system are contradictory. In [14] it is noted that In_2Se_3 has a low – symmetric structure, so author can not induce the debaegram. In [17] the possibility of In_2Se_3 existence in two modifications has been established, in [15-16] it is stated that In_2Se_3 has at least three different modifications: α, β and γ. They are resistant: α - at room temperature, β- over 473 K and γ - 779-873K. At present determination of crystal structure of α-and β - modifications is considered to be finished.

Table 1. Structural parameters of thallium chalcogenides.

Description	Singony	Space group	Lattice periods and angles in degrees (nm)				Number of formula units (Z)	Note	References
			a	*b*	*C*	β			
1	2	3	4	5	6	7	8	9	10
$TlGaSe_2$	tetra-gonal	I4/mcm	0,7620		3,0500		16		[2]
$TlGaSe_2$	tetra-gonal	I4/mcm	0,8053		0,6417		4	Faze of high pressure	[3]
$TlGaSe_2$	mono-clinic	$C_s^4 or C_{2h}^6$	1,0770	1,0770	1,5620	100°	16		[4]
$TlGaSe_2$	mono-clinic	$P2_1/m$	0,7260	0,7270	1,4900	90°20′	8		[5]
$TlGaSe_2$	mono-clinic	$Cc(C_s^4)$	1,0772	1,0771	1,5636	100°6′	16		[6]
$TlGaS_2$	tetra-gonal	I4/mcm	0,7290		2,9900		16		[2]
$TlGaS_2$	mono-clinic	$P2_1/m$	0,7000	0,7600	6,2720	90°20′	32		[7]
$TlGaS_2$	mono-clinic	$C_s^4 or C_{2h}^6$	1,0400	1,0400	1,5170	100°	16		[4]
$TlInS_2$	tetra-gonal	I4/mcm	0,7740		3,0030		16		[2]

$TlInS_2$	tetra-gonal	I4/mcm	0,8000		0,6720		4	α-mod	[8]
1	**2**	**3**	**4**	**5**	**6**	**7**	**8**	**9**	**10**
$TlInS_2$	tetra-gonal	I4/mcm	0,7680		2,9760		16	β-mod	[8]
$TlInS_2$	mono-clinic	$C_s^4 or C_{2h}^6$	1,0950	1,0950	1,5140	100°	16		[4]
$TlInS_2$	mono-clinic	$P2_1/m$	0,7760	0,7760	3,0010	90°15′	16	β-mod	[9]
$TlInS_2$	Hexa-gon	P6/mcm	0,7670		1,4980		8	α-mod	[9]
$TlInS_2$ – II	hexa-gon	P3m	0,3830		2,2230		3	Faze of high pressure	[10]
$TlInS_2$ –III	Hexa-gon	P6/mcm	0,3830		1,4880		2		[10]
$TlInS_2$	Rhom-bic	D_6^2	0,6560	0,3810	1,4940		4		[4]
$TlInSe_2$	tetra-gonal		0,8075		0,6847		4		[11]
$TlInSe_2$	tetra-gonal		0,8494		0,7181		4		[11]
$TlInSe_2$	tetra-gonal		0,8429		0,6865		4		[11]

Existence of thallium selenides have been pointed in the diagram of Tl-Se system state: Tl_2Se (16,19 weight % of Se, $T_{m(melting)}$ = 563K); TlSe (27,28 weight % of Se; $T_{m(melting)}$ = 661K) and Tl_2Se_3 (36,69 weight % of Se). Tl_2Se_3 is melted over the temperature range 547-553 K and has two points of transformation at 445K and 465K [18-19]. Existence of TlSe and Tl_2Se compounds is confirmed by *X*-ray analysis, however, it is not confirmed for Tl_2Se [14,20]. According to electronographic data [21] TlSe is crystallized in tetragonal lattice with constants: a = 0,852; c = 1,268 nm. In Tl-Se system composition of stoichiometric composition TlSe [22] is the most resistant and of interest as semiconductor.

II Phase composition of films Tl-In-S system.

In Tl-S [18] according to the results of thermal and *X*-ray investigations there have been established four stoichiometric compounds: Tl_2S, Tl_4S_3, TlS and TlS_2. Only the phase of the Tl_2S composition has a congruent melting point (623K). In papers [23-24] it is established that there are intermediate phases in Tl-S system: Tl_2S_5 (28,6 at % of Tl), Tl_8S_{17} (32,0 at % of Tl), TlS (50,0 at % of Tl), Tl_4S_3 (57,1 at % of Tl) and Tl_2S (66,7 at % of Tl). With the regard of data [23-24] in [25] there have been given specified version of diagram of Tl-S system state. Phase Tl_8S_{17} in case of long storage at room temperatures and annealing breaks down into Tl_2S_5 and TlS phases. In [25] there have been confirmed existence of Tl_2S_5 which was under suspicion in [18]. Phase Tl_2S_5 is formed peritectically from Tl_8S_{17} and sulphur. In [26] there have been pointed to the production of massive amorphous samples of TlS composition. In [2,4,8-9] existence of phase of $TlInS_2$ composition of different modification has been established.

Solid phases of In-S system are investigated in sections In-In_2S_3. Obtained results show that In_3S_4 does not exist independently and appears in the region of solid solution on the base of In_2S_3(56,3 ÷ 60,0 at % of S) at 873K and 54,5 ÷60,0 at % of S at 973K. In [28] there have been found In_2S as a primary component – pair being in equilibrium with In_2S. Melting temperature of In_2S_3 is 1368K [29]. In [30-31] phase β-In_2S_3 with tetragonal cell period is established: a = 0,7620 nm; c = 3,2300 nm relating to progressive symmetry I4/amd, with 16 formula units in elementary cell and being of non-ordering modification α-In_2S_3 is.

III Phase composition of films of Tl-In-Te system.

According to state diagram in Tl-Te system the following phases are: Tl_2Te_3, TlTe, Tl_2Te and α - phase (Tl_5Te_3) [14,32-36]. There have been contradictory evidence about Tl_2Te. In [32-34] Tl_2Te phase is not revealed, in [14] existence of Tl_2Te phase on the base of *X*-ray analysis of Tl and Te alloys is expected. The presence of Tl_2Te phase in Tl-Te system is established by thermodynamic and roentgen investigations, and microhardness [35-36]. The structure of Tl_2Te compound is not coded. Contradictory data about the existence of Tl_2Te phase can be explained by complexity of preventing of oxidative processes during the work with Tl and its compounds, particularly with Tl_2Te. In fact, authors [35] point to the instability of Tl_2Te phase in the air. According to data [37], thallium hydroxide remaining in Tl_5Te_3 alloy as a pollution in synthesis process prevents crystal growth. Data [14,32-37] by Tl-Te system relate to massive samples with the exception of [38] where films of Tl_5Te_3 composition are formed at evaporation of Tl_2Te alloy.

By chemical and metallographic analysis of samples obtained by zone melting there have been found intermediate compounds In_3Tl_4 and In_3Tl_5 [39]. Formula In_9Tl_7 is assigned to intermediate compounds of in rich content. By investigations [40] existence of In_3Tl_4 is confirmed. Melting temperature of In_3Tl_4 is 938K. In [41] there have been determined InTe and In_2Tl_3 compositions; 50,8±0,1 at. % of Te and 59,7±0,1 at.% of Te, respectively. On the base of *X*-ray analysis it is suggested that range of homogeneity of high–temperature modification In_2Tl_3 (β-In_2Tl_3) is more than low-

temperature modification (α-In_2Tl_3) and unequality undergoes eutectoid decay.

Structure of ternary compound $TlInTe_2$ is determined roentgenographical [11], its melting point (T_m) is 1045K, density (ρ) is 9,31 g/cm^3 [42]. The aim of this paper is the determination of phase composition of Tl-In-Se (S,Te) systems in thin films formed at vacuum condensations of components, determination of kinetic parameters of phase transformations in $TlInSe_2$, $TlGaSe_2$, $TlInS_2$ obtained as at normal conditions of deposition of molecular beam in electric field. There have been considered possibilities of phase transitions from one modification into another and also formation of superlattices of matching one or another phase and not found in massive samples of $TlGaSe_2$, $TlInTe_2$ compositions.

Experimental details.

I. Phase composition of films of Tl-In-Se (S,Te) system is investigated at the component condensation on the substrate of NaCl crystals in vacuum $3\cdot10^{-4}$ Pa. Three sources are placed along the condensation plane so that Tl and In samples are set in outer ones. Distance between samples is 13 cm from each other and they are at the height of 7 cm above condensation plane. The third source with Se (S and Te) is located at the height of 8 cm above the average point of condensation plane between Tl and In sources.

Investigation of films of Tl-In-Se system (S,Te) is of experimental difficulties connected with the oxidation of Tl in the contact with air on the one hand, and with the evaporation of Se (S and Te) by heating in vacuum on the other hand. For prevention of highly evaporating component and oxididatie processes as a result of further thermal treatment of films they are placed in carbon capsules. Preliminary carbon film is applied on the substrate surface of single crystals NaCl by the method of vacuum deposition, then investigated subject is deposited and carbon is applied above again. Maximum thickness of films with the regard of carbon ones does not exceed 50 nm. Phase composition of forming films under the condition of simultaneous and sequential deposition of Tl, In and Se (S and Tl) has been studied by electron- diffracting method for passage on devices ZG, ZGR – 102.

II. Kinetics of phase transitions in thin amorphous films $TlInSe_2$, $TlGaSe_2$, $TlInS_2$ condensed under normal conditions and under the conditions of effect of external electric field has been studied by method of kinematical electron-diffraction examination on device ZG. Amorphous films of $TlInSe_2$, $TlGaSe_2$, $TlInS_2$ compounds for investigation of crystallization kinetics are produced by evaporation of $TlInSe_2$, $TlGaSe_2$, $TlInS_2$ alloy cuts in vacuum ~10^{-4} Pa from tungsten helical tapered furnaces. Small newly made spalls of rock salt are as substrates. The calculated thickness of films applied on crystals NaCl with the rate 1,5 nm/c is ~ 30 nm.

Electric field with strength 3000 v.cm^{-1} is between parallel copper plates with the high – voltage rectifier. Substrates are arranged on the surface of the negative-charged plate. There have been hole in diameter of 5 mm in the upper plate through which molecular beam can pass and reach substrate surface.

Results and their discussions.

I. Phase formation in thin films in Tl-In-Se (S,Te) systems.

1. Electron-diffracting analysis of forming films in Tl-In-Se system showed that at simultaneous evaporation of Tl, In, Se along the condensation plane amorphous films are formed. Values of $S=4\pi Sin\theta/\lambda$ corresponding to diffusion rings on electron-diffraction photographs are given in Table 2.

Table 2. Characteristics of phases of Tl- In- Se systems.

Description	Diffusional ring	S= 4πsinθ/λ (nm^{-1})	Crystal system	Space group	Lattice periods and angles in degrees (nm)			References
					A	*b*	*c*	
Tl_2Se	1 2	21,40 32,90	tetragonal	C_{4h}^3 *P4/n*	0,8520	-	1,2680	[21]
TlSe	1 2 3 4	21,50 33,90 42,90 52,10	tetragonal	I4/mcm	0,8010	-	0,7000	[20]
$TlInSe_2$	1 2 3	20,60 33,90 50,40	tetragonal	I4/mcm	0,8075	-	0,6847	[11]
In_2S_3	1 2 3 4	19,50 32,00 54,00 65,00	cubic initial	-	1,0100	-	-	[43]
InSe	1 2 3	20,00 33,20 60,00	hexagonal	R3m	0,4046	-	2,4960	[44]
In_4Se_3	1 2 3	22,30 40,00 51,50	rhombic	Pnnm	1,5297	1,2308	0,4081	[45]

Crystallization of amorphous films allows six differences according to phase composition and structure Tl_2Se, TlSe, $TlInSe_2$, In_2Se_3, InSe and In_4Se_3 to be established. Crystallization of Tl_2Se and TlSe films are taken place at

493K and 363K, respectively. Ternary compound $TlInSe_2$ is crystallized at 443K. Obtained amorphous films are crystallized on the base of tetragonal crystal system.

By thermal heatment of amorphous phase In_2Se_3 the latest is crystallized in cubic crystal system [43] at 473K. At 653K there have been observed phase transition into lois-symmetric phase described in [43] too. Symmetry of this modification is not revealed yet, it is kept up to 1123K. Above 1123K there have been taken place film melting in capsule. Transition temperature from amorphous into crystalline phase for compounds InSe and In_4Se_3 is 413K and 433K, respectively. Mentioned phases are induced on the base of two crystal systems given in table 2.

Crystallization temperature of films is determined with the accuracy ±5K. We pay attention that amorphous film of Tl_2Se composition is not formed at interaction of Tl and Se [46]. In this case stablization of amorphous state can be explained by the presence of In impurity. It is known that the prescuse of In in Se (up to 10 at.%) retards crystallization process [47] with the formation of rather strong bonds. As it is seen from the given data amorphous formations in films obtain compositions from Tl_2Se up to Se whereas in massive samples they are limited from Tl by composition «$TlSe_2$» [48-49].

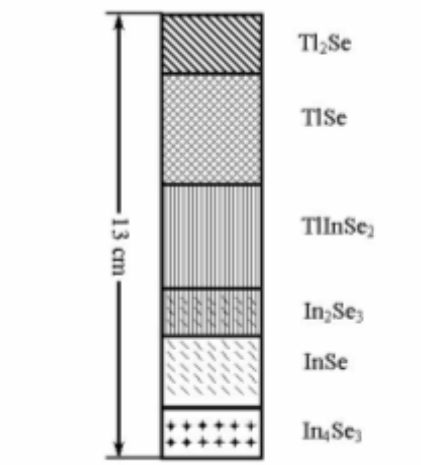

Fig. 1 . Diagram of phase distribution in condensation plane for Tl-In-Se system .

At sequential deposition of Tl, In and Se in vacuum in dependent on evaporation order of phase composition of films does not differ from the case of simultaneous deposition of components. Range extent of forming phases (fig.1) at simultaneous and subsequent depositions of components is similar.

2. There have been formed six amorphous and one crystalline phase at simultaneous evaporation of Tl, Se and In on substrates at room temperature.

Structural characteristics of crystalline phases and values of $S=4\pi Sin\theta/\lambda$ corresponding to diffusion lines on electron – diffraction photographs of amorphous phases – 1) Tl_2S, 2) Tl_4S_3, 3) TlS, 4) Tl_2S_5, 5) $TlInS_2$, 6) In_2S_3 are given in Table 3.

By thermal treatment of films of the first and second amorphous phases there have been formed polycrystalline Tl_2S and textured Tl_4S_3. Annealing of correspon-ding amorphous film at 435K leads to formation of textured TlS. The fourth amorphous phase observed in region abounding in S has been realized by prolonged heating below 373K. This process causes transition of amorphous phase into crystalline with the structure of red Tl_2S_5. Crystallized samples as in case Tl_4S_3 and TlS are textured. Amorphous films of ternary compound of composition $TlInS_2$ and β-In_2S_3 are crystallized at 443 and 433K, respectively. Crystalline phase being formed at simultaneous evaporation of Tl, S and In gives textured diffraction pattern with unsharp lines. Further recrystalline annealing at 100 leads to texture perfection. The comparison of electron-diffraction photographs with powdergram for Tl_8S_{17} [24] allows to consider that crystalline phase has the same composition. Except main diffraction lines coinciding with lines given [24] on electron – diffraction photographs there have been observed weak lines (altogether 40 reflections). Diffraction pattern is induced on the base of primitive cubic lattice with elementary cell parameter a=1,0600 nm.

Taking into consideration that average volume falling at one atom in elementary cell for tallium sulfides V = 2,6600 nm^3 we find that a number of structure unity in elementary cell for Tl_8S_{17} is $z \approx 2$. And calculated value of density $\rho_{calc.}$= *6,0 g/cm*^{3} is well coincided with data for TlS_2 ($\rho_{calc.}$=*5,8 g/cm*^{3}) [50].

Thermal treatment of Tl_8S_{17} films showed that unlike massive samples [24] the films are stable up to 393 K. Further rise of temperature brings about mechanical destruction of films.

Table 3. The structural characteristics of crystal phases and values $S= 4\pi\sin\theta/\lambda$ of amorphous phases of systems Tl-In-S.

Description	**Diffusional ring**	**S= 4πsinθ/λ (nm^{-1})**	**Crystal system**	**Space group**	**Lattice periods and angles in degrees (nm)**				**Note**	**References**
					A	b	c	β		
Tl_2S	1 2 3	14,22 22,01 34,14	hexa-gonal	R3	1,2200	-	1,8170			[18]
Tl_4S_3	1 2	22,03 37,63	monoclinic	$P2_1/a$	0,7720	1,2980	0,7960	103°50′	β-modification	[51]
TlS	1 2 3 4	17,84 21,52 34,31 54,12	tetra-gonal	I4/mcm	0,7790	-	0,6800	-		[14]

TlS_2	-	-	tetra-gonal	$P4_2/nmc$	2,3200	-	5,4800	-		[50]
Tl_2S_5 (red)	1 2 3	14,41 22,03 43,02	rhombic	$P2_12_12_1$	0,6660	0,6520	1,6750	-		[14, 24]
Tl_2S_5 (black)	-	-	rhombic	Pbcn	2,3450	0,8800	1,0570	-		[14]
$TlInS_2$	1 2 3	20,32 26,06 38,43	monoclinic	$P2_1/m$	0,7760	0,7760	3,0010	90°15′	β-modi-fica-tion	[9]
In_2S_3	1 2 3	8,55 27,73 40,62	tetragonal	$I4_1/amd$	0,7620	-	3,2300	-	β-modi-fica-tion	[30, 31]

Decomposition of Tl_8S_{17} massive samples by treatment appears to be connected with partial change of composition at the expense of S (sulphur) volatility that doesn't take place in investigated films placed in coaly capsule up to 393K. Above this temperature vapour pressure of S increases highly inside the capsule and the latter is destroyed with film together.

We note that two phase regions consisting of mixture of mentiond phases are observed on the substrate. At sequential deposition of Tl and S independent on deposition order, on condensation plane by film interaction at room temperature there have been formed four amorphous phases at first: Tl_4S_3, TlS, $TlInS_2$ and In_2S_3. Sample treatment at 373-443K initiates film crystallization and besides mentioned phases another phase of Tl_2S is revealed. Tl_4S_3 and TlS composition phases are textured. Texture axis (axis C) is perpendicular to substrate surface.

3. Electron-diffractometry analysis of films deposited at simultaneous evaporation of Tl, In and Te showed that on condensation plane there have been formed phases known from state diagram of Tl-Te, In-Te and one ternary compound of $TlInTe_2$ composition. On electron-diffraction photograph of film forming in the vinicity of Tl source there have been revealed about 40 diffraction lines. Its calculation and comporison of experimentally obtained interplane distances with *X*-ray data [35] shows the presence of Tl_2Te phase which we induce on the base of primitive cubic lattice with a=1,2620 nm. Tl_2Te phase is formed in a very narrow experimentally hard – established region of composition.

In region enriched in Tl (according to calculation up to 85 at.% of Tl) there have been observed phase with facecentered cubic lattice, space group $F4_132$ a=1,2620 nm which composition we do not establish. This phase is not stable and at 403K it goes over the phase with primitive cubic lattice with the same parameter of elementary cell. With the increase of Te content in the vinicity of Tl_2Te phase there have been observed wide region where γ-phase (Tl_5Te_3) has been found. Electron – diffraction photograph of this phase is well induced on the base of familiar tetragonal lattice with parameters a=0,8920; c=1,2630nm. Thus in thin films both Tl_2Te phase and γ-phase of Tl_5Te_3 composition are realised.

In region enriched in Te there have been observed tetragonal TlTe with parameters of elementary cell a=1,2950; c=0,6180 nm which are in agreement with data [33] and Tl_2Te_3 phase of familiar monoclinic structure with a=1,3500; b=0,6500; c=0,7900nm, β=73° [33]. On condensation plane there have been revealed presence of $TlInTe_2$ ternary compound films with constants of tetragonal lattice a=0,8494; c=0,7181nm [11] and familiar: hexagonal In_2Te_5 with constants of elementary lattice a=1,3270; c=0,3560nm [40] and rhombic In_2Te with a=0,4450; b=1,2580; c=1,5360nm [52]. At sequential deposition of Tl, In and Te substantially different results are not found. Phase composition of films on condensation plane is as in case of simultaneous deposition of components.

II. Crystallization kinetics of amorphous films of $TlInSe_2$, $TlGaSe_2$ and $TlInS_2$.

Study of formation process of kinetics growth and crystallization of semiconductive material films is of great interest for semiconductive science material. The difficulty in study of these problems is that the growth mechanism is unknown. Evidence of growth mechanism and dependence of rate of crystallization on temperature can be obtained by considering temperature – time dependence of film crystallization.

Thermodynamic conditions of new phase formation are established in [53]. Common equation describing kinetics of phase transitions running with the formation of centres of new phase and their subsequent growth providing for statistical character of overlapping centres of increasing phase has been obtained in [54]. Kinetic equation [54] is the general for describing the kinetics of growth as in case of constant speed of originating as in intermediate cases (decreasing speed of originating)

.

$$V_t = V_0[1- exp(-kt^m)] \quad (1)$$

where V_t- fraction of substance volume undergone transformations to moment t, V_0 - initial volume, k – constant of reaction rate. Value m is different for possible types of transformation and depends on measuring of growth. On the base of m exponent value one may infere about possible mechanism of transformation. However it should be noted that for production of reliable results with this theory we must have exact experimental data about value V_t.

Amorphous films $TlInSe_2$ in thickness ~30,00 nm applied by evaporation of synthesized substance on crystals NaCl at room temperature have amorphous structures. Amorphous phase is found in the temperature range of substrate from room temperature up to T_s=403K. On electron – diffraction photographs there have been observed three diffusion rings corresponding to $S=4\pi sin\theta/\lambda$=2,060; 3,390; 5,040nm^{-1} given in fig.1.

Crystallization of amorphous films at 423K leads to formation of polycrystalline tetragonal $TlInSe_2$ being in the agreement with the data of paper [11] .

For determination of kinetic parameters of crystallization from amorphous films $TlInSe_2$ there have been obtained isothermic kinematical electron – diffraction photographs at 403K, 418K, 433K and 453K. We understand that the higher temperature the quicker transition from amorphous state to crystalline is taken place. In case of film overheating at above 453K sharp phase transition is occurred. On kinematical electron-diffraction photographs obtained at mentioned temperatures it is seen that diffusion lines of amorphous phase disappear and lines of crystalline phase $TlInSe_2$ arise. One of these electron – diffraction photographs measured at 433K is given in fig.2.

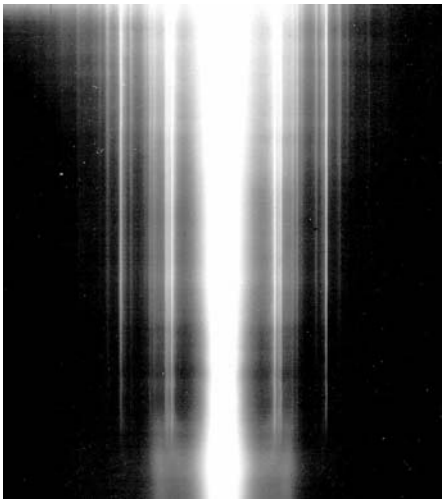

Fig. 2. Kinematical electron-diffraction photograph showing crystallization of $TlInSe_2$ at 433K.

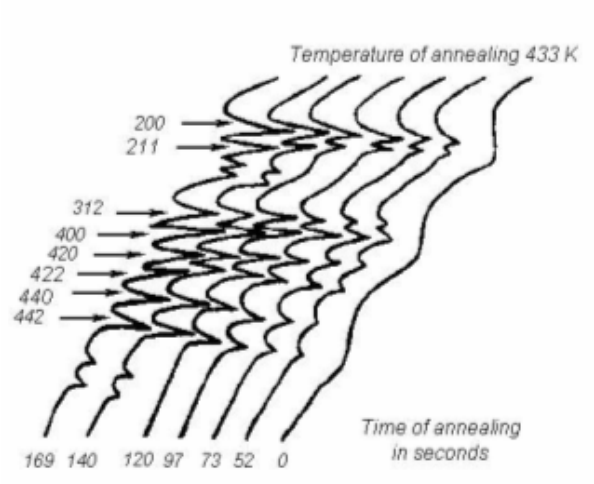

Fig. 3. Microphotographs of isothermal electron-diffraction photograph of $TlInSe_2$ at 433 K. Figures at curves annealing time (sec.)

Region of existence of both phases has been followed. Line intensities of increasing crystalline phase of $TlInSe_2$ corresponding to different time moments are microphotometrically determined. In fig.3 microphotographs of kinematical electron-diffraction photographs measured at 433K are shown. There have been determined diffraction line intensities (200), (211), (312), (400), (420), (422), (440), (442) of crystalline $TlInSe_2$ depending on annealing time. Transition from intensity value to quantity of crystallized substance are carried out by normalization taking into account that in kinematical approximation electron scattering intensity is in proportion to the volume of scattering substance according to paper [55]. In the investigated temperature range there have been carried out kinetic curves of crystallization of amorphous $TlInSe_2$, i.e. dependence of volume of crystallized part of $TlInSe_2$ on time at various temperatures (fig.4).

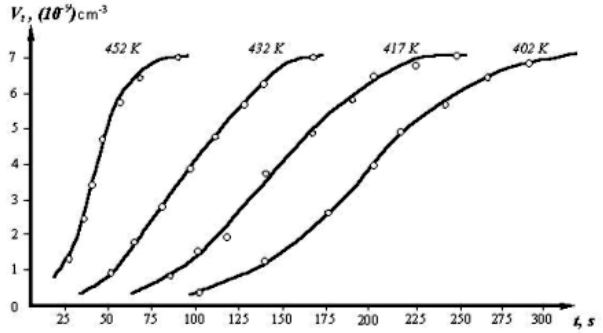

Fig. 4. Kinetic curves of $TlInSe_2$ crystallization. Values of T_c. 1-403, 2-418, 3-433, 4-453K.

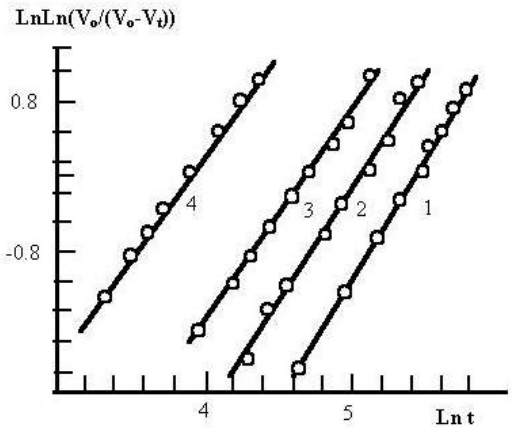

Fig. 5. Dependence of $lnln(V_0/V_0-V_t)$ *on lnt*

There have been carried out dependences $lnln(V_0/(V_0-V_t))$ on *lnt* for 403K, 418K, 433K and 453K (fig.5). Experimental points are arranged on straight lines for all temperatures. Value of "m" exponent in equation (1) determined from shift of given straight lines appeared to be close to three points (m=2,68; 2,73; 2,90 for 453K, 433K, 418K and 403K). It points out that in case of crystallization of amorphous films $TlInSe_2$ in the investigated temperature range two – dimensional growth of chips is taken place. In this case constant k appearing in formula (1) is equal to $1/3\ \pi V_n V_s^2$. Here V_n-rate of crystallization centre formation is as amount of nucleus changing in the center into per unit of time in per unit of volume of metastable phase; V_s-linear rate of crystallization being defined as rate of change of linear sizes of increasing centers of new phase.

Values lnK for various temperatures are the following

K	403	418	433	453
lnK	- 16,70	- 14,66	- 12,62	- 10,44

On the base of mentioned data there have been carried out chart of dependence lnk on reverse temperature which is linear. This dependence indicates that rate of nucleus formation and linear growth of chips can be described by expression of Arrhenius equation [53].

$$\ln k = A - \frac{1}{RT}(E_n + E_s) \qquad (2)$$

where E_n- activation energy of nucleus formation; E_s – activation energy of chip growth; R –universal gas constant; A – constant not depending on temperature .

There have been determined total energy of crystallization activation along the shift of direct dependence lnk on 1/T, which is equal to 45,7 kkal/mol. Activation energy of nucleus formation E_n calculated along the shift of direct dependence $1/\tau$ on lnt (where τ-experimentally observed time for crystallization start – incubation time) which is equal to 16,3kkal/mol.

Activation energy of chip growth E_s from ratio $E_s=E_g-E_n/2$ is equal to 14,7 kkal/mol. Crystallization kinetics investigation of amorphous films $TlInSe_2$ obtained under the effect of external electric field have been made similarly for films obtained under normal conditions.

From the change of diffraction line intensities of increasing crystal phase according to above-mentioned method there have been carried out kinetic curves of crystallization and kinetic parameters of film crystallization of tetragonal $TlInS_2$ [3] and $TlInSe_2$ [2] condensed under normal conditions and under the effect electric film are determined. Values of summary activation energy of crystallization process $E_g=E_n+2E_s$ and magnitudes of activation energy of nucleus formation (E_n) and growth (E_s) are determined. For comparison the obtained values are given in Table 4.

Table 4. Values of activation energy

Description	Electric field strength	m	E_g kcal / mol	E_n kcal / mol	E_S kcal / mol
$TlInSe_2$	E=0	3	45,7	16,3	14,7
$TlInSe_2$	E=3000 B cm^{-1}	3	38,0	11,0	13,5
$TlGaSe_2$	E=0	3	61,8	17,6	22,1
$TlGaSe_2$	E=3000 B cm^{-1}	3	53,3	15,1	19,1
$TlInS_2$	E=0	3	42,0	11,0	9,0
$TlInS_2$	E=3000 B cm^{-1}	3	36,2	9,5	7,7

From the obtained data it is seen that in all three cases there have been observed two-dimensional growth of chips: activation energy values of crystallization for films $TlInSe_2$, $TlGaSe_2$ and $TlInS_2$ obtained under the effect of external electric field are less corresponding magnitudes for films deposited under normal conditions.

Thus with the crystallization of amorphous films $TlInSe_2$, $TlGaSe_2$, $TlInS_2$ under the effect of electric field there have been obtained more unstable states than in case of absence of field.

Influence of electric field on crystallization of amorphous films $TlInSe_2$, $TlGaSe_2$, $TlInS_2$ can be explained that in external electric field, in $TlInSe_2$, $TlGaSe_2$, $TlInS_2$ structures of chained molecules during deposition there have been formed deformations increasing the probability of chain break in short fragments, i.e. it causes increase of their mobility during subsequent thermal treatment and as a result decrease of crystallization activation energy of $TlInSe_2$, $TlGaSe_2$ and $TlInS_2$ is taken place.

III. Formation of superlattices of phase transformations in $TlGaSe_2$ and $TlInTe_2$.

1. $TlGaSe_2$ structure is determined by roentgenographycally and it is shown that it is isostructural with TlSe and it forms individual structural type of space group I4/mcm.

Tetragonal lattice parameters of $TlGaSe_2$ are:a=0,8053; c=0,6417nm, molecule number in elementary cell z=4, [V=41,62nm^3] [3]. Given results in paper [6] published at the same time with [3] are not in agreement with each other. According to [4-6] $TlGaSe_2$ has monoclinic crystal system, phase with tetragonal lattice is not fixed. This circumstance makes open the discussion of possible modifications of the mentioned compound.

Below we present results of formation of the thin films $TlGaSe_2$ and $TlInTe_2$ obtained by vacuum condensation of synthesized compounds on the surface of alkalihaloid compounds of crystals (NaCl, KCl). There have been studied the formation of epytaxial monocrystalline films and the influence of substrate temperature and subsequent thermal treatment on structural characteristics of forming thin films . There have been studied scope for existence of $TlGaSe_2$, $TlInTe_2$ phases depending on films production conditions. There have been considered scope for phase transitions from one modification into another, and also superstructure formations matching one or another phase and not found in massive samples so far.

On the base of investigations we establish the following peculiarities of film formation of $TlGaSe_2$ compound: $TlGaSe_2$ films in thickness ~30,00 nm prepared by deposition of synthesized substance on NaCl, KCl crystals and celluloid at room temperature are formed at amorphous state.

On electron – diffraction photograph there have been observed three diffusion rings corresponding to values $S=4\pi\sin\theta/\lambda=2{,}102;\ 3{,}445;\ 4{,}473\ A^{-1}$. Storage of amorphous films during 4 months at room temperature does not bring about spontaneous crystallization. Amorphous phase on the surface of mentioned substrates up to T_s=413 K. Crystallization of isolated amorphous films from substrate in electron – diffraction examination column at temperature and heating rate 20 deg/sec leads to formation of polycrystalline $TlGaSe_2$ with familiar monoclinic lattice.

Evaporation of $TlGaSe_2$ on heated substrates up to 443K also leads to formation of polycrystalline film. Before increasing temperature of substrates till 483K there have been formed films which electron – diffraction photographs show that observed reflections can be divided into two groups. Diffraction reflexes applies to the first group inducing in monoclinic crystal system with above mentioned parameters of

unit cells. The second group of reflexes (solid lines with arranged points on them) are induced on the base of tetragonal modification [3].With temperature rise of substrates up to 523K the number of monoclinic phase lines is decreased.

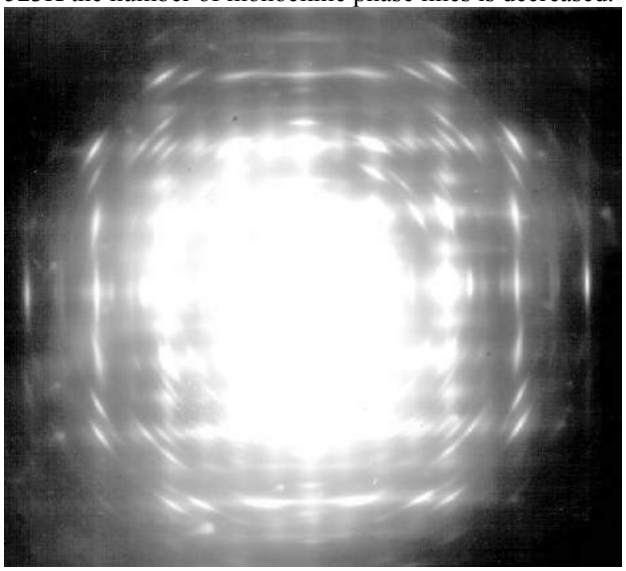

Fig. 6. Electron-diffraction photograph of $TlGaSe_2$ textured films.

Films obtained on NaCl, KCl substrates at T_s=543K with subsequent holding at given temperature over 30 minutes detect the presence of only tetragonal phase $TlGaSe_2$. This phase is retained at room temperature. Co-existence of these two structures is due to process of phase transition accompanied by change of atom coordination and bond characteristics between them. Quite a different picture emerges during the production of films on NaCl substrates heated above. Electron-diffraction photographs of forming films under these conditions indicate about the presence of predominant orientation of chips. However formed texture is not perfect. Reflections on electron – diffraction photographs are diffused out, reflection splitting is observed. Intensity distributions in the sports do not follow any regularities. Finally at the temperature of substrates of the order of 330 we obtain samples on which electron – diffraction photographs there have been reflections arranged closely along layer lines. By electron – diffraction photographs of mentioned films (fig.6) it is established that $TlGaSe_2$ chips form texture with axis "*c*" being perpendicular to substrate. Parameters of tetragonal lattice with periods are determined: *a*=0,8050; *c*=1,3050nm. Extinction system brings about space group $I\bar{4} - S_4^2$ other than initial phase referring to group I4/mcm. Here period "*a*" is unchanged but there is value for period "c" which is close to the value of body diagonal of cell of initial tetragonal phase. It points to the appearance of some ordering taking place not along all the directions of cell but only along axis "*c*".

$TlGaSe_2$ films grown on (NaCl) monocrystalline substrates at T_s=623-643K are monocrystalline with different degree of perfection. By point electron – diffraction photographs there have been determined lattice periods (photography with NH_4Cl standard) which are equal to: *a*=1,5980; *c*=1,1680nm. In fig.7 electron-diffraction photograph of monocrystalline film of superstructure $TlGaSe_2$ is presented. Period "c" is determined by electron-diffraction photographs measured with the angle φ=35°. Space group $I4_1/amd$ $\left(D_{1n}^{19}\right)$ is established.

Good crystallographic agreement of conjugating substrate planes and new phase is responsible for formation of perfect monocrystalline films with superperiods. By epytaxial growth of $TlGaSe_2$ on NaCl one elementary cell of phase superstructure is conjugated with three cells of NaCl, and comparative incompalility of conjugated lattices is 5%. Monocrystalline films $TlGaSe_2$ are orientated by the plane [001] paralleled to face [100] of NaCl. According to data [3] cell includes 4 formula units. Consequently there must be 16 formula units in cell of $TlGaSe_2$ superstructure, i.e. 16 atoms of Tl, Ga and 32 atoms of Se. Over crystallization occurs at higher temperature and compound leaning by high-volatile component is possible, as a consequence stabilization of tetragonal phase [3] is possible too. For explanation and coordination of *X*-ray data we suggest the following. $TlGaSe_2$ structure is laminated and is alternating packets of two opposite big tetrahedral group of (Ga_4Se_{10}) composition combined by Van- der -Waals forces [3,6].

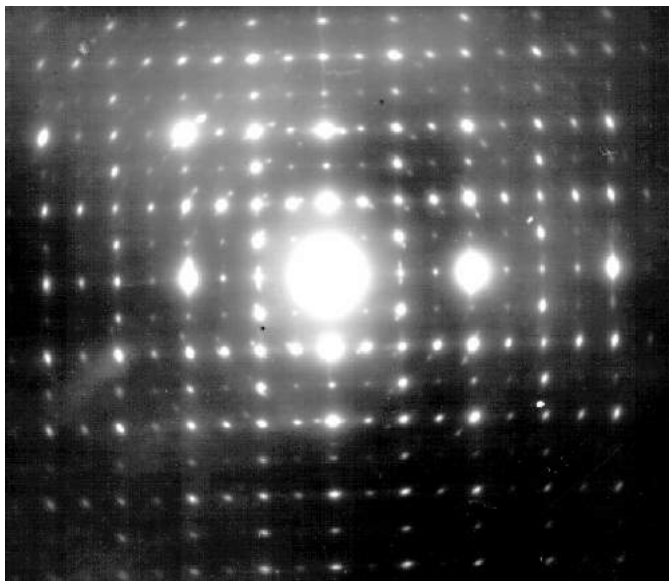

Fig. 7. Electron-diffraction photograph of $TlGaSe_2$ single crystal.

Distances between packets are 0,3 nm. We assume that the presence of such weak link while the thermal treatment undergoing deformation in dynamic conditions monoclinic laminated structure $TlGaSe_2$ falls apart into separate fragments arranging in chain tetragonal structure of TlSe – type. Thus it is shown that phase transformation connected with layer reconstruction in $TlGaSe_2$ brings about formation of its tetragonal modification. Similar processes of tetragonal phase formations are observed under investigation of phase transformations in thin films of IB subgroup chalkogenides of periodic system. In [56] it is shown that tetragonal modification is the intermediate formation and is manifested due to enrichment (leaning) of subject by one of components. It is possible that similar processes are realized for system under investigation. Period difference of revealed superlattices (in the fiest case it is the period "*a*", in the second case both period «*a*» and period «*c*») can be connected with different degree of atom ordering and vacancies of selenium in tetragonal lattice. They are due to the change of selenium content in different positions, in consequence in structure on the whole. Superstructural phase is formed as a result of ordering of selenium atom defect positions.

2. Below we consider formation conditions of $TlInTe_2$ thin films with different substructure and growth peculiarities of epytaxial layers.

We do not suggest that during evaporation there have been arisen substance decomposition or oxidation of this compound, films with different conditions of preparation have been obtained i.e. due to rate of evaporation and substrate temperature. With point electron-diffraction photographs of single crystal there have been obtained electron-diffraction photographs of polycrystal inducing completely on the base of tetragonal lattice with periods: a=0,8494; c=0,7181 nm space group I4/mcm $\left(D_{4h}^{18}\right)$; z=4 [11].

We obtain amorphous films under specific conditions for this compound. We establish that $TlInTe_2$ layers can be obtained on substrate cooled tentatively up to 213K. In having films on substrates with temperature above 213K there have been observed mesophase transition into crystalline structure. On electron-diffraction photographs of amorphous films three diffusion rings with corresponding $S=4\pi\sin\theta / \lambda$=0,275; 0,335; 0,453 nm^{-1} have been observed. Later on the base of investigations there have been established the following peculiarities of film formation of $TlInTe_2$ compound: films in thickness ~30 nm obtained by evaporation of synthesized substance on NaCl, KCl crystals and celluloid at 223K up to room temperature and at 443K they are obtained in polycrystalline state. During sublimation of ternary alloy $TlInTe_2$ on newly made spall of KCl single crystal heated up to 493K there have been observed film formation with mosaic crystal structure. On electron-diffraction photographs of such films there have been presented point reflections indicating the prescuse big chips in film closely oriented in an azimuth about each other however these electron-diffraction photographs cannot be induced on the base of tetragonal crystal system by relations c/a.

On all electron-diffraction photographs of monocrystalline films forming on the surface of single crystal heated up above 493K there have been observed superstructural lines which intensity rises with temperature and at 563K these lines reach good sharpness. At T close to 593K substrates form monocrystalline films with perfect structure and periods: a=2,500 nm. Period "c" is also tripled and equal to 2,185 nm. Between lattice periods a_0 and c_0 of initial and superstructural phases simple relationship are taken place:

$$a_{sup.stp.} = 3a_0 = 2{,}500\ nm;\ c_{sup.stp.} = 3c_0 = 2{,}185\ nm;$$

And one elementary cell of superstructural phase is conjugated with four cells of substrate, relative incompatibility of conjugated lattice period is 4,8%. Exact extension law being in agreement with space group $I4_1/amd$ $\left(D_{4h}^{19}\right)$ is established.

As base area of superstructural cell is nine times as much as base area of initial phase there must be 36 formula units in superstructural cell $TlInTe_2$, i.e. 36 atoms of Tl, In and 72 atoms of Te. $TlInTe_2$ monocrystalline films is oriented by plane (001) parallel to KCl face (100).

Observed orientation relations during epytaxial growth of $TlGaSe_2$ and $TlInTe_2$ films as in $TlInSe_2$ [56] are defined by relationship of atomic configuration of metal layers in crystal lattice of growing film and substrate surface. In $TlGaSe_2$ and $TlInTe_2$ lattices metal atoms form orthogonal lattices with distances between points equal to 0,402 and 0,421 nm, respectively. Similar orthogonal lattices with distances between 0,399 and 0,444 nm point form cations or anions on NaCl and KCl crystal face (100), respectively.

However in [56] for TlSe clear epytaxial relationship is not realized in although incompability parameter conjugating lattices is only Δ=0,5% and three different crystallographic orientations is realized at which $\Delta\approx$40%. Similar phenomenon is known for the case of epytaxial growth of metals on alkalaloid crystals [57-58] and is due to the fact, that the relationship of parameters of conjugating lattices defines perfect epytaxy at initial phases of growth according to Frank-van-der-Merve mechanism [59] but it does not bear the responsibility for epytaxial relationship in Folmer-Veber mechanism.

As the substances under investigation are characterized by mixed covalent and ionic links there must be Folmer-Veber mechanism characteristics for weak adhesion between crystal and substrate.

Superstructural phase formation is connected with ordering of chalkogen atom vacancies forming at temperature rise because of its volatility. Ordering of point defects can play an important role in compensation of parameter incompability of conjugating lattices at epytaxial growth of thin – filmed samples [60] that takes place in our experiment in $TlGaSe_2$, $TlInTe_2$ and according to [56] in $TlInSe_2$ thin films. Nucleation and ordering of point defect vacancies in experimentally grown film appears to be brought about decrease of incompability stress in them and formation of more perfect monocrystalline samples. It seems that observed orientation relations for pair "film – substrate" are defined by relationship of atomic configuration $TlGaSe_2$ –NaCl, $TlInTe_2$-KCl and that brings about formation of perfect monocrystalline films with super periods.

CONCLUSIONS.

1. At sequential deposition of Tl, In and Se evaporation order and simultaneous evaporation of components there have been isolated six differences in composition and compound structure Tl_2Se, TlSe, $TlInSe_2$, In_2Se_3, InSe, In_4Se_3. Formed at room temperature films are amorphous and ranges over compositions from Tl_2Se to Se, that are considerably wider than range in massive samples obtained by quick cooling of melts limiting from Tl by Tl_2Se composition. Amorphous films are stable at room temperature and are crystallized at 363-373K.

2. In case of simultaneous deposition of components in Tl-In-S system there have been observed one crystalline and six amorphous phases which are stable at room temperature and ranges over composition from Tl_2Se to Tl_2S_5 much wider than the range obtained by quick cooling of melts (TlS-Tl_2S_5). For the first time there have been obtained phase Tl_8S_{17} where primitive cubic lattice with period a=1,060 nm with number of structural units in elementary cell z=2.

3. At simultaneous and sequential evaporation of Tl, In and Te by interaction on the substrate there have been possible production of all phases of system Tl_2Te, Tl_5Te_3, TlTe, Tl_2Te_3 and ternary compound $TlInTe_2$. There have been established existence of metastable phase with FCC lattice and elementary cell parameter a=1,262 nm, space group $F4_132$ which changes over the phase Tl_2Te at ~ 403K crystallizing into primitive cubic lattice with the same parameter «a».

4. Values of activation energy of crystallization for $TlInSe_2$, $TlGaSe_2$ and $TlInS_2$ films obtained under the effect

of external electric field are less corresponding values for films deposited at standard conditions. In both cases two-dimensional growth of $TlInSe_2$, $TlGaSe_2$ and $TlInS_2$ chips are observed.

5. For the first time there have been established three superstructural phases of $TlGaSe_2$ and $TlInTe_2$ compounds, two of them are formed by epytaxial growth of $TlGaSe_2$ on NaCl and one phase of $TlInTe_2$ composition on KCl. Good crystallographic agreement of conjugating planes of substrates and new phases is responsible for formation of perfect monocrystalline films with superperiods.

[1] *G. R .Offergeld.* U. S. Patent, 11, 1963, 685.
[2] *H. Hahn, B. Wellman.* Naturwissenchaften, 4, 1967, 42.
[3] *K. J. Range, G. Mahlberg and S. Obenland.* Z. Naturforsh., 32B, 1977, 1354.
[4] *D. Muller, F. E. Poltman, H. Hahn.* Z. Naturforsch., 29B, 1974, 117.
[5] *T. Z. Isaacs, R. H. Hopkins.* Z. Cryst. Crowth., 9, 1975, 121.
[6] *D. Muller, H. Hahn*. Z. Anorg. Allg. Chem., 438, 1978, 258.
[7] *T. Z. Isaacs.* Z. Appl. Cryst., 6, 1973, 413.
[8] *G. D. Guseinov, E. Mooser, E. M. Kerimova, R. S. Gamidov, I. V. Alekseev, M. Z. Ismailov.* Phys. Stat. Sol.,34, 1969, 33.
[9] *T. Z. Isaacs. Z. F. Krist.* 141, 1974, 104.
[10] *K. Range, G. Engert, W. Muller, A. Weise.* Z. Naturforsch., 29B, 1974, 181.
[11] *D. Muller, G. Eulenberger and H. Hahn.* Z. Anorg. Allg. Chem., 398, 1973, 207.
[12] *G. D. Guseinov, G. B. Abdullayev, E. M .Gojayev*. Res. Bull., 7, 1972, 1497.
[13] *M. B. Babanli, A. N. Mamedov, A. A. Kuliyev*. Z. Phys. chem., 50, 1976, 1888.
[14] *H. Hahn, W. Kingler.* Z. Anorg. Allg. Chem., 260, 1949, 110.
[15] *H. Hahn*. Naturwissenchatten, 44, 1957, 534.
[16] *H. Miyazawa, S. Sugaike*. Z. Phyz. Soc. Jap., 12, 1957, 312.
[17] *K. Osamura, Y. Murakami, Y. Tomite*. Z. Phyz. Soc. Jap., 21, 1966, 1848.
[18] *M. Hansen,K. Anderko.* M. Metallurgizdat, 2, 1962, 488.
[19] A. P. Obuhov, N.S.Bubireva. AN USSR, Izv. sektora Fiz. Chem. aralia, 19 (1944) 276.
[20] *Z. A. Ketelear, W. H. Thart, M. Moerel, D. Polder*. Z. Kristallogr., A101, 1939, 396.
[21] *M. M. Stasova, B. K. Vaynshteyn.* Kristallografiya, 3, 1958, 141.
[22] *H.P.Nempel, H.Lauckner, H.Thumann.* Z.Naturtorsch., 164, 1961, 1402.
[23] *V.P.Vasilyev, A.V.Nikolskaya, Y.I.Gerasimov*. dokl. ANSSSR, 199, 1971, 1094. (in Russian).
[24] *V. P. Vasilyev, A. V. Nikolskaya, Y. I. Gerasimov.* Izv. AN SSSR ser. Neorg. Mater., 9, 1973, 553. (in Russian).
[25] *V. P. Vasilyev, A. V. Nikolskaya, V. V. Chernishev, Y.I.Gerasimov.* Izv. AN SSSR ser. Neorg. Mater., 9, 1973, 900. (in Russian).
[26] *L. Cervinka, A. Hruby*. Journ. Of Non-Crystalline Solids, 30, 1978, 191.
[27] *A. R. Muller, A. W. Searcy.* Z. Phys. Chem., 69, 1965, 3826.
[28] *A. R. Muller, A. W. Searcy.* Z. Phys. Chem., 67, 1965, 2400.
[29] *R. E. Jhonson.* Z. Electrochem. Soc., 110, 1963, 593.
[30] *Goodyear, G.A. Steigmann.* Prog. Phys. Soc., 78, 1961, 491.
[31] *S. King.* Acta Cryst., 15, 1962, 512.
[32] *A. P. Obuhov, N. S. Bubireva.* Izv. Sektora fiz.-xim. analiza, 19, 1949, 276.
[33] *A. Rabenau, Astegher, P. Eckerlin.* Z. Metallkunde, 51, 1960, 295.
[34] *E. Cruccenau*. Z. Metallkunde, 60, 1969, 852.
[35] *V. P. Vasilyev, A. V. Nikolskaya, Y. I. Gerasimov Kuznetsov*. Izv. AN SSSR ser. Neorg. Mater., 4, 1968, 1040. (in Russian).
[36] *M. M. Asadov, M. B. Babanli, A. A. Kuliyev*. Izv. AN SSSR ser. Neorg. Mater., 13, 1977, 1407.
[37] *A. Zoudakis, C. R. Kannewurf.* Z. Appl. Phys., 39, 1968, 3003.
[38] *L. I. Man, R. M.Imamov, Z. G. Pinsker*. Kristallografiya, 16, 1971, 122.
[39] *F. A. Shunk.* Constitution of Binary Alloys, Second Supplement, MeGraw-Hill Book Company, 1973, 479.
[40] *S. Geller, A. Jayarman, G. W. Hull.* Z. Phys. Chem. Solids, 26, 1965, 122.
[41] *E. G. Grochowski, D. R. Mason, G. A. Schmitt, P. H. Smith.* Z. Phys. Chem. Solidi, 25, 1964, 551.
[42] *G. D. Guseinov, A. M. Ramazanzade, E. M. Kerimova, M. Z. Ismailov*. Phys.Status Solidi, 22, 1967, 117.
[43] *S. A. Semiletov*. Докl. AN SSSR 137, 1961, 584.
[44] *K. C. Nadral, S. Z. Ali, Z. Pure*. Appl.Phys, 13, 1975, 258.
[45] *Z. Trotter*. Structure reports, 38A, 1972, 107.
[46] *F. I. Aliev, D. I. ismailov, R. M. Sultanov, R. B. Sharifzade*. VINITI, 722, 1988, 34.
[47] *V. G. Sidyakin.* FTT, 3, 1961, 3527.
[48] *Z. Zirke, C. Dromer, A. Tausend, D. Wobid*. Z. Non-Cryst. Solids, 24, 1977, 283.
[49] *L. Cervinka, F.Hruby.* Z.Non-Cryst.Solids, 34, 1979, 275.
[50] *M. Soulard, M. Tournoux.* Bull. Soc. Chem. France, 3, 1974, 791.
[51] *B. Leclerc, M. Baielly*. Acta Crystallogr., 29, 1973, 2334.
[52] *Y. I. Gerasimov.* DAN SSSR, 147, 1962, 835.
[53] *J.V.Gibbs*. Main principles of statistical mechanisms, Гостехнтеоретиздат, 1946, 203.
[54] *M. Avrami.* Z.Chem.Phys., 8, 1940, 212.
[55] *B.K.Vainshten*. Structural electron-diffraction examination, M., Izd, ANSSSR, 1965. 315. (in Russian).
[56] *D.I.Ismailov, R.M.Sultanov, F.I.Aliyev, R.B.Shafizade.* Thin Solid Films , 205, 1991, 1.
[57] *R.P.Ferrier, I.M.Prado, M.R.Anseau*. I.Non – Cryst.Solids, 8-10, 1972, 798.
[58] *G.A.Veneables, G.D.Spillirt, M.Hanbucken*. Reports of program in phys., 47, 1984, 399.
[59] *A.A.Chernov, E.I.Givargizov, Kh.S.Bagdasarov, V.A.Kuznetsov, L.N.Demyanetz, A.N.Lobatchev*. Modern crystallography. M. Izd. “Nauka” 3, 1980, 407. (in Russian).
[60] *L.S.Palatnik, M.Ya.Fuks. V.M.Kosevitch*, Formation mechanism and structure of condenced films , M. Izd.“Nauka”, 1972, 319.(in Russian).

C. İ. İsmayılov

$A^3B^3C_2^6$ – BİRLƏŞMƏLƏRİNDƏ FAZA KEÇİDLƏRİNİN ELEKTRONOGRAFİK TƏDQİQİ

Elektronoqrafik üsul ilə $A^3B^3C_2^6$ qrupuna daxil olan birləşmələrin, nazik təbəqələr vəziyyətində alınma xüsusiyyətləri tədqiq edilmişdir. Göstərilmişdir, ki otaq temperaturunda formalaşan amorf təbəqələrin tərkiblərinin təşkil etdiyi interval, həcmli nümunələrinkindən daha genişdir. Adi şəraitdə və xarici elektrik sahəsinin təsiri altında alınmış $TLInSe_2$, $TLGaSe_2$ və $TLInS_2$ nazik amorf təbəqələrin faza kecidlərinin kinetik parametrləri təyin olunmuşdur. Epitaksial böyümə nəticəsində $TLInTe_2$ təbəqələrinin KCl, $TLGaSe_2$ təbəqələrinin isə NaCl monokristalları üzərində böyüməsi nəticəsində uyğun olaraq 1 və 2 ədəd ifrat quruluşlu fazaların mövcudluğu müəyyən olunmuşdur.

Д. И. Исмаилов

ЭЛЕКТРОНОГРАФИЧЕСКОЕ ИССЛЕДОВАНИЕ ФАЗОВЫХ ПЕРЕХОДОВ В СОЕДИНЕНИЯХ $A^3B^3C_2^6$

Электронографическими исследованиями установлены особенности формирования пленок соединений группы $A^3B^3C_2^6$. Показано,что интервал составов аморфных пленок при комнатной температуре значительно шире интервала в массивных образцах. Определены кинетические параметры фазовых превращений в аморфных пленках $TLInSe_2$, $TLGaSe_2$ и $TLInS_2$ полученных в обычных условиях и в условиях воздействия внешнего электрического поля. Установлены 3 сверхструктурные фазы составов $TLGaSe_2$ и $TLInTe_2$, две из которых формируются в результате эпитаксиального роста $TLGaSe_2$ на NaCl и одна - состава $TLInTe_2$ на KCl.

Received: 08.01.04

DƏRİ İMPEDANSINA GÖRƏ ELEKTROSTİMULYATORUN AVTOMATİK QOŞULMA SİSTEMİ

N.Ə. SƏFƏROV
Azərbaycan EA Fizika İnstitutu
371143, Bakı, Cavid pr., 33

Ş.Ş. ƏMİROV, F.A. AXUNDOVA
Azərbaycan Dövlət Tibb Universiteti
371022, Bakı, Bakıxanov küç., 23

Təklif olunan avtomatlaşdırılmış sistemdə diaqnostik məlumat kimi dərinin impedansı parametri götürülmüşdür. Barmaqlara bağlanmış elastik braslet dəri müqavimətini qeyd edərək onu emosional halı təyin edən cihaza ötürür. Sonra isə cihazdan bu siqnal personal kompüterin səs platasındakı "Game" portuna ötürülür. Xüsusi proqram təminatının köməyi ilə alınan məlumatlar işlənilir və pasient təyin edilmiş alqoritm üzrə diaqnoz edilir. Diaqnozun və müalicənin proqramlaşması, onların avtomatik sistemdə işlənib hazırlanması, tətbiq edilməsi belə müalicə metodlarının effektivliyini artırır, həkim personalının təsadüfi səhvlərinin qarşısını alır. Bu sistem əsasən personalın emosional vəziyyətlərini təyin etmək, onların hər biri üçün gündəlik arxiv bazası yaratmaq və bu arxivdən istifadə etməklə baxış keçirməyə imkan verir.

Müasir dövrdə diaqnostikanın etibarlılığını və effektivliyini artırmaq üçün kompüter və yeni texnikadan istifadə etmək tələb olunur. Avtomatlaşdırılmış sistemin effektivliyi həlledici dərəcədə diaqnostikada istifadə olunan alqoritimin etibarlılığından asılıdır. Belə sistemlər üçün optimal hazırlanmış alqoritmlər müxtəlif xəstəliklərin kifayət qədər etibarlılıqla müəyyən olunması ilə yanaşı, həmçinin kütləvi baxış zamanı nəticələri qiymətləndirməyə imkan verir.

Toxumaların impedansı təkcə aktiv müqavimət ilə deyil, həm də tutum müqaviməti ilə müəyyən olunur. Məlum olduğu kimi orqanizm toxumalarının impedansı onların fizioloji halından asılıdır. Məsələn, reoqrafiya adlanan diaqnostik metod ürək-damar sisteminin fəaliyyəti zamanı onun halından asılı olaraq impedansın dəyişməsinə əsaslanıb [1]. Ölçməni adətən körpü sxemi ilə aparırlar ki, bu da həssaslığın kifayət qədər olmaması ilə nəticələnir. İnsanın emosional halını təyin edən cihaz çox zaman istintaq praktikasında tətbiq edilir. Belə ki, müəyyən edilmişdir ki, cinayətkarlar yalan danışdıqda və ya təqsiri boynuna almadıqda bu hal əsəb gərginliyi ilə müşaiət edilir ki, nəticə etibari ilə müxtəlif fizioloji hadisələr baş verir: qan təzyiqi qalxır, üz qızarır, dərinin müqaviməti dəyişir [2]. Adi halda dəri müqaviməti 3…100kOm təşkil edir, həyəcanlanmanın təsirindən isə təxminən 5% dəyişir. Çıxış sıxacına ya qalvanometr ya da özüyazan maşın qoşulur[3]. Məlumatın bu cihazlardan alınıb və onların işlənməsi tibb personalı tərəfindən fərdi qaydada yerinə yetirilir, ki bu zaman subyektivliyə və texniki səhvlərə yol verilə bilər.

Təklif olunan avtomatlaşdırılmış sistem aşağıdakı kimi işləyir:

Diaqnostik məlumat kimi dərinin impedansı parametri götürülmüşdür. Barmaqlara bağlanmış elastik braslet dəri müqavimətini qeyd edərək onu emosional halı təyin edən cihaza – 1 ötürür. Sonra isə cihazdan bu siqnal personal kompüterin - 3 səs platasındakı "Game" portuna ötürülür. Xüsusi proqram təminatının köməyi ilə alınan məlumatlar işlənilir və pasient təyin edilmiş alqoritm üzrə diaqnoz edilir. Diaqnozun nəticəsindən asılı olaraq kompüterin displeyində elektrostimulyasiyanın verilib – verilməməsinə dair təklif çıxır. Diaqnoz hər hansı bir pasientin cari impedansının qiymətinin arxiv verilənlərin orta qiymətindən fərqinə əsasən aparılır. Bu fərqin faizlə miqdarı, təklif olunan elektrostimulyasiya prosedurlarının sayı və onların təsir müddəti fizioterapevt tərəfindən əvvəlcədən sifariş edilir və alqoritmə daxil edilir. Diaqnozun nəticəsindən asılı olaraq impedansın orta qiymətinin normadan kənara çıxması zamanı sistem stimulyatoru - 2 pasientə qoşur. Diaqnozun və müalicənin proqlaşması, onların avtomatik sistemdə işlənib hazırlanması, tətbiq edilməsi belə müalicə metodlarının effektivliyini artırır, həkim personalının təsadüfi səhvlərinin qarşısını alır.

Bu sistem əsasən personalın emosional vəziyyətlərini təyin etmək, onların hər biri üçün gündəlik arxiv bazası yaratmaq və bu arxivdən istifadə etməklə baxış keçirməyə imkan verir. Bundan əlavə sistem hər hansı bir şəxsin emmosional vəziyyətini müəyyən edən müddətdə onun emosional vəziyyəti normadan kənara çıxdıqda avtomatik surətdə stimulyasiya blokunu birləşdirmək üçün fizioterapevtin təsdiqini gözləyir (şək. 1). Bundan sonra təyin edilən vaxt muddətində pasient stimulyasiya olduqdan sonra təkrar ölçmə aparılır. Bu proses müəyyən olunmuş dövrdə davam etdirilir, stimulyasiya olmaqla emmosional vəziyyət normaya uyğun vəziyyətə gətirilir. Ölçmənin nəticələri bütün hallarda arxivləşdirilir.

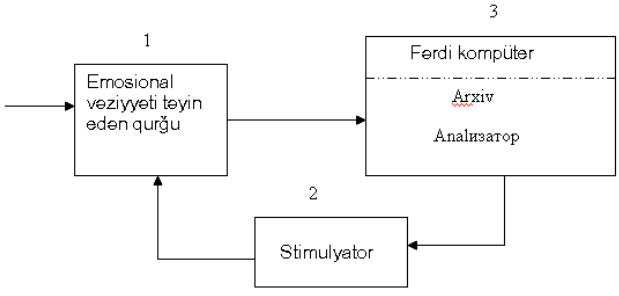

Şək. 1. Sistemin məntiqi blok sxemi

Sistemin işləməsi üçün minimal tələbat kimi, əməliyyat sistemi olaraq – WINDOWS əməliyyat sisteminin hər hansı bir versiyası, texniki tələbat kimi isə HDD- 0.4 Gb, operativ yaddaş- 8 Mb olması kifayətdir.

Proqramda istifadə olunan menyular haqqında:

İnput information menyusu sistemin informasiya bazasına fizioterapevt tərəfindən lazımı informasiyaları daxil etmək (lazım gəlsə onları redakte etmək) və pasientlərin emmosional vəziyyətini ölçmək üçün nəzərdə tutulub

Parametrs alt menyusu əsasən parametrlərin qiymətlərini daxil etmək üçün nəzərdə tutulub

Looking information menyusu hər hansı seçilmiş pasientin emosional vəziyyəti haqqında arxiv məlumatlara baxmaq üçün nəzərdə tutulub. Bunun üçün onun adını və ya kodunu daxil etdikdən sonra "advanjed information'' düyməsini basmaq lazımdır

Testing menyusu emosional vəziyyəti ölçmək üçün nəzərdə tutulub. Bundan sonra ekrana çıxmış pəncərədə (şək.2) average (old) mətn qutusunda seçilmiş pasientin emosional vəziyyətini xarakterizə edən kəmiyyəti lazım gəlsə ilk dəfə fizioterapevt dəyişdirə bilər. Bundan sonra pasientin barmaqlarına elektrodları bağlayıb ölçməyə başlamaq üçün start düyməsini basmaq lazımdır.

Qeyd edək ki, ölçmənin nəticəsindən asılı olaraq nəticə normaya uyğun olduqda nəticə arxivdə yadda saxlanılır, əks halda isə stimulyasiya rejimi avtomatik işə salınır.

Bu menyuların hər hansı birindən **Exit** düyməsini basmaqla çıxmaq olar.

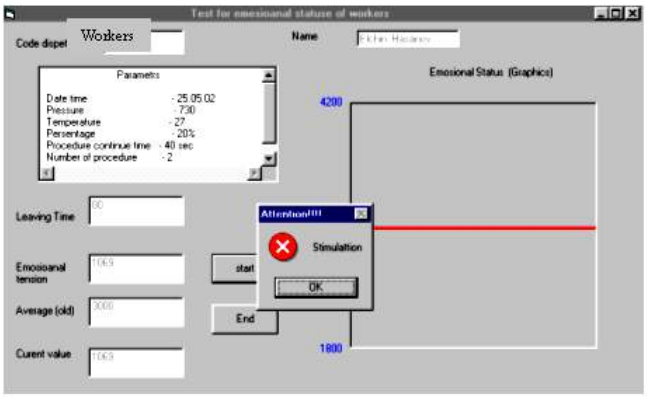

Şək. 2 Displeydə sistemin işçi pəncərəsi

Sistemin əsas üstün cəhətlərdən biri diaqnoz və müalicənin avtomatik sistem vasitəsi ilə effektiv üsulla aparılması, operativlik və sadələşdirilmiş iş qaydasıdır. Digər fərqlərdən biri isə məlumatın kompüterə ötürülməsi və qəbulu zamanı standart giriş portundan istifadədir ki, bu da xüsusi təyinatlı çevirici qurğulardan istifadə etmək zəruriyəti yaratmır. Bu isə öz növbəsində sistemin maya dəyərinin xeyli azalmasına və adi fərdi kompüterlərin bu məqsədlə istifadəsinə geniş imkanlar açır.

[1] *A.N. Remizov*. Kurs fiziki, glektroniki i kibernetike dlə mediüinskix institutov. Moskva "Vısş. şkola" , 1982, str.265

[2] Spravoçnik po sxemotexnike dlə radiolöbitelə. Kiev, "Texnika",1987, str.211

[3] Texnika i metodiki fizioterapevtiçeskix proüedur/ Pod red. *V.M.Boqolöbova*. – M.: Mediüina, 1983, 352s.

N.A. SAFAROV, Sh.Sh. AMIROV, F.A. AKHUNDOVA

AUTOMATIC SYSTEM OF CONNECTION OF THE ELECTROSTIMULATOR ON THE SKIN IMPEDANCE

In the suggested automated system as diagnostic parameter it is taken a skin impedance. The elastic bracelet fixed on finger registers skin resistance and transfers in the device for definition emotional conditions of the person. After that the signal from this device is sent on "Game" port of a computer. The received information will be processed with the help of the special software and on the certain algorithm the patient diagnosis. Depending on result of diagnostics on the screen of the display there is a recommendation on inclusion of an electro stimulator. Programming of diagnostics and therapy, application of the automated system raises efficiency of therapy, promote elimination of possible omissions and mistakes in medical practice. This system serves the basic for definition emotionalo a condition of personnel's, creation for each of them of everyday archival base and using this base permit to inspect. The basic advantages is carrying out of diagnostics and therapy in an automatic mode, efficiency, simplicity works and use of standard entrance ports at a sending of the information to a computer.

Н.А. САФАРОВ, Ш.Ш. АМИРОВ, Ф.А. АХУНДОВА

АВТОМАТИЧЕСКАЯ СИСТЕМА ПОДКЛЮЧЕНИЯ ЭЛЕКТРОСТИМУЛЯТОРА ПО КОЖНОМУ ИМПЕДАНСУ

В предложенной автоматизированной системе как диагностический параметр взят кожный импеданс. Эластичный браслет, закрепленный на пальцах, регистрирует кожное сопротивление и передает в прибор для определения эмоционального состояния человека. После этого сигнал с этого прибора посылается на "Game" порт компьютера. Полученная информация обрабатывается с помощью специального программного обеспечения и по определенному алгоритму пациент диагнозируется. В зависимости от результата диагностики на экране дисплея появляется рекомендация по включению электростимулятора. Программирование диагностики и терапии, применение автоматизированной системы повышает эффективность терапии, способствуют устранению возможных упущений и ошибок во врачебной практике. Эта система в основном служит для определения эмоционального

состояния персонала, создание для каждого из них каждодневной архивной базы и, используя эту базу, позволяет провести осмотр. Основными достоинствами является проведение диагностики и терапии в автоматическом режиме, оперативность, простота работы и использование стандартных входных портов при посылке информации к компьютеру.

Received: 16.01.04

THE MAGNETIC AND ELECTRIC PROPERTIES OF $CoCr_2Te_4$

A.A. ABDURRAGIMOV, K.Z. SADIKHOV, SH.O. ORUDJEVA
Institute of Physics of Azerbaijan Academy of Sciences
370143, Baku, H.Javid ave. ,33

The magnetization, electroconduction and thermoelectromotive force of the compound $CoCr_2Te_4$ were investigated in the temperature interval 80-300K. It is shown, that compound is ferrimagnetic with Curie temperature 275K and electric characteristics have changes in the magnetic transformation region.

In the refs [1, 2] Hall effect and the magnetic resistance, and in the ref [3] the heat properties of $CoCr_2Te_4$ were investigated. In the given refs the authors discovered the influence of the magnetic order in $CoCr_2Te_4$ on the investigated physical properties. However, the character of the magnetic order in $CoCr_2Te_4$ is unclear, because of the absence of magnetic investigations.

With the aim of the definition of the magnetic order character in the given paper, the temperature and field dependences of the magnetization of the $CoCr_2Te_4$ compound have been investigated. The influence of the magnetic order on the several electric properties of the $CoCr_2Te_4$ has also investigated.

The synthesis of the samples for the measurement was carried out in the evacuee quartz ampoules in the result of the interaction of the initial high purity components in the following consequence. The temperature in the metallurgical furnace increases slowly till 950K, was keeping at this temperature during 4 days, and later it was cooled till the room temperature with the velocity 100 grad/h. The obtained powdery samples were carefully crushing, later they were pressing above high pressure~ 6t/sm^2 and were carrying out by annealing at the temperature 500K during 10 days.

The roentgenphased analysis of the samples was carried out on the diffractometer DRON-3M in CuK_α-radiation.

The angular permission of the film was~0,1°. The diffractogram was recording continuously, the diffraction angles were defined by the measurements method on the intensity peak. The mistake of the definition of reflection angles didn't be higher than ±0,02°.

The roentgenphase analysis shows, that compound $CoCr_2Te_4$ is crystallized in the monoclinic structure with lattice parameters a=6,70; b=3,77; c=12,52Å; β=90°20[1], that agrees with the results [1,2].

The magnetization has measured on the pendulum magnetometer Domenikalli, thermoconduction and thermoelectromotive force have measured by compensation method.

The measurements have been carried out in the temperature interval 77÷300K. The spontaneous magnetization at the fixed temperature is defined by extrapolation of magnetization, measured in the different fields, on the zero field.

On the fig.1 the dependence of the specific magnetization of $CoCr_2Te_4$ on the magnetic field at 80K is given. As it is seen from the figure, the dependence M(H) is characterized for the materials with the spontaneous magnetization and the considered paraprocess is observed after the final of the technical magnetization.

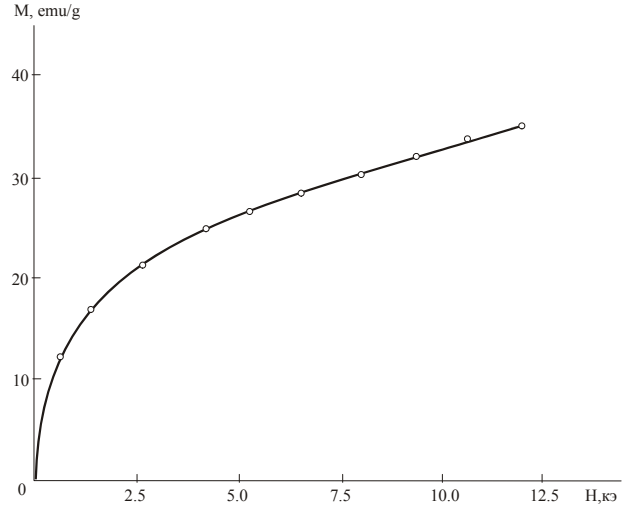

Fig.1. The dependence of the specific magnetization of $CoCr_2Te_4$ on the magnetic field at 80K.

The similar dependence M(H) is observed in the ferrimagnetic materials with the different crystal structure, including the several sublattices (in the dependence on the member of the magnetic ions). In the compound $CoCr_2Te_4$ such sublattices are formed by the two-and trivalent ions Co^{2+} and Cr^{3+}.

If we propose, that in $CoCr_2Te_4$ is any weaked intrasublattice and intersublattice changeable interaction (for example, interaction Co^{2+}-Co^{2+} Cr^{3+}-Cr^{3+}), then in it the big number of disoriented by the thermal motion spins can exist, at the low temperatures, which are responsible the intensive paraprocess.

It is noted, that intensive paraprocess in $CoCr_2Te_4$ can be also the consequence of spin orientation by the magnetic field, disoriented near defects of compound crystal lattice, in the result of local change of the changeable interaction.

At 80K the magnetic moment $CoCr_2Te_4$ has calculated in the magnetic field 10,8ke, which was equal to 3,9μb. This experimental value is some higher than theoretical value (3μb) of the magnetic saturation moment, calculated as the difference of the spin magnetic moments of the sublattices, having Co^{2+} and Cr^{3+} ions.

It can be connected with the noncollinear of the magnetic moments in the sublattices, having Co^{2+} ions. In this case the magnetic moment of this sublattice increases and the resulting magnetic moment of the compound increases, correspondingly.

The temperature dependence of the specific magnetization, measured in the magnetic fields 6,7,9,5 and

10,8 kE, is evidence of the spontaneous magnetization in $CoCr_2Te_4$ fig. 2. .

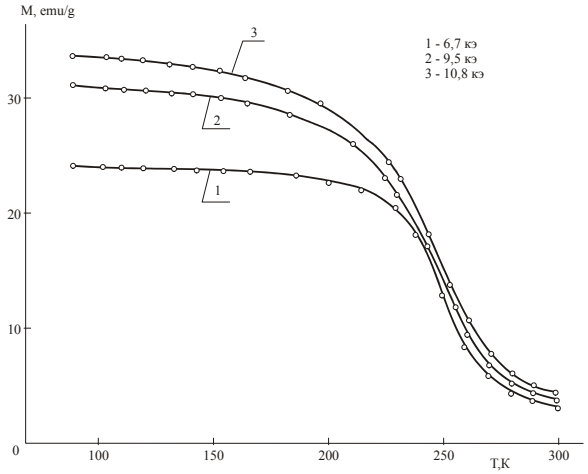

Fig.2. The temperature dependence of the specific magnetization of $CoCr_2Te_4$.

With the aim of definition Curie temperature of $CoCr_2Te_4$ in the magnetic transformation region the thermodynamical coefficient method is applied [4]. The transition temperature of ferrimagnetic-paramagnetic was equal to 275K and equal to the value, defined by the extrapolation of the spontaneous magnetization on the temperature axis.

The magnetic order in $CoCr_2Te_4$ influenced on the electroconduction and thermoelectromotive force of this compound (fig.3). As it is seen from the fig.3, the electroconduction decreases slowly with the temperature, in the temperature region 100-275K б practically doesn't depend on the temperature higher than~275K (magnetic transformation region).

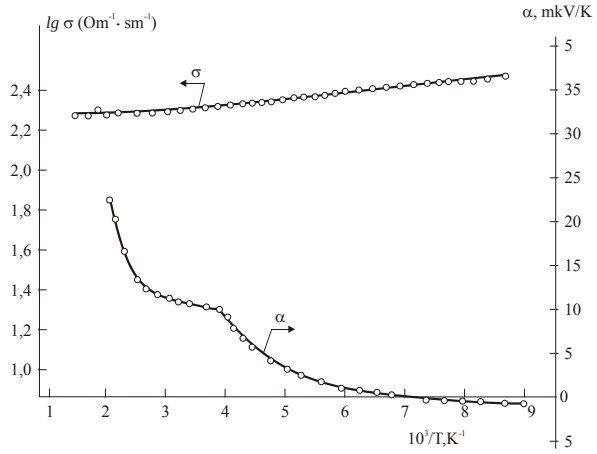

Fig.3. The temperature dependencies of the electroconduction and thermoelectromotive force of $CoCr_2Te_4$.

The thermoelectromotive force of $CoCr_2Te_4$ is positive at the low temperatures, i.e. in this region the compound has p-type conductivity. The thermoelectromotive force coefficient decreases slowly with the increase of the temperature, and at~ 150K the sign inversion takes place, after that α increases with the increase of the temperature. The some bending takes place in dependence $\alpha(T)$ in the region~275K, that can be connected with the magnetic phase transition ferrimagnetic-paramagnetic.

Thus, investigations show, that compound $CoCr_2Te_4$ is ferrimagnetic with Curie temperature 275K, at which some electric characteristics have changes.

[1] *L.M. Valiyev, I.G. Kerimov, A.A. Abdurragimov, N.B. Nabiyeva*. Izv. AN Azerb. SSR, ser. Fiz.-tekh. i mat.nauk, 1976, N1, s. 52. (in Russian).

[2] *L.M. Valiyev, I.G. Kerimov, A.A. Abdurragimov, N.B. Nabiyeva*. Neorganicheskiye materiali, 1977, t. 13, N4, s. 51. (in Russian).

[3] *A.A. Abdurragimov, M.A. Aljanov, N.G. Guseinov, A.G. Guseinov*. Phys. Stat. Sol. (a), 1989, v. 113, p. k207.

[4] *K.P. Belov, A.N. Goryacha*. Fizika metallov I metallovedeniye. 1956, t. 2, N3, s. 441. (in Russian)

Ə.Ə. Əbdürrəhimov , R.Z.Sadıxov, Ş.O.Orucova

$CoCr_2Te_4$ MADDƏSİNİN MAQNİT VƏ ELEKTRİK XASSƏLƏRİ

80-300K temperatur intervalında $CoCr_2Te_4$ maddəsinin elektrik keçiriciliyi, termo e.h.q və maqnitlənməsi tədqiq edilmişdir. Müəyyən edilmişdir ki, bu maddə Küri temperaturu, 275K olan ferrimaqnetikdir və maqnit keçidi oblastında elektrikkeçirmə, termo e.h.q-si dəyişikliyə uğrayır.

А.А.Абдуррагимов, Р.З.Садыхов, Ш.О.Оруджева

МАГНИТНЫЕ И ЭЛЕКТРИЧЕСКИЕ СВОЙСТВА $CoCr_2Te_4$

В интервале температур 80-300К исследованы намагниченность, электропроводность и термоэдс соединения $CoCr_2Te_4$. Показано, что соединение является ферримагнетиком с температурой Кюри 275К и электрические характеристики испытывают изменения в области магнитного превращения.

Received: 24.01.04

NGR AND THE MAGNETIC SUSCEPTIBILITY OF THE LAYERED CRYSTALS $Bi_{m+1}B_mO_{3m+3}$ (B=Ti, Fe)

G.D. SULTANOV, M.A. ALDJANOV, A.B. ABDULLAYEV, M.D. NADJAFZADE, M.B. GUSEINLY

Institute of Physics of Azerbaijan Academy of Sciences
370143, Baku, H. Javid ave.,33.

In the given paper the discussion of the results of magnetic and mossbauer investigations of the compounds $Bi_{m+1}B_mO_{3m+3}$(B=Ti, Fe) revealing in the result of the specific of crystal structure, properties, which are character for the thin magnetic films has been carried out. It was shown, that the influence of the concentration of the magnetic iron ions on the magnetic transition temperature in these compounds significantly differs from the similar influence in the three-dimensional magnetic substance.

The structure of the compound with the general formulae $B_{m+1}B_mO_{3m+3}$ (where m is number of monooctahedronic layers in the perovskite-like packet) is build by the following principle: in the direction [001] the perovskite-like layers (packets) $[Bi_{m-1}B_mO_{3m+1}]^{2-}$take turns with the bismuthooxigen layers $[Bi_2O_2]^{2+}$ (fig.1) [1]. The thickness of the perovskite-like layers is defined by the m value, including in the formulae: these layers have oxygen octahedrons, connected by their vertexes. Inside the oxygen octahedrons are B cations, where B-Ti, F. Because of the octahedron positions are as the magnetic ions of iron, so and the diamagnetic ions of Ti, so these compounds can be considered as the magnetodiluted systems. The magnetic properties of such systems, particularly, the temperature of the transition in the magnetoordered state, depend on the concentration of the magnetic ions.

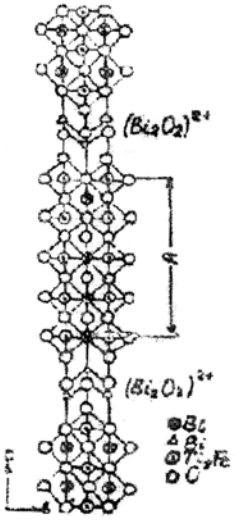

Fig.1. The cell projection of compound $Bi_{m+1}B_mC_{3m+3}$ with the layered structure (m=5) on (001).

In the refs [3-5] it is shown, that compounds $B_{m+1}B_mO_{3m+3}$ reveal the properties, which are characteristic for the thin magnetic films. The revealing of the properties, which are characteristic for the thin magnetic films, by the given crystals is caused by the following reason. In these compounds the magnetic ions of iron, situated in the one packet, are divided from the iron ions, being in the neighbour perovskite-like packets, by the layer, consisting on the diamagnetic ions Bi^{3+} and O^{2-}. That's why the magnetic properties of the investigated crystals will be defined by the interaction of the iron ions only inside the packet, i.e. each packet can be considered as the thin magnetic film. The thickness of such film will be defined by the number of the ionooctahedron layers in the one packet, i.e. by m. It is known, that the magnetic properties of the thin magnetic films are strongly differ from the thickness of the films. Firstly, the dependence of the spontaneous magnetization with Curie point (Neel), values of the internal magnetic field on the nucleus from film thickness and the revealing of its supermagnetic behaviour in the wide temperature region can be considered in these properties. All these peculiarities of the investigated crystals were revealed in the refs [3-5]. The big interest is the following question. If the compounds $B_{m+1}B_mO_{3m+3}$, in the respect of the magnetic properties, behave themselves as the magnetic films, so the influence of magnetic ion concentration on the magnetic properties (particularly on the magnetic transition temperature) will depend on the film thickness and differ from the similar influence for the massive three-dimensional magnetic substance. And with this point of view in the given paper the discussion of the results of mossbauer and magnetic investigations is carried out.

The values of concentration © of iron magnetic ions in the octahedron positions, leading to the appearing of the magnetic order, investigated compounds are defined by method [2] and given in the table1.

Table1

Compound	*C*	*M*
$Bi_6Ti_8Fe_2O_{18}$	0,4	5
$B_6Ti_2Nb_{0,5}Fe_{2,5}O_{18}$	0,5	5
$Bi_7Ti_3Fe_3O_{21}$	0,6	6
$Bi_2Ti_3Fe_5O_{27}$	0,62	8

The mossbauer measurements were carried out in the temperature interval 5-300K, but magnetic measurements - 77-950K. In the compounds $Bi_6Ti_8Fe_2O_{18}$ and $B_6Ti_2Nb_{0,5}Fe_{2,5}O_{18}$ the number of the octahedron layers in the perovskito-like packet are equal, i.e. the thicknesses of the films are equal. However, the magnetic ion concentrations in the octahedron states of these compounds are different: $Bi_6Ti_3Fe_2O_{18}$ c=0,4, and in $Bi_6Ti_2Nb_{2,5}O_{18}$ c=0,5. From the mossbauer investigations of these compounds it follows, that magnetic transition temperature in $Bi_6Ti_2Fe_3O_{18}$ is between 20-30, but in $Bi_6Ti_2Nb_{0,5}Fe_{2,5}O_{18}$ is between 150-170K. Under the magnetic transition temperature is meant the temperature, lower of which in the spectrum begin to appear the lines of the magnetic fission. It is seen, that the change of

the magnetic ion concentration in the octahedron positions on 0,1 leads to the change of the transition temperature on 130-140°C.

In the compound $Bi_9Ti_3Fe_5O_{27}$ the number of the monooctahedron layers in the perovskito-like packet is equal to 8. The iron magnetic ion concentration in the octahedron positions is equal to 0,62. The lines of the superthin magnetic structure in the mossbauer spectrums of this compound disappear between 260 and 280K, i.e. the magnetic transition temperature is in this region.

The lines of the magnetic fission in the mossbauer spectrums of $Bi_7Ti_3Fe_3O_{21}$ compound, in which the number of the monooctahedron layers and magnetic ion concentration in the octahedron positions are equal to 6 and 0,5 accordingly, and disappear between 200 and 220K. The temperature difference of the magnetic transition, defined from the mossbauer measurements in the compounds $Bi_9Ti_3Fe_5O_{27}$ and $Bi_7Ti_3Fe_3O_{21}$ is ~60°C. The more high value of the magnetic transition temperature in $Bi_9Ti_3Fe_5O_{27}$ with the comparison of the transition temperature in $Bi_7Ti_3Fe_3O_{21}$ is caused by two reasons. The first reason is the number of layers (thickness on the film) in is $Bi_9Ti_3Fe_5O_{27}$ more, than in $Bi_9Ti_3Fe_5O_{27}$ is also more, than in $Bi_7Ti_3Fe_3O_{21}$. It is followed, that it can be proposed that in these compounds the temperature difference, caused by the only increase of the concentration of magnetic ions, will be less than 60°.

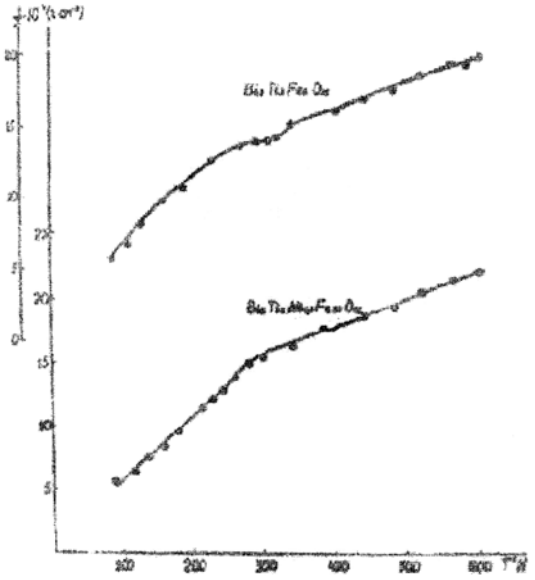

Fig.2. The temperature dependences of the reversible specific magnetic susceptibility of compounds $Bi_7Ti_3Fe_3O_{21}$ and $Bi_6Ti_2Nb_{0,5}Fe_{2,5}O_{18}$.

Later let's consider the results of the magnetic measurements. On the figures 2 and 3 the temperature dependencies of the inverse specific magnetic susceptibility are given. For all compounds at the high temperatures the Weiss-Curie law $\chi = \frac{C}{T + \theta}$ is carried out. The effective magnetic moment, on the each iron ion, defined from these curves, well agrees with the theoretical value 5,92μ for the trivalent iron. About the trivalent state of the iron ions the values of the isomer shifts, defined from the mossbauer spectrums of the investigated compounds at the room temperature is also evidence.

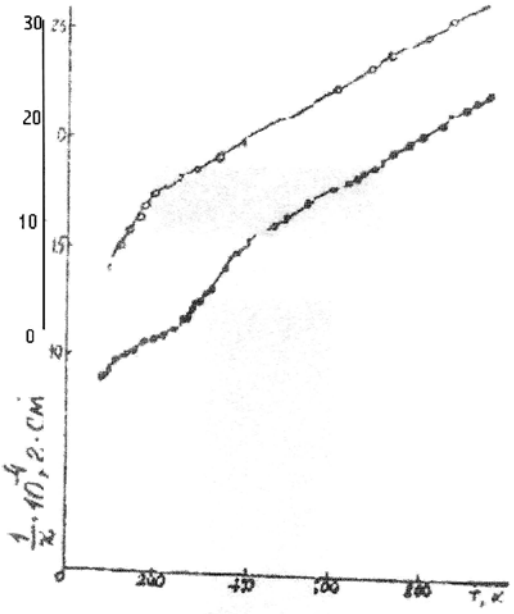

Fig.3. The temperature dependences of the reversible specific magnetic susceptibility of compounds $Bi_6Ti_3Fe_2O_{18}$ and $Bi_9Ti_3Fe_5O_{21}$ (low curve).

The negative values of the paramagnetic Curie O temperatures, given in the table 2, show on the antiferromagnetic interactions between iron ions in the compounds $Bi_{m+1}B_mO_{3m+3}$ in the magnetoordered phase.

Table2.

Compound	m	θ,K	$T_{Nmag.}$	$T_{Nmoss.}$
$Bi_6Ti_3Fe_2O_{18}$	5	-390	120	20-30
$B_6Ti_2Nb_{0,5}Fe_{2,5}O_{18}$	5	-550	260	150-170
$Bi_7Ti_3Fe_3O_{21}$	6	-560	330	200-220
$Bi_9Ti_3Fe_5O_{27}$	8	-780	400	260-280

At the decrease of the temperature, the change of inclination of the curve of temperature dependence of the inverse magnetic susceptibility takes place. The temperatures, at which the change of inclination of curve $\chi(T)$ takes place, for the different compounds are different. They are given in the table2 ($T_{N\,mag}$).

As it is seen from the figures 2 and 3, the behaviour of the magnetic susceptibility of the compounds $Bi_{m+1}B_mO_{3m+3}$ lower, than T_N, differs from the behaviour of the massive three-dimensional samples lower the temperature of antiferromagnetic order. In the difference from the massive three-dimensional samples, the increase of the magnetic susceptibility value of the compounds $Bi_{m+1}B_mO_{3m+3}$ is lower than the temperature of antiferromagnetic order can be explained, if these compounds are lower than T_N, defined from the magnetic measurements, transfer in the supermagnetic state, i.e. the state with the antiferromagnetic order with spin fluctuation.

Firstly, the theoretical propositions of the essential increase of the magnetic susceptibility of antiferromagnetic substance, being in the supermagnetic state, were given by Neel (see example 6). These propositions were proved in the refs [7,8].

It is noted, that lines of the magnetic fission, showing on the magnetic order, in the mossbauer spectrums of the compounds $Bi_{m+1}B_mO_{3m+3}$ appear at the more low

temperatures (these temperatures are also given in the table2), than T_N, defined from the magnetic measurements, are the transition temperatures of the compounds $Bi_{m+1}B_mO_{3m+3}$ in the superparamagnetic state. Indeed, vice versa, if Tn, defined from the magnetic measurements, would be the transition temperatures in the stable (without spin fluctuation) antiferromagnetic state, so the lines of the magnetic fission in the mossbauer spectrums should be appear , lower than Tn at once.

The absence of the lines of the magnetic fission in the spectrums in the temperature region from mag. till mes. connects with that in this temperature region the fluctuation frequency of spins (ω_{ii}) is more, than the frequency of Larmor precession (ω_i) [9]. At the decrease of the temperature, as ω_{ii} becomes the ω_i degree, so in the spectrum began to appear the lines of magnetic fission.

Now we carry out the comparison of the results of mossbauer and magnetic measurements for two couples of compounds. The first couple $Bi_6Ti_3Fe_2O_{18}$ and $Bi_6Ti_2Nb_{2,5}O_{18}$, in which the magnetic ion concentrations differ on 0,1. The second couple are compounds $Bi_9Ti_3Fe_{0,5}O_{27}$ and $Bi_7Ti_3Fe_3O_{27}$. The concentrations of iron ions in these compounds differ on 0,125, i.e. not the more, than for the first couple of compounds.

From mossbauer investigations of first couple of compounds it follows, that temperature difference of the magnetic transition is 130-140°C. Such difference of the transition from the paramagnetic state in the supermagnetic state takes place for this couple from the magnetic measurements. For the second couple of compounds the considering differences are ~60-70°C.

It is noted, that dependence of magnetic transition temperature in the massive three-dimensional magnetodiluted systems on the magnetic ion concentrations were studied in refs [10, 11].

Thus, from the obtained results we can do the conclusion, that in the compounds with the less number of monooctahedron layers in the perovskito-like packet (in more thin film), the change of the magnetic transition temperature, than in the compounds with big number of the monooctahedron layers in the perovskito-like packet (in more thick film).

[1] *I.G. Ismailzade, V.I. Nesterenko, F.A. Mirishli, P.G. Rustamov.* Kristallografiya, 1967, t.12, N3, s.468-473. (in Russian).

[2] *J.S. Smart*. J. Phys. Chem. Sol., 1969, vol. 16, N3-4, p.169-172.

[3] *S.A. Kidzhayev, G.D. Sultanov, F.A. Mirishli*. FTT, 1973, t. 15, N1, s. 297-300. (in Russian).

[4] *G.D. Sultanov, N.G. Guseynov, I.G. Ismailzade, R.M. Mirzababayev, L.A. Aliyev*. FTT, 1975, t.17, s. 1940-1943. (in Russian).

[5] *G.D. Sultanov, N.G. Guseynov, R.A. Mirzababayev, F.A. Mirishli*. FTT, 1976, t. 18, s. 2562-2564. (in Russian).

[6] *S.V. Vonsovskiy*. Magnetizm, M., Izd-vo"Nauka", 1971, s. 1032. (in Russian).

[7] *J. Cohen, K.M. Green, R. Rauthenet*. J. Phys. Soc. Japan, 1962, vol. 17, Suppl., B-1, p.685-688.

[8] *G.J. Muench, S. Aragts, F. Matievich*. J. Appl. Phys., 1981, vol. 52, N3, p.2493-2494.

[9] *I.P. Suzdalev*. Dinamicheskiye effekti s gamma-rezonansnoy spektroskopii. M., Izd-vo "Atomizdat", 1979, 192 s. (in Russian).

[10] *S. Krupichka*. Fizika ferritov i rodstvennikh im magnitnich okislov. T. 1, Izd-vo "Mir", 1976, 353 s. (in Russian).

[11] Khimicheskiye primemeniya messbauerovskoy spektroskopii. M., Izd-vo "Mir"1970, 502 s. (in Russian).

Q.C. Sultanov, M.Ə. Alcanov, A.M. Abdullayev, M.C. Nəcəfzadə, M.B. Hüseynli

$Bi_{m+1}B_mO_{3m+3}$ (B=Ti, Fe) LAYLI KRİSTALLARDA NQR VƏ MAQNİT QAVRAYICILIĞI

Bu işdə laylı quruluşa malik $Bi_{m+1}B_mO_{3m+3}$ (B=Ti, Fe) birləşmələrinin maqnit və messbauer tədqiqatlarının nəticələri müzakirə edilmişdir. Müəyyən edilmişdir ki, dəmir ionlarının konsentrasiyasının maqnit keçidi temperaturuna təsiri, üçolçülü maqnetiklərdəkindən kəskin fərqlənir.

Г.Д. Султанов, М.А. Алджанов, А.М. Абдуллаев, М.Ж. Наджафзадя, М.Б. Гусейнли

ЯГР И МАГНИТНАЯ ВОСПРИИМЧИВОСТЬ СЛОИСТЫХ КРИСТАЛЛОВ $Bi_{m+1}B_mO_{3m+3}$ (B=Ti, Fe)

В настоящей работе проведено обсуждение результатов магнитных и мессбауровских исследований соединений $Bi_{m+1}B_mO_{3m+3}$ (B=Ti, Fe), прявляющих вследствии специфичности кристаллической структуры свойства, характерные для тонких магнитных пленок. Показано, что влияние концентрации магнитных ионов железа на температуру магнитного перехода в этих соединениях существенно отличается от подобного влияния в трехмерных магнетиках.

Received: 20.04.04

THE INVESTIGATION OF GELATINCREATION PROCESSES IN THE SYSTEM OF AGAROSA-WATER-CARBAMIDE

E.A. MASIMOV, V.V. PRUDKO, A.A. GASANOV, R.N. ISMAYLOVA
NII"Physchemistry of macromolecule solutions" of physic facultee
of Baku State University,
370148, Baku c, ac. Z. Khalilov str., 23.

In the given paper the influence of carbamide on the gelatincreation process on the structuring in the water agarosa solutions with the use of the dispersion method of the optical density, has been studied. The temperature dependences of the optical density at the cooling of the solutions and heating of gelatins are obtained. The temperatures of gelatincreation and melting, sizes and number concentration (particle number in the volume unit) of the submolecular particles, are obtained. It is established, that carbamide dumps the gelatincreation process, shifting the temperatures of the melting and the beginning of the gelatincreation to the region of more low temperatures. Carbamide, destroying the intermolecular and helium communications, the water structure, weakens the gelatin strength.

Key words: *agarosa, carbamide, water solutions, gelatincreation, structuring, gelatincreation temperature, melting temperature, gelatin strength, hysteresis.*

The solutions of some polymers at the definite concentration and conditions have the possibility of the gelatincreation. This takes place after the achieving of such state, at which the energy of the polymer interaction with the solvent becomes less, than the energy of macromolecul interaction [1]. In the result between macromolecules, and between their associates and agregates also are the local communications, leading to the grid creation. At the detail considering of the gelatin structure it is need to take into consideration, that the submolecular structures of the fluctuation character with the different continuous of "life" appear besides of the stable compounds in the polymer systems. Gelatins, formed by polymer solutions at the change of the temperature and composition are heterogeneous and that's why they have the such high light scattering, as the colloid systems. In the dependence on the gelatincreation conditions, the number and size of dispersion phase particles change and the light scattering intensity changes correspondingly. The gelatin of the solutions of many polymers can be achieved by the addition of the precipitant to them, and at the change of the chemical composition of the solved polymer, also. In all these cases the gelatin takes place in the result of the system transition in the state of the limited compatibility of the polymer with the solvent.

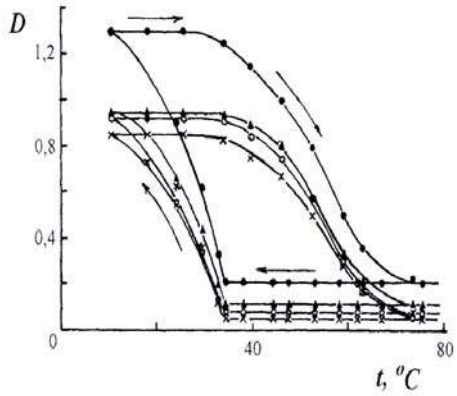

Fig.1. The temperature dependences of optical for 1% agarosa solution at the different wave length: • - 400, ▲ - 490, o -540, x - 670.

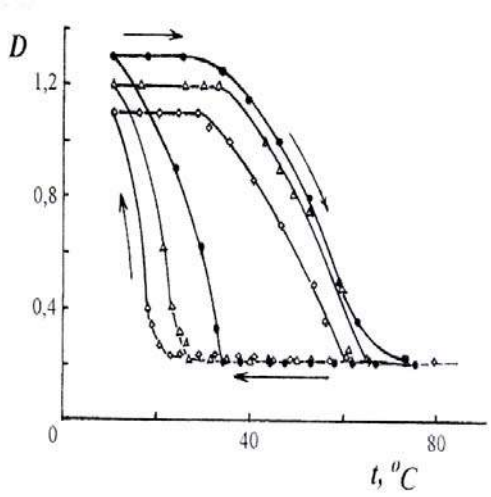

Fig.2. The temperature dependencies of optical density of 1%water agarosa solutions without (•) and at the carbamide addition: 1M(Δ) and 3M(◊) λ=400nm.

In the given paper the gelatin of the water solutions of the one from the gelatincreating polymers is considered, especially agarosa at the change of the temperature and solvent composition. Using the concentration photoelectric calorimeter (KFK-2), the temperature dependencies of the optical density of the (D) solutions, given on the fig.1 with the dependence $D=f(t°)$ for 1% agarosa solution at the different wave lengths, were fixed. (Such dependencies had been obtained for the rest solutions).The agarosa concentration was kept constant -1%, but carbamide concentration, used as the addition, was 1,5 and 3 moles. The dependencies $D=f(t°)$ for the all investigated solutions at λ=400nm were given on the fig.2. The technique of investigation is described in [2]. The temperature dependences of the optical density were obtained as at the cooling from ≈80°C till the room temperature, so at the heating from the room temperature till the gelatin melting temperature (t_{ml}). These temperature dependences don't combine, but they create the hysteresis loops, because of the discombination of the gelatin and melting temperature. It is well known [3] that in always gelatincreating system the melting temperature is higher, than gelatin temperature (t_{gel}). The hysteresis reason of the melting and gelatin is in the clear difference of the mechanisms of the creation and melting of the gelatins. The gelatin creation takes place

through the consequence of many steps, demanding the definite cooling and time, but melting of the gelatin has all signs of the cooperate transitions. The system turbidity increases at the agregiroation and creation of the grid points. In the overwhelming majority of the gelatins the grid points are created by submolecular elements or so-called by the submolecular particles (SMP), the sizes of which change with the temperature and solvent nature. For the defining of the R sizes and number concentration of N particles (number of particles in the volume unit), the method, worked by Clenin with collaborations [4] on the base of Mi theory and being in the optical density measurement at the different wave lengths of the fallen light, is used.

Taking into consideration the experimental data, we can say the following. According to the generally accepted Ris model for the polysaccharides [5], one of which agarosa is, macromolecules in the solution at the high temperatures are rolled in balls. They unroll at the temperature decreases and create the spirals, later bispirals. These bispirals join in the aggregates (SMP). As at the high temperatures the optical density doesn't change, so it is clear, that sizes of these particles are small yet. The SMP increase at the temperature decrease, and when their size becomes enough, the turbidity takes place, at which is equal to the strong increase of the optical density (fig.1 and 2). In this time the first local communication between SMP appear, i.e. the rudiments of the space gelatin grid also appear. This is equal to the bendings on the cooling curves $D=f(t°)$. Temperature, considering to such is the temperature, beginning with which the creation of gelatin (t_{gel}) is possible. At the later temperature decrease the number of communications increases, leading finally to the creation of the gelatin grid. For the clarity t_{gel} was fixed also by kinetic dependencies of the optical density $D=f(t°)$, where t is time. Moreover, the D values in the bending region were taken through 1°C or 0,5°C. For example, in the paper the such dependencies $D=f(t°)$ for 1% solution of agarosa (fig. 3) are given. As it is seen from the fig.3, the optical density at the temperatures, which are higher, than t_{gel}, is kept constant. But at the first signs of gelatin creation, i.e. at $t \le t_{gel}$, the temperature becomes change with time. After the full forming of the gelatin, the optical density again stays constant with the time change.

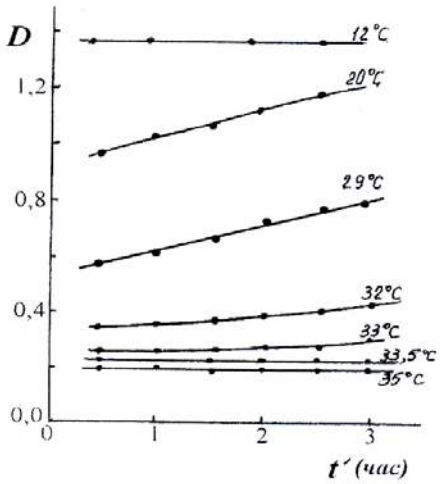

Fig.3. The kinetic dependencies for 1% water agarosa solution at λ=400nm

If we consider the heating curves, that it is seen on them, that with the temperature increase the optical density firstly doesn't change till the definite temperature, considering to the be beginning of the gelatin destruction, but later it decrease till the temperature of full gelatin melting (t_{mel}), at which the optical density becomes equal to D at high temperatures, from which the measurements of cooling curves had begin. The defined by such way, t_{gel} and t_{mel} are given in the table 1.

Table1

System:1% agarosa+water+carbamide

Concentration of carbamide, mole	Squares of hysteresis, S_h				t_{gel}, °C	t_{mel}, °C
	λ=400	λ=490	λ=540	λ=670		
-	31.9	27.65	24.1	23.6	33.0	73.5
1.5	30.3	26.73	22.9	22.48	26.5	66.0
3.0	29.3	24.55	21.1	21.78	21.0	60.0

On the base of the experimental data and according to the ref [4], the sizes of SMP and their number concentration in the dependence on the temperature for all investigated solutions, taking into consideration the optical density values, obtained at the cooling of the solutions, had been calculated. The temperature dependences of values R and N are given on the figures 4-6. From the figures it is seen, that dependencies $R=f(t°)$ are analogical to the dependencies $D=f(t°)$. In the high temperature region the particle sizes stay constant, but beginning from the some temperature $t \le t_{gel}$, the growth of these particles, which continues till the room temperature, when solution transfer to gelatin, takes place. For the SMP number the inverse dependence is observed, i.e. if there are polymer chains join, so there are many R, and there are less N.

Let's consider the influence of the carbamide on the gelatincreation process in the water solutions of agarosa. It is known, that carbamide destroys the water structure, increasing the part of water in the monomolecular state, and by this increases the growth of its activity as solvent [6.7]. The creation of stable helium communications of water molecules with carbamide molecule, leads to the such orientation of water molecules, which difficulties the creation of the helium communications in the solvent and this is caused the water structure destruction. In the ref [8] for the water solutions of carbamide the structure temperatures (T_{str}), characterising the degree of the solution structuring in respect to the pure water, are defined. The structure temperatures, given in the ref [8] for the carbamide water solutions in the wide interval of its concentrations, decrease from T_{str} for pure water (≈147°K) till 0°K at carbamide

concentration, which is equal to 10 moles, that proves about decrease of water structuring with the increase of carbamide concentration till full destroying at 10 moles of carbamide. The investigation of 0,1% solution of agarosa, not creating the gelatin [8], shows, that with the addition of carbamide (from 1 till 8 moles), the structure temperature of solutions decreases and although T_{str} of agarosa solutions is higher than T_{str} for pure water at carbamide concentrations 1,5 and 3 moles, it becomes lower, than T_{str} for the agarosa water solution without carbamide (table2). This says about that although carbamide destructures the water and increases of its solving capability, that leads to the T_{str} of agarosa water solutions with carbamide, but agarosa itself keeps some structuring capability to the water, and weakens the carbamide action on the water.

Table 2

System:Agarosa (0,1%)+carbamide+water(data of ref [8])

Carbamide concentration, mole	Structural temperature of carbamide water solutions T_{str}, K	Structural temperature of agarosa water solutions with carbamide T_{str}, K
-	147	253
1	135	193
1.5	126	180
3	110	154
5	88	138
7	65	130
8	55	114

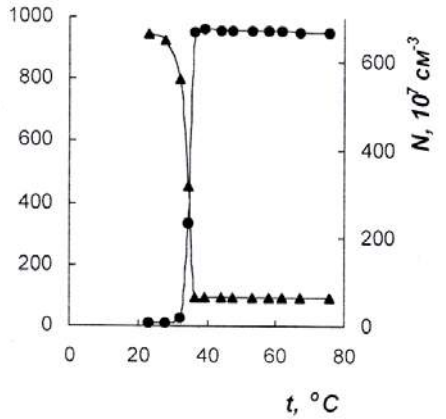

Fig.4. The temperature dependencies of *R* and *N* for 1% water agarosa solution.

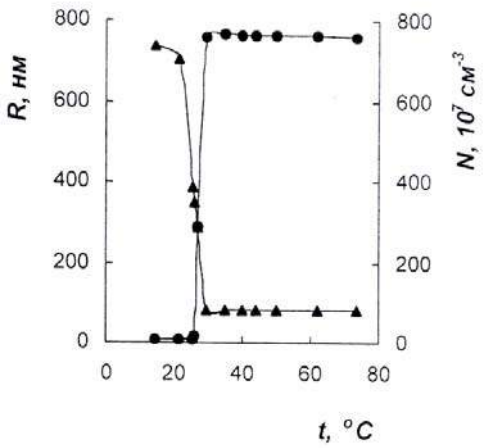

Fig.5. The temperature dependencies of *R* and *N* for 1% water agarosa solution at the presense of 1,5M carbamide.

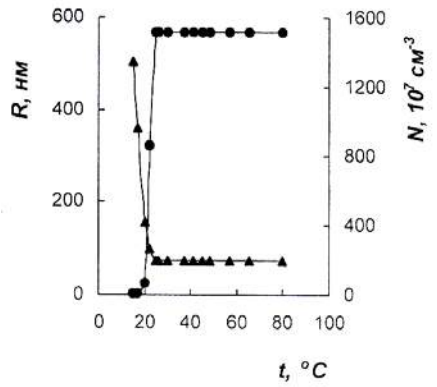

Fig.6. The temperature dependencies of *R* and *N* for 1% water agarosa solution at the presence of *M* carbamide.

In the case of solutions, creating the gelatins, besides the carbamide influence on the water, carbamide molecules act on polymoleculaes, destroying the helium communications. It all should be lead to worth of gelatin and decrease of parameters, characterising the gelatincreating systems, that is proved in ref [9,10], where reological investigations, carried out with the water solutions of agara and agarosa at urea concentrations from 1 till 10 moles, show the strong carbamide influence on the gelatin creation processes in these solutions. The results of the given paper prove this. The values D, t_{gel}, t_{mel} and R with the carbamide addition (fig.2,4-6 and tables), i.e. with the increase of activity, i.e/ the solving capability of solvent (water) strongly decrease, that is proved about weak of points of the space grid of gelatin and destruction of gelatin itself. It is possible, that the influence of intermolecular and helium communications decreases, that leads to the decrease of the intensity of gelatins in urea presence. This also proves the decreases about creation of less intensive gelatins at the addition of carbamide.

[1] Enciklopediya polimerov. M.: izd. Sov. enc., 1977, t. III, s. 556. (in Russian).

[2] *S.A. Gadziyev, E.A. Masimov, V.V. Prudko.* Izv. AN Az. SSR, 1981, № 4, s. 90-95. (in Russian).

[3] *L.Z. Rogovina, G.L. Slonimckiy.* Uspekhi kimii, 1974, t.XLIII, vip. 6, s 1102-1135. (in Russian).
[4] *V.I. Klenin, S.Yu. Shshegolev, V.I. Lavruilin*. Kharakteristicheskiye funkcii svetorasseyaniya dispersnikh system. Izd. Saratovskogo gosud. Un-ta, 1977. (in Russian).
[5] *D.A.Rees*. Structure, conformation and mechanism in the formation of polysaccharide gels and network. – Adv. Carbohydrate Chem. Biochem., 1969, v. 24, p.267-332.
[6] *S.P.Moulik, D.P.Khan*. Activation parameters for fluidity of water influenced by glucose, sucrose, glycerol, mannitol, sorbitol. – Indian J.Chem., 1978, v. 16A, p.16-19.
[7] *K.Ueberreiter.* Change of water structure by solvents and polymers. Part 3. – Colloid and Polym. Sci., 1982, v. 260, № 1, p. 37-45.
[8] *E.A. Masimov, A.A. Gasanov, R.N. Ismailova.* Fizika, izd. Elm, Baki, 2000, cild VI, №4, s. 55-58.
[9] *E.A. Masimov, V.V. Prudko, L.I. Khomutov.* Khimiya i kim. tekhnologiya, 1985, t. 28, vip. 11, s. 74-77. (in Russian).
[10] *E.A. Masimov, V.V. Prudko.* Strukturno-mekhanicheskiye svoystva vodnikh I vodno-organicheskikh studney agarozi i agara. V sb. Elektronniye yavleniya v tverdikh telakh i gazakh. Baku, izd. AGU, 1982, s. 57-61. (in Russian).

E.Ə.Məsimov, V.V.Prudko, A.A.Həsənov, R.N.İsmailova

AQAROZA-SU-KARBAMİD SİSTEMİNDƏ GELƏMƏLƏGƏLMƏ PROSESİNİN TƏDQİQİ

İşdə optik sıxlığın dispersiyası metodu ilə karbamidin aqarozanın sulu məhlullarında geləmələgəlmə prosesinə təsiri öyrənilmişdir. Məhlulların soyudulması və qızdırılması prosesində optik sıxlığın temperatur asılılığı alınmışdır. Məhlulların geləmələgəlmə və ərimə temperaturları, molekulüstlü hissəjiklərin konsentrasiyası və ölçüləri təyin olunmuşdur. Müəyyən olunmuşdur ki, karbamid geləmələgəlmə prosesini ləngidir və onların temperaturun kiçik qiymətləri istiqamətində sürüşdürür. Karbamid molekullararası hidrogen rabitələrini qırır və bununla da gelin möhkəmliyini azaldır.

Э.А.Масимов, В.В.Прудько, А.А.Гасанов, Р.Н.Исмаилова

ИССЛЕДОВАНИЕ ПРОЦЕССОВ СТУДНЕОБРАЗОВАНИЯ В СИСТЕМЕ АГАРОЗА-ВОДА-КАРБАМИД

В данной работе изучено влияние карбамида на процесс студнеобразования, на структурирование в водных растворах агарозы с использованием метода дисперсии оптической плотности. Получены температурные зависимости оптической плотности при охлаждении растворов и нагревании студней. Определены температуры студнеобразования и плавления, размеры и числовая концентрация (число частиц в единице объема) надмолекулярных частиц. Установлено, что карбамид тормозит процесс студнеобразования, сдвигая температуры плавления и начала студнеобразования в область более низких значений. Карбамид, разрушая межмолекулярные и водородные связи, разрушая структуру воды, ослабляет прочность студней.

Received: 05.02.04

THE UNIVERSAL THEORY OF THE THREE-WAVE OZONOMETRIC MEASUREMENTS

H.G. ASADOV, M.M. ALIYEV, A.A. ISAYEV
Azerbaijan National Aircosmic Agency

In the paper "Universal theory of three-wave ozonometric measurements" the theoretical possibility of almost full compensation of sum error of three-wave ozonometer measurement, used for the measurement of the common ozone content in the atmosphere is shown. The algorithm of working of device is presented; the theoretical substantiation of compensation is given.

Key words: The common ozone content, aerosol error, ozonometer, optical density, two-wave technique.

As it is known [1], nowadays the base method for the common content of ozone in the atmosphere is the two-wave method of measurement, based on the reducing law of the radiation in the atmosphere - Buger law, which has the following form:

$$S_\lambda = S_{\lambda_0} \cdot 10^{-\left| \alpha_\lambda X \mu + \beta_{\lambda_0} m + \delta_\lambda m_1 \right|} \qquad (1)$$

where S_λ is the flux of the direct sun radiation on Earth surface; S_{λ_0} is the same flux on the top surface of the atmosphere; α_λ is the absorption index of the ozone radiation, to the wave length λ; X is the sum ozone in the atmosphere;, measured in atm/cm; β_{λ_0} is the optical density of the reley atmosphere; δ_λ is the optical density of the atmospheric aerosol for the wavelength λ; μ, m, m_1 are relative optical densities of the ozone layer of the reley atmosphere and aerosol layer, which are ratios of the considering optical densities in the gradient direction to the mentioned optical densities in the vertical direction.

The physical mean of the formulae (1) is that reducing of radiation in the atmosphere takes place because of: 1) absorption in the band; 2) stray radiation in the pure air; 3) reducing of the radiation in the aerosol.

Also, it is known [1], that common error of the measurement of the common ozone content (COC) by the two-wave method is defined as

$$\frac{\Delta X}{X} = \frac{(\beta - \beta')\, m}{(\alpha - \alpha')\, \mu\, X} + \frac{(\delta - \delta')\, m_1}{(\alpha - \alpha')\, \mu\, X} . \qquad (2)$$

In the ref [2] the three-wave ozonometer was given, allowing to increase the exactness of the ozonometric measurements. Before, that we consider the functional possibilities of the given ozonometer, we note the conventional signs, which will be used in the following explanations:

$\delta=\delta(\lambda)$ is the functional dependence of aerosol optical density on the radiation wave length. According to the ref [1], $\delta(\lambda)$ is the line function in the diapazon300-340 nm, practically:

$\beta=\beta(\lambda)$ is the functional dependence of the reley atmosphere optical density on the radiation wave length:

λ_1 is the first main wave length, where the first main calculation (measurement) S_{λ_1} takes place;

λ_2 is the second correct wave length, where the second auxiliary calculation (measurement) S_{λ_2} takes place;

D_1 is the operator of the calculation working S_1 and S_2 for the obtaining of the following calculated values:

1) Calculated value S_p, depending S_{λ_1} and S_{λ_2}, i.e. $S_p = f_1(S_{\lambda_1}, S_{\lambda_2})$;

2) Calculated value β_p, depending on β_{λ_1} and β_{λ_2}, i.e. $\beta_p = f_2(S_{\lambda_1}, S_{\lambda_2})$;

3) Calculated value δ_p, depending on δ_{λ_1} and δ_{λ_2}, i.e. $\delta_p = f_1(S_{\lambda_1}, S_{\lambda_2})$;

4) Calculated value length λ_p, defined or on δ_p or on β_p;

5) λ_3 is the third main wave length, where the third main calculation (measurement) S_3 takes place;

6) D_2 is the operator of λ_3 change;

7) D_3 is the operator of the operations carrying out under the exit values D_1 and D_2 for the calculation of the found value X.

The algorithm of the three-wave measurer working has the different form at the carrying out of the COC measurements in the dependence on the concrete given aim. That's why it is needed to consider the tasks, which are solved by the three-wave method step by step.

The algorithm of the three-wave COC measurer working generally has the following form (fig.1).

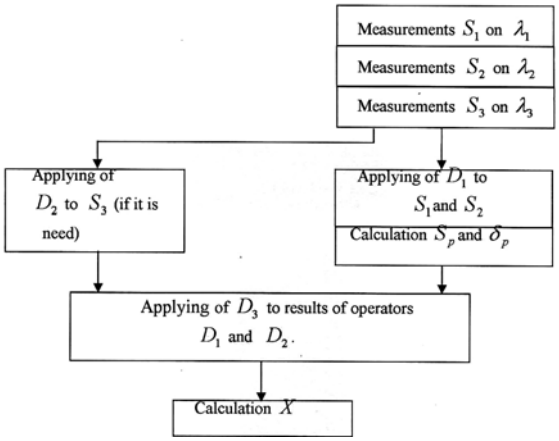

Fig.1. Common algorithm of three-wave oozonometric measurements.

By words, the algorithm of the device working can be expressed in the form of the following consequence of the carried out operations:

1) Carrying out of the measurements S_i on λ_1 (i=1,2,3)
2) Applying of D_1 to S_1 and S_2
3) Applying of D_2 to S_3

4) Applying of D_3 to the exit values D_1 and D_2

The private algorithms of the device are differ from the general algorithm, i.e. in this case operators D_1, D_2, D_3 have the concrete mathematic meaning.

1. USING OF THREE-WAVE METHOD FOR THE DECREASE OF THE AEROSOL ERROR.

As it is known [1], the relative aerosol error in the two-wave ozonometer is calculated as

$$\frac{X - X'}{X} \cdot 100\% = \frac{(\delta - \delta') \cdot 100\%}{(\alpha - \alpha')X} \quad , \qquad (2)$$

where the first three of parameters (X, δ, α) are equal to the wave length л1, but second three parameters (X', δ' α') are equal to the wave length λ_2.

The operator D_1 for the three-wave ozonometer has the meaning of the following consequence of the mathematic operations

$$D_1 = M \cdot R$$

where M is multiplication operation; R is

The operator D_2 in the given case has the shift meaning $S_3(\lambda_3)$ till the value $S_3'(\lambda_3 \pm \Delta\lambda_3)$.

The cases, when the applying of D_2 isn't necessary, are possible. The operator D_3 in the given case has the meaning of the fission and logarithmic of the D_1 and D_2 results.

Thus, the algorithm of the three-wave ozonometric measurements with the aerosol error compensation has the form (fig.2).

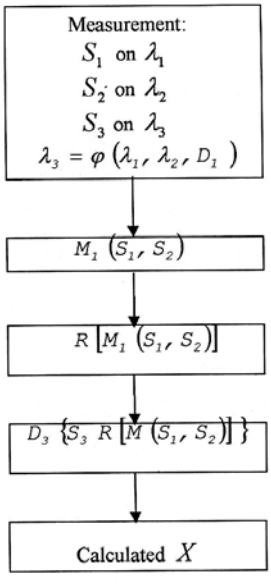

Fig.2. The algorithm of three-wave ozonometric measurements with compensation of aerosol component.

In the device in the given case the equality δ_{λ_3} and δ_{λ_p}, where δ_{λ_p} is the aerosol density of the considering to the calculated wave length λ_p, takes place.

As it was mentioned earlier, λ_p can be defined on the base λ_1 and λ_2, on the dependence $\delta(\lambda)$ or on dependence $\beta(\lambda)$ (in the dependence on the given aim). In the considered case

$$D_1 = M \cdot R \,,$$

where M is the multiplication operation; R is λ_p is calculated by the formulae

$$\lambda_p = \frac{\lambda_1 + \lambda_2}{2}$$

Moreover, ideally the condition $\lambda_3 = \lambda_p$ should be kept. However, there are set of reasons, because of which $\delta_{\lambda_3} \neq \delta_{\lambda_p}$. They are:

1) Error of λ_p calculation
2) Error of $\delta(\lambda)$ nonlinearity.

For the clearing of the given error, the measurer algorithm is changed by the way of the input of the operator R (fig.3) regulation possibility.

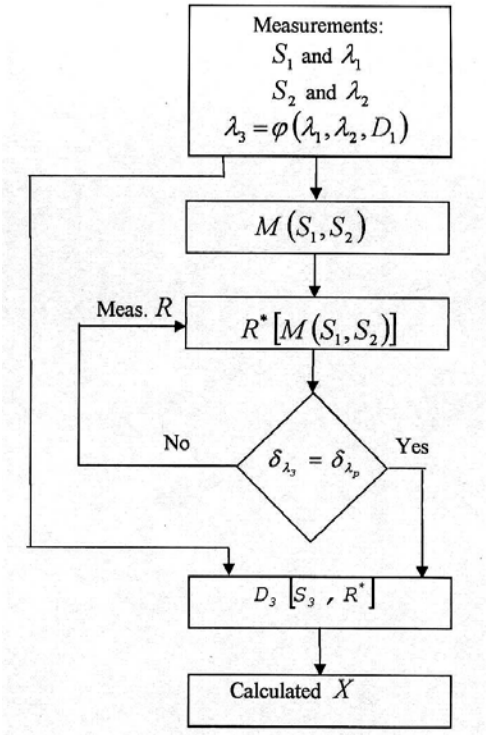

Fig. 3. Correction of error by the way of R^* regulation.

The meaning of that correction is in the some shifting of λ_p, in order to obtain $\delta_{\lambda_3} = \delta_{\lambda_p}$.

Such correction also can be obtained by the shifting of λ_3, however this would need the applying of set of filters with the nearest pass bands (set of bands), that is connected with the technical difficulties.

2. EFFECT OF FULL COMPENSATION OF SUM ERROR IN THE THREE-WAVE OZONOMETER.

As it was also mentioned, the full error of the two-wave ozonometer at the absence of the external impurity in the atmosphere is calculated by the formulae (2). In general case

$$\chi_{\Pi} = \chi_1(\beta) + \chi_2(\delta) \quad ,$$

where χ_{Π} is the full error of ozonometer; $\chi_1(\beta)$ is error component because of the scattering of pure atmosphere; $\chi_2(\beta)$ is error component because of aerosol influence.

The common conception of the mutual compensation of components $\chi_1(\beta)$ and $\chi_2(\beta)$ is in the such choose of the calculated wave length λ_p, that χ_1 and χ_2, calculated on the results of measurements in λ_3 and λ_p, would have the opposite signs and equal values on the absolute value. For the achieving of the given condition, the two ways can be used:

1) The regulation of operator R^*, i.e. the regulation in the calculated device, in the result of which λ_p will be differ from $\frac{\lambda_1 + \lambda_2}{2}$ on the value $\pm\Delta\lambda^*$, i.e. $\lambda_p = \frac{\lambda_1 + \lambda_2}{2} \pm \Delta\lambda^*$

2) λ_3 regulation by the way of using of many optical filters with the band in λ_{3i}; $i = \overline{1,n}$. However, as it was mentioned earlier, this way unpractical and too difficult.

Block is circuit of algorithm working of device is shown on the fig.4.

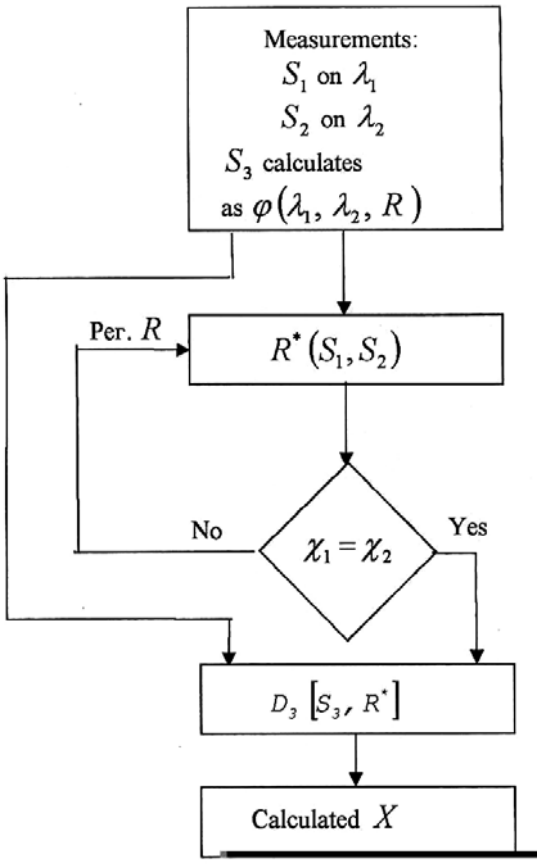

Fig.4. Block is circuit of algorithm of working of device.

The condition of practically full mutual compensation of error components χ_β and χ_δ can be expressed by the following way:

$$|\chi_\beta| = |\chi_\delta|$$

or

$$\left|\beta(\lambda_3^*) - \beta_p^*\right| m = \left|\delta(\lambda_3^*) - \beta_p^*\right| m_1 \quad . \qquad (4)$$

Thus, the meaning of the full compensation of sum error of three-wave ozonometer is in the carrying out of regulation λ_3^* or β_p^* with the aim of the carrying out of the condition (4).

Let's give the graphic interpretation of the mutual compensation of the above considered error components.

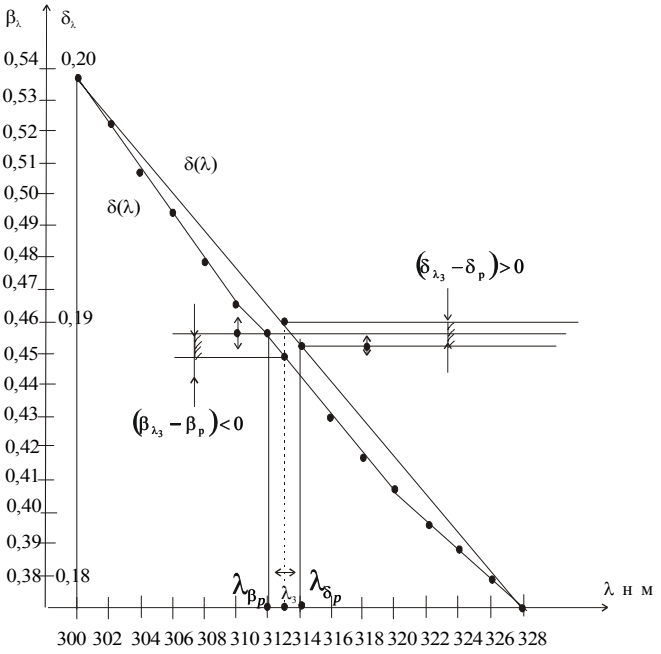

Fig.5. The graphics of dependencies β_λ and δ_λ on wave length λ.

The graphics of the dependencies β_λ and δ_λ on the wave length λ are shown on the fig.5. Taking into consideration $m \approx m_1$, effect of the mutual compensation from the graphic statements can be expressed by the following way:

$$\left|\beta_{\lambda_3} - \beta_p\right| = \left|\delta_{\lambda_3} - \delta_p\right|,$$

where β_{λ_3} is the value of reley scattering of atmosphere on the wave length λ_3; δ_{λ_3} is aerosol optical density on the wave length λ_3; β_p is the calculated value of β component, calculated on the curve $\beta(\lambda)$, from the condition $\beta_p = \frac{\beta_{\lambda_1} + \beta_{\lambda_2}}{2}$; δ_p is the value of δ component on the calculated wave length λ_{p_δ}, calculated on the curve $\delta(\lambda)$ from the condition $\delta_p = \frac{\delta_{\lambda_1} + \delta_{\lambda_2}}{2}$.

In the end we note, that revealed additional possibilities of later increase of the three-wave ozonometer clarity are realized by the famous technical means and don't present any difficulty in the practical realization plan.

[1] *G.P. Gushshin, N.N. Vinogradov*. Summarniy ozon v atmosphere. Leningrad, Gidrometeoizdat, 1983. (in Russian).

[2] Polojitelnoye resheniye № a20030134 ot 23.06.03 o vidache Patenta Azerbaijanskoy Respubliki na izobreteniye "Tryekhvolnoviy ozonometr"avtorov*: Kh.G. Asadova, A.A. Isayeva*. (in Russian).

H.H. Əsədov, M.M. Əliyev, A.A. İsayev

ÜÇDALĞALI OZONOMETRİK ÖLÇMƏLƏRİN ÜMUMİ NƏZƏRİYYƏSİ

"Üçdalğalı ozonometrik ölçmələrin ümumi nəzəriyyəsi" məqaləsində atmosferdə ozonun ümumi miqdarının ölçülməsi üçün istifadə edilən Dobson spektrofotometrinin üçdalğa modifikasiyasının jəm ölçmə xətasının tam kompensasiyası imkanının nəzəri mümkünlüyü göstərilmişdir. Ölçmə qurğusunun iş alqoritmi və kompensasiya şərtlərinin nəzəri əsasları verilmişdir

Х.Г. Асадов, М.М. Алиев, А.А. Исаев

ОБЩАЯ ТЕОРИЯ ТРЕХВОЛНОВЫХ ОЗОНОМЕТРИЧЕСКИХ ИЗМЕРЕНИЙ

В статье "Общая теория трехволновых озонометрических измерений" показана теоретическая возможность почти полной компенсации суммарной погрешности измерения трехволнового озонометра, используемого для измерения общего содержания озона в атмосфере. Приведен алгоритм работы устройства, дано теоретическое обоснование условия компенсации.

Received: 25.12.03

THE UNIVERSAL INTERCOMMUNICATION AND MUTUAL CAUTION OF THE CRYSTAL PROPERTIES

N.A. ABDULLAYEV
The Institute of Physics of NAS of Azerbaijan,
Baku Az - 1143, av. Javid, 33.

In the present paper the intercommunication, interaction and mutual caution of the main five crystal properties are discussed. On the example of the real physical laws it is shown, that these intercommunication, interaction and mutual caution are observed clearly and revealed.

It is known, that the dialectical approach to the nature perception proposes, that non effect can't be understood, if it takes in the isolate form, out of the connection with the surrounding phenomena. The dialectics considers the nature not as the accidental accumulation subjects, separating, isolating and independent from each other, but as the unit ones; where subjects and phenomena are connected with each other organically, depend and cause each other. In the above mentioned context, the physical phenomena and physical crystal properties aren't the exception. Moreover, the thermodynamical development, addition of the thermodynamical principles to the reversible processes has revealed, that for every from the physical effects, connecting these or that physical properties, the reversible effects should exist. For example just in 1887, the electrocaloric effect, reversible to the pyroelectric one, was predicted by Calvin on the base of thermodynamics. Analogically, firstly the existence of the inverse piezoelectric and many other effects was theoretically predicted, later it was experimentally proved.

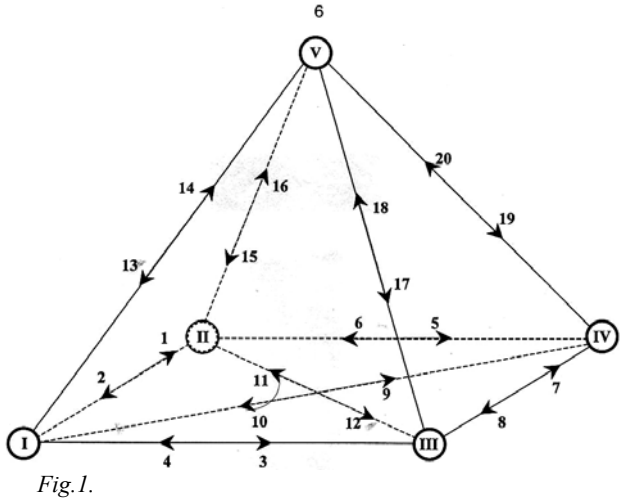

Fig.1.

Earlier the attempts of the circuit considering of the set of physical crystal properties in their interaction and mutual caution were considered. For example, the Heckman triangle, described in the famous book of J.Nai in details and Kedy tetrahedron exist, with the help of which the authors show clearly the intercommunication, interconnection and mutual caution of three (mechanical, heat and electric properties) [1] or four (mechanical, heat, electric and magnetic properties) [2] of the main physical crystal properties. In the present paper, the pyramid is given by author (fig.1), with the help of which the interconnection, interaction and mutual caution of the five main physical crystal properties - mechanical heat, electric, magnetic and optical ones. On the coincidence that the experiments were carried out by the author of present paper and the mechanical (Grunaisen parameters and elastic constants) [3], heat (heat expansion and heat conduction) [4,5], electric anisotropy of electric conduction and jump conduction), [6], galvanomagnetic (Hall effect and magnetoresistance) [7], and optical (the influence of the uniaxial deformation on the exciton energetic position in the absorption spectrums) [8] crystal properties were studied. Therefore, in all cases the temperature dependencies of physical characteristics - from the helium temperatures till room temperatures were investigated.

In the vertexes of the given pyramid (fig.1), characterising the intercommunication, interaction and mutual caution of five main physical crystal properties, the Rome numbers are dedicated:

I - heat properties
II - electric properties
III - optical properties
IV - magnetic properties
V - mechanical properties

It is need to note the several peculiarities of the given pyramid. The first peculiarity is the presence in the vertexes of so-called main effects, inherent to each of physical properties. The main effects are expressed by the very simple ratios (line and one-argument functions) mathematically, but in the different forms. For example, in scalar form - heat ($\Delta Q=C\Delta T$) and optical properties (Plank formulae $E=h\nu$), in vector form - electric($\vec{D} = \varepsilon \vec{E}$) and magnetic ($\vec{B}=\mu \vec{H}$) properties, in tensor form - elastic properties (Guk law $\sigma_{ik}=c_{iklm}u_{lm}$). In these main effects the intercommunication between action of the external "forces" is revealed, in role of which are temperature change ΔT, frequency ν, strengths of electric $\vec{E}$ and magnetic $\vec{H}$ fields, voltage σ_{ik} and crystal reaction, which are quantity of heat ΔQ , energy E, electric $\vec{H}$ and magnetic $\vec{B}$ inductions, deformation u_{im}, accordingly.

The second peculiarity is the fact, that all physical effects in crystals, characterising this or that physical crystal property reveale, interact between each other and are described with the help of the fields, theoretically. Heating the crystal in the definite place, we create the temperature gradient or temperature field. The electric and magnetic properties of the compounds are revealed especially with the help of electric and magnetic fields. The light is optical radiation presenting itself the electromagnetic field. Giving

the some mechanical action on the crystal, we create the field of the mechanical stresses in the crystal.

Third, by the number, but not by the importance, peculiarity is interconnection and mutual caution of physical properties and effects, that show the mutual direction of the communications in the pyramid (fig.1). For example, the communication of the heat **I** and electric properties **II** is mutual. From the one side (the direction of the pointer **1**), the temperature change in the crystal can be followed by the electric induction (pyroelectricity) or electric current (thermoelectricity, Zeebek effect), that is caused the existence and change of the electric resistance, but from the other side (pointer **2**) - the existence of the effects of heat generation or absorption, caused by the electric field (electrocaloric Jouel-Lenz effect, Peltye effect). The communication of the heat **I** and optical **III** properties is also mutual. As it is known, the heat bodies radiate (heat radiation) – pointer **3** and vice versa of optical pyrometers is based on the effect of the heat radiation influence – pointer **4**. The intercommunication of the electric II and magnetic IV properties is also mutual (pointers **5, 6**) and are described by the well known Maxwell equations, and galvanomagnetic and other effects also. The communication of the optical **III** and magnetic **IV** properties is also mutual - in the magnetic field (pointer **7**) is the rotation of polarization plane of the transmitted beam (Faradei effect) and the rebuilding of the atom energetic levels (Zeeman effect), from the other side the light is the electromagnetic wave with the magnetic field component of the electromagnetic field. The physical properties are also mutual, being on the diagonal of the pyramid base **I** and **IV**, and **II** and **III** also. For example, the temperature dependence of the magnetic susceptibility (Curie-Lanjevena law) or the existence of Curie point in the ferromagnetics - pointer **9** and the effect of the obtaining of the ultralow temperatures by the technique of adiabatic demagnetization or the effect of the temperature gradient appearance, perpendicular to the magnetic field and electric current (Ettingshausen effect) - pointer **10**. The photoelectric effects in the crystals (photoeffect, photoconduction and others) – pointer **11** and from the other side, electrooptical effects, acts of light absorption and radiation, rebuilding of the energetic levels under electric field action (Stark effect) – pointer **12**.

The fourth peculiarity is that circumstance, that in the vertex of pyramid the mechanical properties are situated- **V**. This is evidence to the fact, that the character sizes of the crystal, parameters of the crystal lattice are the more sensitive characteristics, mostly defining its crystal properties. The essential role of deformation effects in the layered crystals was described in the review [9]. The interconnection and mutual caution of mechanical V and other physical properties are shown on the fig.1. Heating the body is caused by its deformation as a result of the thermal expansion effect (pointers **14**), and vice versa, the elastic adiabatic deformation of the crystal is caused by change of its temperature - so-called thermoelastic effect (pointer **13**). The set of the crystals crystallise at the deformation (piezoelectric effect) - pointer **15**, and vice versa, the polarization under electric field action is caused by the mechanical deformations of the crystal (so-called inverse piezoelectric effect or electrostriction effect, differ from it) - pointer **16**. The light gives the mechanical pressure (Stoletov experience), under the light action the elastic properties of the crystal change (photoelectric effect) – pointer **18**, but from the other side under deformation action the index of substance refraction changes (piezoelectric or photoelectric effect), the rebuilding of the energetic levels takes place (deformation potential theory) – pointer **17**. The sizes of the magnetic substance change at the magnetization (so-called the magnetostriction effect) – pointer **20**, and vice versa, the magnetic state of the crystal changes at its deformation (piezomagnetism, magnetoelastic effect) – pointer **19**.

The practical treasure of the above mentioned pyramid circuit of the intercommunications of the physical properties and effects is that firstly all possible ways of the interactions and interdependencies are clearly seen at the considering any physical functional dependence. For example, as it is known, the temperature change of the forbidden band width in the semiconductors is caused mainly by two factors: electron-phonon interaction and deformation of crystal lattice. In the given pyramid circuit (fig.1) this transition from the heat properties **I** to the optical ones **III** takes place with the help of the more two ways, besides the direct way - heat radiation (pointer **3**): on the pointer **1** (intrinsic interaction of electron and phonon), later on the pointer **12** (act of the phonon absorption with small energy) or on the pointer **14** (heat deformation of the crystal lattice as a result of the thermal expansion), later on the pointer **17** (rebuilding of the energetic spectrum with the help of deformation potential). The induction effect at the temperature change (transition from the heat properties **I** to the electric ones **II**) can be done or by direct way on the pointer **1** (pyroelectric effect), either by indirect way on the pointer **14** (heat deformation of the crystal lattice as a result of the thermal expansion), later on the pointer **15** (piezoelectric effect).

Secondly, from the given circuit it is seen, that besides the direct way of the interaction, the other side ways of physical process are possible. This leads to the appearance of the “false” effect, besides “true” one. Therefore, in several cases the “false” effect can be higher in several times, than “true” effect. For example, we can mention the above mentioned pyroelectric effect. The “false” pyroelectric effect, caused firstly by the mechanical deformation at the temperature change (i.e. thermal expansion, pointer **14**) with the latest electric induction as a result of the mechanical deformation (piezoelectric effect, pointer **15**) is possible besides the “true” pyroelectric effect, which is the electric induction effect at the temperature change (pointer **1**). Analogically we can say about “true” and “false” effects of the thermal expansion in the piezoelectric crystals. The “true” effect is caused by the crystal deformation at the temperature change (pointer **14**), but “false” effect is caused firstly by the electric induction appearance at the temperature change (pyroelectric effect, pointer **1**) with the following later mechanical deformation (inverse piezoeffect, pointer **16**).

It is need to add, that in the case of the solids it is need to distinguish the heat conductivity at the constant voltage and the heat conductivity at the constant deformation or elastic constants at the constant temperature (isothermic) and at the constant entropy)adiabatic). Thus, taking into consideration the above mentioned, at the considering of the values of that kind it is need to clarify also if the electric field and

polarization should be constant. As the alternating mechanical stress, so the electric alternating field as a result of the electrocaloric effect leads to the quantity of heat change.

Thus, in the present paper the intercommunication, interaction and of the main five physical crystal properties are shown on the example of the real physical effects. The given pyramid circuit more fully shows the functional dependencies of crystal physical values and allows to establish the presence of the "false" physical effects.

[1] *J.. Nay.* Fizicheskiye svoystva kristallov. M., Mir, 1967, 386s. (in Russian).

[2] *U. Kedi.* Piezoelektrichestvo I ego prakticheskiye primeneniya. M.:Inostr. Lit-ra, 1949, 719s. (in Russian)..

[3] *N.A. Abdullayev.* FTT, 2001, 43, 4, 697. (in Russian).

[4] *G.L. Belenkiy, R.A. Suleymanov, N.A. Abdullayev, V.Ya. Shtenshrayber.* FTT, 1984, 26, 12, 3560. (in Russian).

[5] *N.A. Abdullayev, M.A. Aljanov, E.M. Kerimovaва*. FTT, 2002, 44, 2, 213, (in Russian).

[6] *N.A. Abdullayev, R.A. Suleymanov, M.A. Aljanov, L.N. Aliyeva.* FTT, 2002, 44, 10, 1775. (in Russian).

[7] *G.L. Belenkiy, N.A. Abdullayev, V.N. Zverev, V.Ya. Shtenshrayber.* Pisma v JETF,1988, 47, 10, 498. (in Russian).

[8] *N.A. Abdullayev, M.A. Nizametdinova, A.D. Sardarli, R.A. Suleymanov*. FTT, 1993, 35, *1*, 77.

[9] *N.A. Abdullayev, A.D. Sardarli, R.A. Suleymanov*. FTT, 1993, 35, 4, 1028.

[10] *S.G. Abdullayeva, N.A. abdullayev, G.L. Belenkiy, N.T. Mamedov, R.A. Suleymanov*. FTP, 1983, 11, 2068.

[11] *G.L. Belenkiy, E.Yu. Salayev, R.A. Suleymanov.* UFN, 1988, 155, 1, 89.

N. A. Abdullayev

KRİSTALLARIN FİZİKİ XASSƏLƏRİNİN ÜMUMİ QARŞIRIQLI ƏLAQƏSİ VƏ QARŞIRIQLI ŞƏRTLƏNMƏSİ

Məqalədə kristalların beş əsas fiziki xassələrinin qarşırıqlı əlaqəsi, qarşırıqlı təsiri və qarşırıqlı şərtlənməsi müzakirə olunur. Konkret fiziki qanunların misalında göstərilmişdir ki, bu qarşırıqlı təsir, qarşırıqlı əlaqə və qarşırıqlı şərtlənmə dəqiq nəzərə çarpır və özünü göstərir.

Н.А. Абдуллаев

ВСЕОБЩАЯ ВЗАИМОСВЯЗЬ И ВЗАИМООБУСЛОВЛЕННОСТЬ ФИЗИЧЕСКИХ СВОЙСТВ КРИСТАЛЛОВ

В настоящей статье обсуждается взаимосвязь, взаимодействие и взаимообусловленность основных пяти физических свойств кристаллов. На примере конкретных физических законов показано, что эта взаимосвязь, взаимодействие и взаимообусловленность чётко отслеживается и проявляется.

Received: 14.02.04

ELECTRICAL FIELDS AND DISCHARGES IN PROCESSES OF SEWAGE PURIFICATION

A.M. HASHIMOV, N.M. TABATABAEI*, R.N. MEHDIZADEH, M.J. OKHRAWI*
Institute of Physics, Azerbaijan National Academy of Sciences
**Tarbiat Moallem University of Azerbaijan, Tabriz, Iran*

In the paper the results of researches processes of complex purification of sewage with application of electrical discharge effect. It is shown that application of electrical discharge barrier type and ozonizing significantly raises the efficiency of adsorptive clearing of sewage from impurities. Offered method represents the very promising purification technology for industries' sewage.

In conditions of a snowballing of various industries problems of water reclamation as means of conservation of water resources, sewage purification and ordering of water consumption at the factories are actual for today and demand the urgent solution. Sewage of the various industrial factories contain suspended matters in the composition - calcium, magnesium, sodium+kalium, hydro carbonates, carbonates, sulfates, chlorides, ammonia (on nitrogen), nitrates, nitrites, phosphorus, mineral oil, organic compounds (including phenol), ions of metals, salts of barium, bismuth, strontium, iron, zinc, aluminum, titanium, kalium. In some events sewage appear is radioactive infected, contain in the composition heavy atoms of iodine and other impurities which getting as the waste in reservoirs or ground, pollute them and intoxicates living and vegetable organisms.

Presence of an affluent spectrum of impurities in sewage demands development of qualitatively new purification processes providing hard ecological requirements.

Most of cleaning technique of waste waters now is are periodic, multiphase processes having series of an essential limitation. The basic key defect existing methods is that with the purposes of clearing waste water from admixtures there are used the contact them to acids, alkali and other reagents that clears water from admixtures, but at the same time remain in water and by that negatively effects on a nature.

From put into practice cleaning technique of waste waters the adsorptive methods with use of solid natural adsorbents, have some advantages [1]. The adsorptive processes taking place at contacting a liquid with solid surface are widely used in a chemical industry and other branches of engineering. Availability of the adsorptive method, requirement of practice demand study of possibilities of the further application of the adsorptive processes, developing of control facilities by them during carrying out of processing steps.

One of such control facilities is influence of electric fields and discharges on the adsorptive process [2-4]. Effectiveness of influence electric discharge on sorption processes is determined not only a possibility of control but also other advantages of electrical influence: a possibility of direct effect in passing sorption process, small power consumption and manufacturability.

In the present work results of researches on sewage purification on the plastic manufacturing plant, the thermal electric station and gas processing factory and oil seam waters are given.

The combined physicochemical methods of purification including reagent and adsorptive purifications at action of the ozone, the strong electric fields and discharges were used in processes [5].

Experiments were carried out on samples of water, both taken immediately from a concrete industrial installation and synthetically prepared in laboratory conditions.

Let's consider results on reagent purification of water from salts of hardness in conditions of action of electric discharge of barrier type. The offered purification method is carried out as follows.

The water containing salts of hardness was treated by mixture consisting of 97 % weight Silicate of alkali metal, 0,6 % weight Alcohol and 2,4 % weight Calcium chloride at environing temperature, and before compounding silicate of alkali metal was exposed by electric discharge.

Action of electric discharge was carried out in the glass pot with the built - in electrode system formed the configuration of weak non-uniform electric field with dielectric barriers in an interelectrode interval. At the application to electrode system the sufficient value of alternating voltage there was an electric discharge of barrier type in the interelectrode interval. Silicate of alkali metal was passed with fixed velocity through an interelectrode interval in which the discharge was initiated. Laboratory experiments have shown that action of electric discharge during even 30 seconds apparently increases effect of water purification by silicate of alkali metal. Therefore for optimization of process the reagent was exposed the discharge within (1-5) minutes. After treatment the water is fed on settling. The allocated sediment as gel was separated from solution by centrifugation.

Purified water can be used in the industrial and technical purposes in a cycle of self-contained water service, and the sediment can be used for preparation the construction materials or fertilizing, or for the further processing. Action of electric discharge on the mixture's basic component - silicate of alkali metal, considerably activates it that results in increasing of water purification velocity. As a result of faster sedimentation of salts of hardness the productivity of process increases.

Besides the activation of silicate of alkali metal causes smaller specific expenses of the reagent that results both in reduction in price of purification process, and to absence or sharp decreases of reagent traces in water.

The mixture of composition, weight, treated the initial water with hardness, equal 200 mg.equ/l, incorporating the salts of barium, bismuth, strontium, iron, zinc, aluminum, titanium and kalium. %:

Silicate of sodium - 97
Alcohol - 0,6
Calcium chloride - 2,4

The mixture is introduced as 1,5 % of water solution. Thus silicate of sodium is not exposed to electric discharge.

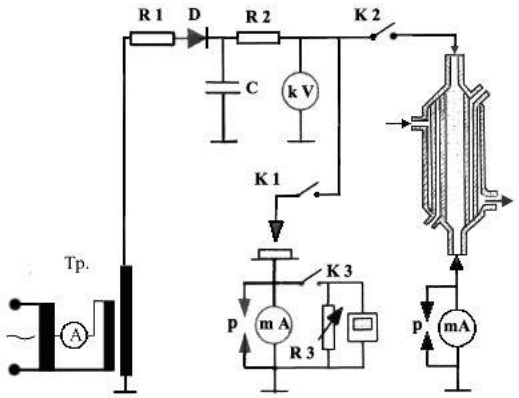

Fig. Principal electric scheme of discharge action at clearing process

The charge of mixture makes 70 g / m^3. The processed water settled within 1,5 hours, then the allocated sediment was separated by centrifugation. As has shown analysis, purified water has zero hardness. In the following experiment, saving identical all requirements of experiment, before compounding carried out action of electric discharge on silicate of sodium at the voltage between the electrodes of 16 kV (fig.). The average value of field intensity in a discharge gap of 4 mm was equal 40 kV/cm. Action of the discharge on a reagent carried out during 3 minutes. In the given experiment the charge of an mixture made 50 g / m^3, and the processed water was settled within 1 hour, then the sediment was separated. Purified water also had zero hardness.

From comparison of results it is visible, that action by electric discharge on silicate of sodium gives an opportunity to reduce the charge of a reagent and to reduce the sedimentation time till 1 o'clock. The further experiments in this direction have shown, that the preliminary activation of silicate of alkali metal by means of electric discharge results in the considerable expansion of cleared impurities assortment in water, such, as mineral oil, organic compounds (including phenol), ions of metals.

In work researches of clearing processes with use of ozone actions are carried out. Results of researches have shown that ozone is effective at clearing of the various factories sewage from such bonds, as ethylene amine, ammonia, polyesters, sulfur-containing bonds, etc.

In an event of application of ozone during sewage clearing, besides a direct effect of a disinfecting of water, the positive side effect, the bound with sharp decrease of sedimentations on the walls of pipelines and reactors is observed still. Results of work can be the useful at polymeric materials manufacturing, for a wood pulp and paper industry, for the slate factories, in dyeing business, a dry-cleaner, etc. Ozonization is an efficient method of deodorization of water polluted by mineral oil. At ozonization of the water keeping mineral oil in concentration 1 mg/l, i.e. approximately in 10 times is higher than their threshold on an smell, the complete deodorization of water was observed as a result of 3-5 minute treatment by ozone dose of 3 mg/ l.

By researches it fixed, that use of actions of electric discharges in various gaseous environments allows increasing efficiency of the adsorptive methods of sewage purification essentially.

In work as adsorbents Silica Gel of KCM mark, synthetic zeolites and natural zeolite of Ay-Dag deposits (Azerbaijan) were used.

On the basis of obtained results, in dependence on impurities composition of initial water, some alternatives of clearing processes that are successfully tested in laboratory conditions are offered. Some results have been tested and introduced in the relevant industrial factories.

[1] *Giglio. E. Chim.* Industria 1972, 54, №1, pp. 59-62.

[2] *Ch. Juvarli, A.M. Gashimov, R.N. Mehdizadeh and others.* Method of water clearing from salts of rigidity. Thesis on USSR Patent delivery, No.5012721/26, 1992 (Russian)

[3] *Ch. Juvarli, A.M. Gashimov, R.N. Mehdizadeh and others.* Environmental problems in thermal power generation industry: effect of strong electric field and discharge application to the cleaning of industrial wastes.Fourth Baku International Congress. Baku, Azerbaijan Republic. Sept. 23-26, 1997

[4] *A.M. Gashimov, R.N. Mehdizadeh and others.* Some electrophysical processes in power engineering objects at effect of the electrical discharges. The sixth Baku International Congress "Energy, Ecology, Economy", Baku, May 30- June 3, 2002, pp. 3-4

[5] *A.M. Gashimov, R.N. Mehdizadeh and others.* New designees for processes of sewage purification. Seventh Baku International Congress "Energy, Ecology, Economy" 26-27 June,2003.

A.M.Həşimov, N.M.Tabatabaei, R.N.Mehdizadə, M.C.Oxravi

TULLANTI SULARIN TƏMİZLƏNMƏSİ PROSESLƏRİNDƏ ELEKTRİK SAHƏLƏRİ VƏ BOŞALMALARININ TƏTBİQİ

Məqalədə elektrik boşalmalarının təsiri vasitəsilə tullantı suların adsorbsiya üsulu ilə təmizlənməsinin tədqiqindən əldə edilmiş nəticələr verilmişdir. Göstərilmişdir ki, arakəsməli elektrik qaz boşalmasının və ozonlaşmanın təsiri tullantı suların adsorbsiya üsulu ilə təmizlənməsinin effektivliyini nəzərə çərpacaq dərəcədə yüksəldir. Təklif olunan üsul sənaye tullantı suların təmizlinməsi texnologiyası üçün əhəmiyyət kəsb edir.

А.М. Гашимов, Н.М. Табатабаеи, Р.Н. Мехтизаде, М.Дж. Охрави

ЭЛЕКТРИЧЕСКИЕ ПОЛЯ И РАЗРЯДЫ В ПРОЦЕССАХ ОЧИСТКИ СТОЧНЫХ ВОД

В статье приводятся результаты исследований процессов адсорбционной очистки промышленных сточных вод с использованием воздействия электрического разряда. Показано, что использование воздействия электрического разряда барьерного типа и озонирования значительно повышает эффективность адсорбционной очистки сточных вод от примесей. Предлагаемый метод представляет интерес для технологии очистки промышленных сточных вод.

Received: 24.05.04.

THE PHASE DIAGRAM AND MAGNITODIELECTRIC PROPERTIES OF THE HOMOGENEOUS PHASES OF $TlInS_2$-$TlCoS_2$ and $TlGaSe_2$-$TlCoS_2$ SYSTEMS

R.K. VELIYEV, MIR-GASAN U. SEIYIDOV, E.M. KERIMOVA, F.M. SEYIDOV, R.Z. SADIKHOV, A.I. JABBAROV

The Institute of Physics of National Academy of Sciences of Azerbaijan, Az-1143, Baku, H. Javid ave., 33.

The interaction in the quasi-binary systems $TlInS_2$-$TlCoS_2$ and $TlGaSe_2$-$TlCoSe_2$ has been studied. The regions of the homogeneous phases in these systems are revealed. In the temperature interval 77-400K the dielectric properties of $TlInS_2$, $TlgaSe_2$ and magnetic and electric properties $TlCoS_2$, $TlCoSe_2$ also have been investigated. The experimental results showed, that $TlInS_2$. $TlGaSe_2$ are ferrooelectrics, $TlCoS_2$ is ferrimagnetic-semimetal, $TlCoSe_2$ is ferrimagnetic-metal. The coexistence of polar and magnetic order in the crystals $TlIn_{1-x}Co_xS_2$ and $TlGa_{1-x}Co_xSe_2$ is proposed.

1. Introduction

The triple disulfides and diselenides of thallium with the common crystalchemical formulae $TlMeX_2$ (where Me=Ga, In, Cr, Fe, Co; X=s, Se) presents themselves the wide class of the strong -anisotropic (layered, chained) compounds with the physical properties , having practically all investigation range in the modern region, of condensed state. Between them are semiconductors (for example, $TlGaS_2$) [1,2] ferroelectrics - semiconductors $TlInS_2$, $TlGaSe_2$ [3÷6], ferromagnetic substance ($TlCrS_2$, $TlCrSe_2$) [7,8], ferrimagnetic substance ($TlCoS_2$-semimetal, $TlCoSe_2$-metal) [9], antiferromagnetic substance-semiconductors ($TlFeS_2$, $TlFeSe_2$, $TlMnS_2$, $TlMnSe_2$) [10-12], disorder structures ($TlInS_2$, $TlGaSe_2$) [3-6, 13] and e.t.c. Moreover, each of the components can be in the different phase states in the dependence on the temperature, hydrostatic pressure and defection degree, and transfer from one phase state to another (in respect of $TlInS_2$, $TlGaSe_2$, see refs [14-17]). However, the most interest and important from the scientific point of view is the possibility of the purposeful variation of the factual chemical composition of above mentioned compounds with the aim of the obtaining in the one crystal the state, of the coexistence of the polar and magnetic order (ferromagnetic substance).

2. Phase diagrams of $TlInS_2$-$TlCoS_2$ and $TlGaSe_2$-$TlCoSe_2$ systems.

For the solving of the given physical problem it is need to identify the solubility intervals in the ferroelectrics $TlInS_2$, $TlGaSe_2$ of above mentioned magnetic substance. The polythermal cuttings of $TlInS_2$-$TlCoS_2$ and $TlGaSe_2$-$TlCoSe_2$ have been investigated by us by the method of the differential-thermal; analysis (DTA).

For the construction of phase diagram of $TlInS_2$-$TlCoS_2$ the 14 compositions had been prepared. The initial phases of $TlInS_2$ and $TlCoS_2$ were synthezed by the forward melting of the elements, suspended in the stoichiometric ratio, in vacuum quartz ampoules, having the residual pressure $1{,}3\cdot10^{-2}$ Pa. The phase synthesis mode, suspended in the equimolecular ratio on the base of the initial triple compositions, already done in the fine-disperse state, was chosen with the orientation of the melting point of $TlInS_2$ (1050K) and $TlCoS_2$(690K). The quartz ampoules with the compounds were done the vacuum ones, after that put into furnace, heated higher than melting points of the initial compositions and kept at this temperature during 6-7 hours. The synthesized alloys for the homogenization are annealed during 27 days at 700K in the case of alloys, enriched by In and during 29 days at 460K, in the case of alloys, enriched by Co. The annealed alloys were investigated by the DTA method, which was carried out on the device NTR-73, allowing to fix the temperatures of phase transformations with exactness ±10K. The heating velocity was 2-4K/min. The temperature was controlled by Pt-Pt/Rh-thermocouple, measured on reference substances in the interval 430÷1560K.

The phase diagram of system state $TlInS_2$-$TlCoS_2$, constructed on DTA results is represented on the fig.1. This system is quazibinary of the eutectic type with wide regions of solid solutions on the base of $TlInS_2$ and $TlCoS_2$, reached till 35 mol%. The eutectic melts at 400K and has the composition $(TlInS_2)_{0,5}$ and $(TlCoS_2)_{0,5}$.

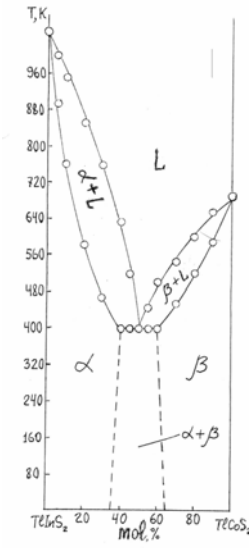

Fig.1. The phase diagram of the system $TlInS_2$-$TlCoS_2$.

For the construction of phase diagram of state $TlGaSe_2$-$TlCoSe_2$ was prepared the 13 compositions. The triple compounds $TlGaSe_2$ and $TlCoSe_2$ were synthesized in the vacuum quartz ampoules (the residual pressure $1{,}3\cdot10^{-2}$Pa) by the element allowing, suspended in the stoichiometric ratio. The phase synthesis mode, suspended in the equimolecular ratio on the base of the initial triple compounds, already done

in the fine-disperse state, was chosen in the orientation of the melting points of $TlGaSe_2$ (1080K) and $TlCoSe_2$(650K). The quartz ampoules with the compositions were done the vacuum ones, after that put into furnace, higher than melting points of the initial compounds and kept during 5-6 hours at this temperature. The obtained alloys for the homogenization were annealed during 23 days at 810K in the case of the alloys, enriched by Ga and - 25 days at 520K in the case of alloys, enriched by Co, after that investigated by DTA method.

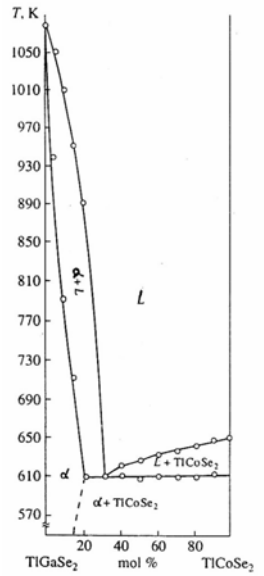

Fig.2. The phase diagram of the system $TlGaSe_2$-$TlCoSe_2$.

The phase diagram of the system $TlGaSe_2$-$TlCoSe_2$, constructed on DTA results, is given on the fig.2. This system is quazibinary of the eutectic type. The eutectic melts at the temperature 610K and has the composition $(TlGaSe_2)_{0,69}(TlCoSe_2)_{0,31}$. In the left part of the diagram between eutectic point and $TlGaSe_2$ at 300K appear the solid solutions on the base of $TlGaSe_2$ with the dissolution of $TlCoSe_2$ till 14mol%. In the right part of the diagram (between eutectic point and $TlCoSe_2$) appears the simple eutectic.

3. The preparation of the samples and the experimental techniques.

For the investigation of the temperature dependence of the dielectric constant ($\varepsilon(T)$) of the layered crystals TlInS2, TlGaSe2, the samples in the form of the plates of polar cut, catted from the monocrystal ingots of the both compounds, grown by the modificated method by Bridgemen-Stockbarger, were used. In the capacity of the electrodes the silver paste was applied. $\varepsilon(T)$ of $TlInS_2$ and $TlGaSe_2$ were measured with the help of the alternating current bridge on the frequency 1kHc.

The temperature dependence of the magnetic susceptibility ($\chi(T)$) of the magnetic substance $TlCoS_2$, $TlCoSe_2$ was investigated by Faradei method on the magnetoelectric scales.

The temperature dependences of the electric conductivity ($\sigma(T)$) and thermoelectromotive force ($S(T)$) of $TlCoS_2$, $TlCoSe_2$ were investigated by the tetrazond compensated method. The samples for the measurements had the form of parallelepiped with sizes 7,15·4,86·2,06mm^3 ($TlCoS_2$) and 9,72·4,85·2,37mm^3 ($TlCoSe_2$). The Ohmic contacts were created by the way of the electrodeposition of cuprum on the edges of the samples.

The investigations were carried out in the temperature interval 77-400K in the quazistatic mode, moreover the velocity of temperature change was 0,2K/min. During the measurements the samples were inside of the nitrogen cryostat and in the capacity of the temperature gauge the differential cuprum-constantan, the thermojunction of which was stationary fixed on the crystalokeeper near the sample, was used. The supporting thermojunction stabilized at the temperature of the thawing ice.

4. The experimental results and their discussion.

The temperature dependence of the dielectric constant TlInS2, measured at the atmosphere pressure given on the fig.3. As it is seen from the figure, the curve $\varepsilon(T)$ is characterized by the set of anomalies in the maximum forms at 206,3K and 202,4K and the existence of the some bending in the neighbourhood 201K, also. As it is known, the layered crystal $TlIn\ S_2$ with the temperature decrease at the atmosphere pressure has the complex consequence of the structural phase transitions (PT), including the PT in the noncommensurable(NC) and the commensurable© ferroelectric phases [3-6]. The initial paraelectric phase $TlInS_2$ is characterized by the space symmetric group (Ssg) C_{2h}^6 PT in NC -phase connects with the soft water condensation (at T_i=216K) in the Brillyoin band point with the wave vector $\vec{k}_i$ =*(δ; δ; 0,25)*, where δ is the noncommensurable parameter [13]. At T_c~201K the δ value transforms by jump in the zero and the crystal $TlInS_2$ transfers in the no intrinsic ferroelectric (vector of spontaneous polarization is situated in the plane of layer) C-phase with the wave vector $\vec{k}_c$ =(0; 0; 0,25) [13-17].

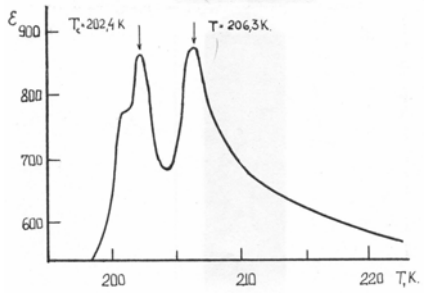

Fig.3. The temperature dependence of the dielectric constant of $TlInS_2$.

Comparing our results with data, given in [3-6,17] one can conclude that curve $\varepsilon(T)$ of the investigated crystal strongly differs from the analogical curves, given in the literature, as by the number of anomalies, so by their temperature states. Let's note, that the color of the investigated sample $TlInS_2$, differed by orange shadow, whereas crystals of $TlInS_2$, chosen from the different parties and investigated in the refs [3-6] on the color gamma had the different shadows of the yellow color. Taking into consideration the data of refs [15, 16] in which the strong sensitivity of the physical properties (PT temperature also) of the layered crystal $TlInS_2$ to the impurity quantity in the

sample and to the defect degree of its crystal structure, is fixed so it can be proposed that observed by us anomaly on the curve $\varepsilon(T)$ at 206,3K connects with PT in NC-phase, but at 202,4K - with PT in commensurable ferroelectric phase. Moreover, "bending"in the neighbourhood ~201K is the temperature interval of the remainder co-existence of the undistorted solutions of NC-phase and domains of the low temperature C-phase [3].

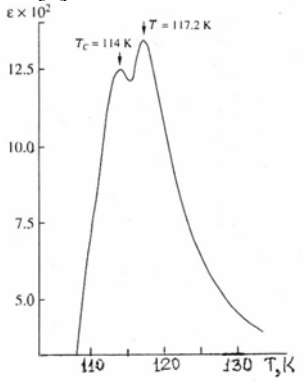

Fig.4. The temperature dependence of the dielectric constant of $TlGaSe_2$.

The temperature dependence of e of $TlGaSe_2$, measured at the atmosphere pressure was given on the fig.4. As it is seen from the figure, the dependence curve $\varepsilon(T)$ of $TlGaSe_2$ is characterised by the anomalies in the maximum form, connected with the phase transition points in the noncommensurable phase at T=117,2 and commensurable ferroelectric phase at T_c=114K. In the both crystals the temperature curve e in the paraelectric and ferroelectric phases is well approximated by Curie -Weiss law with the value of Curie constant ~10^3K. It is noted, that temperature state of the anomalies on the curve $\varepsilon(T)$, and the value of Curie constant also $TlGaSe_2$ are well agreed with the refs [5,18,20].

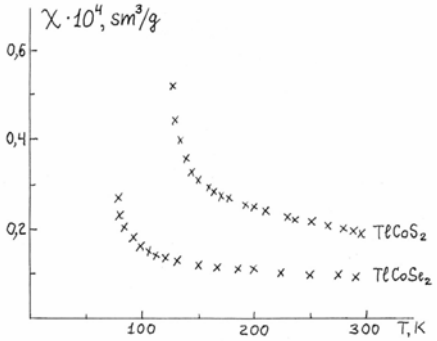

Fig5. The temperature dependence of magnetic susceptibility of $TlCoS_2$, $TlCoSe_2$.

The temperature dependence χ of the compounds $TlCoS_2$ and TlCoSe2 is given on the fig.5. As it is seen from the dependence $\chi(T)$ for the both compounds has the parabolitic form, characteristic for the ferrimagnetic order of spin system, caused by the competing influence of two types of magnetic interactions-ferromagnetic substance (inside the layers) and antiferromagnetic substance (between layers).

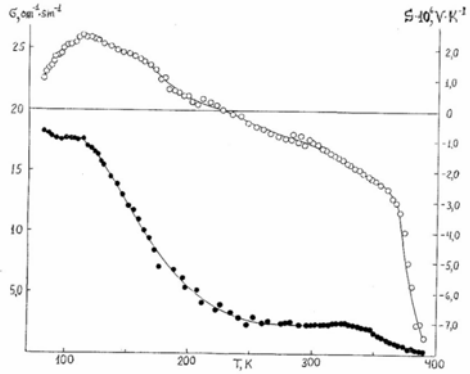

Fig.6. The temperature dependences of electric conductivity (.) and thermoelectromotive force ($_0$) of ferrimagnetic semi-metal $TlCoS_2$.

The temperature dependence σ and S of ferrimagnetic $TlCoS_2$ is given on the fig.6. As it is seen from the figure, σ decreases with the temperature increase from 77K. In the neighbourhood 113K on the curve $\sigma(T)$ of $TlCoS_2$ the bending is observed, caused as it is known from the literature of the ref [21], by the electron scattering on the spin nonhomogeneous, forming at the transition of the spin magnetic spin system from the magnetoordered state to the paramagnetic one. The decrease of the electroconduction of $TlCoS_2$ is observed till ~250K, then б increases insignificantly in the interval 250÷325K. The later decrease of conduction of$TlCoS_2$ in the interval 325÷400K, connects with the achieving of the intrinsic conduction temperature of semi-metal $TlCoS_2$. From the fig.6 it is seen that $S(T)$ of TlCoS2 increases insignificantly in the temperature interval 77÷113K, achieving its maximum value (2,42mkV/K) at ~113K. After that with the increase of the temperature the change of the conduction type from p- till n-type is observed. Let's note that temperature (~113K), at which on the dependencies $\sigma(T)$ and $S(T)$ of $TlCoS_2$, the anomaly, close to the temperature T_c=112Kof phase transition of spin ferrimagnetic system TlCoS2 takes place from the magnitoordered state to the paramagnetic, defined in the ref [9], takes place.

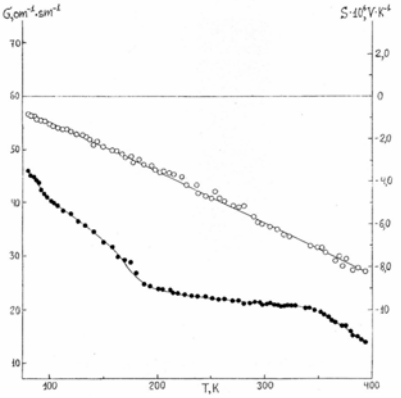

Fig.7. The temperature dependencies of the electric conductivity (.) and thermoelectromotive force ($_0$) of ferrimagnetic metal $TlCoSe_2$.

The temperature dependences б and S of compound TlCoSe2 are presented on the fig.7. As it is seen from the figure, the curve $\sigma(T)$ and $S(T)$ of $TlCoS_2$ has the metallic character in all investigated temperature interval.

Thus, basing on the carried out investigations, we can prove that in the crystals TlIn1-xCoxS$_2$(0<x<=0,35) and

$TlGa_{1-x}Co_xSe_2$($0<=x<=0,14$) the coexistence of the polar and magnetic order is possible, i.e. the changes of the dielectric constant of the ferroelectrics $TlInS_2$, $TlGaSe_2$ are possible from the applied electric and magnetic fields with the solubility of ferrimagnetic substance TlCoS2(till 35%mol), TlCoSe2(till 14%mol) in them, correspondingly.

[1] *G.D. Guseinov, G.B. Abdullayev, S.M. Bidzinova, M.Z. Ismailov, A.M. Pashayev*. J.Phys. Letters, 1970, 33A, 7, 421.

[2] *G.D. Guseinov, A.M. Ramazanzade, E.M. Kerimova, M.Z. Ismailov*. J.Phys. State Sol., 1967, 22, K117.

[3] *F.M. Salayev, K.R. Allahverdiev, F.A. Mikailov*. J. Ferroelectrici, 1992, 131, 1-4, 163.

[4] *R.A. Suleymanov, M.Yu. Seidov, F.M. Salayev, F.A.Mikailov*. FTT, 1993, 35, 2, 348. (in Russian).

[5] *K.R. Allakhverdiyev, N.D. Akhmed-zade, T.G. Mamedov, T.S. Mamedov, M.Yu. Seidov*. FNT, 2000, 26, 1, 76. (in Russian).

[6] *F.A. Mikailov, T. Bauaran, T.G. Mammadov, M.Yu.Seyidov, E. Senturk*. J. Phisika B, 2003, 334 /1-2, 13

[7] *M. Rosenberg, A. Knulle, H. Sabrowsky, C. Platte*. J.Phys. Chem. Solids, 1982, 43, 2, 87.

[8] *M. Aljanov, M. Nadjafzade, Z. Seidov, M. Gasumov*. Turkish Journal of Physics, 1996, 20, 9, 1071.

[9] *R.Z. Sadikhov, E.M. Kerimova, Yu.G. Asadov, R.K.Veliyev*. FTT, 2000, 42, 8, 1449. (in Russian).

[10] *Z. Seidov, H.-A. Krugvon Nidda, J. Hemberger, A. Loidl, G. Sultanov, E. Kerimova and A. Panfilov*. J.Phys. Rev. B, 2001, 65, 014433.

[11] *S.N. Mustafayeva, E.M. Kerimova, A.I. Jabbarli*. FTT, 2000, 42, 12, 2132. (in Russian).

[12] *R.Z. Sadikhov, E.M. Kerimova, R.K. Veliev, A.I.Jabbarov*. 13th International Conference on Ternary and Multinary Compounds. Book of abstracts, 2002, P1-13.

[13] *S.B. Vakhrushev, V.V. Dzhdanova, B.E. Kvatkovskiy, N.M. Okuneva, K.R. Allakhverdiyev, R.A. Aliyev, R.M. Sardarli.* Pisma v JETF, 1984,39, 6, 245. (in Russian).

[14] *K.R. Allakhverdiyev, A.I. Baranov, T.G. Mamedov, V.A. Sandler, Ya.N. Sharifov*. FTT, 1988, 30, 6, 1751. (in Russian).

[15] *S. Ozdemir, R.A. Suleymanov, E. Civan.* Solid State Comm., 1995, 96,10, 757.

[16] *S. Ozdemir, R.A. Suleymanov, E. Civan, T. Firat*. Solid State Comm., 1996, 98, 5, 385.

[17] *R.A. Aliyev, K.R. Allakhverdiyev, A.I. Baranov, N.R.Ivanov, R.M. Sardarli*. FTT, 1984, 26, 5, 1271. (in Russian).

[18] *H. Hochheimer, E. Gmelin, W. Bauhofer*. Z.Phys. B: Condens. Matter., 1988, 73, 2, 257.

[19] *R.M. Sardarly, O.A. Samedov, I.Sh. Sadyhov.* Solid State Comm., 1991, 77, 6, 453.

[20] *A.K. Abiyev, N.A. Bakhishov, A.E. Bakhishov, M.S.Gadzhiyev*. Izv. Vuzov, Fizika, 1989,12, 84. (in Russian).

[21] Fizika magnitnikh materialov,pod. red. *V.A. Ignatchenko i G.A. Petrakovskogo*, Nauka, Novosibirsk, 1983, 82-101. (in Russian).

R. Q. Vəliyev, Mir-Həsən Y. Seyidov, E.M. Kərimova, F.M. Seyidov, R.Z. Sadıqov, A.İ. Cabbarov

$TlInS_2$-$TlCoS_2$ və $TlGaSe_2$-$TlCoSe_2$ SİSTEMLƏRİNİN HAL DİAQRAMMASI VƏ HOMOQEN FAZALARININ MAQNİTODİELEKTRİK XASSƏLƏRİ

$TlInS_2$-$TlCoS_2$ və $TlGaSe_2$-$TlCoSe_2$ kvazibinar sistemlərində qarşılıqlı təsir öyrənilmişdir. Bu sistemlərdə homoqen faza oblastları aşkar olunmuşdur. 77K÷400K temperatur intervalında $TlInS_2$, $TlGaSe_2$-nin dielektrik xassələri və həmjinin $TlCoS_2$, $TlCoSe_2$-nin maqnit və elektrik xassələri tədqiq olunmuşdur. Təçrübi tədqiqatlar $TlInS_2$, $TlGaSe_2$-seqnetoelektrikdir, $TlCoS_2$ - ferrimaqnetik- -yarımmetaldır, $TlCoSe_2$ isə ferrimaqnetik-metaldır. $TlIn_{1-x}Co_xS_2$ və $TlGa_{1-x}Co_xSe_2$ kristallarında polyar və maqnit nizamlanmasının birgə olması gözlənilir.

Р. К. Велиев, Мир-Гасан Ю. Сеидов, Э.М. Керимова, Ф.М. Сеидов, Р.З. Садыхов, А.И. Джаббаров

ДИАГРАММА СОСТОЯНИЯ И МАГНИТОДИЭЛЕКТРИЧЕСКИЕ СВОЙСТВА ГОМОГЕННЫХ ФАЗ СИСТЕМ $TlInS_2$-$TlCoS_2$ и $TlGaSe_2$-$TlCoSe_2$

Изучено взаимодействие в квазибинарных системах $TlInS_2$-$TlCoS_2$ и $TlGaSe_2$-$TlCoSe_2$. Выявлены области гомогенных фаз в этих системах. В интервале температур 77К÷400К исследованы диэлектрические свойства $TlInS_2$, $TlGaSe_2$, а также магнитные и электрические свойства $TlCoS_2$, $TlCoSe_2$. Экспериментальные результаты показали, что $TlInS_2$, $TlGaSe_2$ являются сегнетоэлектриками, $TlCoS_2$ -ферримагнетиком –полуметаллом, $TlCoSe_2$ - ферримагнетиком – металлом. Предположено сосуществование полярного и магнитного упорядочения в кристаллах $TlIn_{1-x}Co_xS_2$ и $TlGa_{1-x}Co_xSe_2$.

Received: 05.02.04

EFFECT DEFORMATİON İN M1 TRANSİTİONS BETWEEN STATES WİTH DİFFERENT SHAPES

M. GÜNER [1], E. GULİYEV [2]

[1] *Sakarya Univ.,Fac. of Science.and Art, Dept. of Math., 54100 Mithatpasa-Adapazarı*

[2] *Institute of Physics, Azerbaijan National Academy of Science, Baku, Azerbaijan*

In Random Phase Approximation (RPA), using the analytic properties of the nucleus transition matrix elements and by means of contour integrals and residue theorem, we obtain an analytic formula containing the dependence of deformation of the energy-weighted sum rule (EWSR) for the magnetic dipole transformations. Numeric calculations show that the transition probability between levels, which have different forms decreases sharply compatible with experimental data.

Keywords: sum rules, transitions M1, Residue theorem and contour integrals.

Microscopic nuclear models are successfully used to investigate the properties of nuclear collective excitations [1]. Approximate calculation methods are used to investigate the structure of nucleus within the framework of assumed models. In order to evaluate the success of used methods and nucleus models, the obtained results are compared with suitable experimental data.

In quantum mechanics, the transition probability of the system from one state to the other is restricted to the sum rules which are independent from the model and subject to transitions matrix elements. The sum rules in nucleus physics are very important to finding parameters and understanding the reliability of used models [2]. Experimental reviews in heavy nuclei show that the theoretical values of sum rules of matrix elements of the electromagnetic transition parameters are greater by a factor of almost 1,5-2 than the experimental values corresponding to them. The reason for this disagreement between the theory and the experiments is not exactly explained. According to our hypothesis, the main reason of these disagreements is the change of nucleus shape caused by the transitions between different energy levels. It is experimentally known that in some nuclei, the velocity of transition between levels having different structure decrease [4,5].

While investigating the structure of nucleus, electromagnetic and β-transition probabilities play a very important role in determination of spin forces among nucleons in nucleus. For this reason, analytically calculating the sum rules for the transition matrix elements in levels, which have deformation parameters different from the ground state is very important.

There are two types of sum rules: Energy-weighted sum rule and none energy-weighted sum rule and the energy-weighted sum rule (EWSR) is widely used in the nucleus physics:

$$\sum_{k>0}(E_k-E_0)|\langle k|M|0\rangle|^2=\frac{1}{2}\langle 0|[M^+,[H,M]]|0\rangle. \quad (1)$$

Here energy E_k and wave function $\langle k|$ are eigenvalues and eigenfunctions of Hamiltonian operator of nucleus, respectively. M is transition operator, E_0 and $|0\rangle$ also denote the energy and wave function of the ground state, respectively. Since the right-hand side of the sum rule (1) does not contain the internal movement parameters of nucleus, this is independent from models and has constant values. On the other hand, since the left-hand side of the sum rule (1) contains wave functions and energy levels of nucleus, its values depend on models and used methods. Thus, the sum rule (1) is very important in investigating the structure of nucleus. In Ref. [6], assuming that the spin forces creates 1^+ excitations in deformed nuclei, the Hamiltonian describing these levels can be expressed in the following form [6]:

$$H = H_{sqp} + V_{\sigma\tau} \quad (2)$$

where

$$V_{\sigma\tau} = \frac{1}{2}\chi_{\sigma\tau}\sum_{i\neq j}\sigma_i\sigma_j\tau_i^z\tau_z^j. \quad (3)$$

Here $V_{\sigma\tau}$ and H_{sqp} denote isovector spin forces and quasi-particle Hamiltonian in the model of superfluid, respectively. Further, σ and τ are Pauli matrices which represent respectively spin and isotopic spin. All relations which are used and not explained all relations in this paper are similar to those in Ref. [6]. In RPA, the wave functions of 1^+ states can be viewed as single-phonon function:

$$|k\rangle = Q_k^+|0\rangle = \frac{1}{\sqrt{2}}\sum_\mu(\psi_\mu^k C_\mu^+ - \varphi_\mu^k C_\mu)|0\rangle \quad (4)$$

Where Q_k^+ and $|0\rangle$ describe, respectively, phonon-creation operator and phonon vacuum corresponding to the ground state in even-even nuclei. Our system has a discrete spectrum and the wave functions $|k\rangle$ form complete set satisfying $\sum_k |k\rangle\langle k| = 1$. Thus, two quasi-particle amplitudes ψ_μ ve φ_μ corresponding to the operator C_μ and C_μ^+ are normalized as follows:

$$\sum_\mu\left(\psi_\mu^i\psi_\mu^k - \varphi_\mu^i\varphi_\mu^k\right) = \delta_{i,k}. \quad (5)$$

In order to find the eigenvalues and the eigenfunctions of Hamiltonian H, by solving the motion equation

$$\left[H_{sqp} + V_{\sigma\tau}, Q_k^+\right] = \omega_k Q_k^+ \quad (6)$$

and using the well-known RPA procedure, dispersion equation for ω_k roots which are energy of 1^+ states is taken in the form:

$$D(\omega_k) = 1 + \chi\left(F_k^n(\omega_k) + F_k^p(\omega_k)\right) = 0 \quad (7)$$

where

$$F_k^\tau(\omega_k) = 2\sum_\mu{}^{\tau} \frac{\varepsilon_\mu \sigma_\mu^2 L_\mu^2}{\varepsilon_\mu^2 - \omega_k^2}, \quad \tau = \text{n,p.} \quad (8)$$

Here ε_μ and σ_μ are quasi-particle energy of nucleons and single-particle matrix elements of the spin operator, respectively. Two-quasi particle amplitudes ψ_μ and φ_μ have the form:

$$\psi_\mu^i = \frac{1}{\sqrt{Y(\omega_i)}} \cdot \frac{\sigma_\mu L_\mu}{\varepsilon_\mu - \omega_i} \quad (9)$$

$$\varphi_\mu^i = \frac{1}{\sqrt{Y(\omega_i)}} \cdot \frac{\sigma_\mu L_\mu}{\varepsilon_\mu + \omega_i} \quad (10)$$

where

$$Y(\omega_i) = 4\omega_i \sum_i \frac{\varepsilon_\mu \sigma_\mu^2 L_\mu^2}{(\varepsilon_\mu^2 - \omega_i^2)^2}. \quad (11)$$

On the other hand, since energies of the magnetic dipole 1^+ states are the solutions of the function $D(\omega_i)$, we can write

$$Y(\omega_i) = \frac{1}{\chi} D'(\omega_i) \quad (12)$$

where

$$D' = \frac{dD(z)}{dz}.$$

Due to the symmetry between the used spin-spin forces and magnetic dipole operator, the most characteristic quantity of the 1^+ states is transition matrix elements M1 from ground state to all excited states in nucleus:

$$M_k = \langle k | M | 0 \rangle \quad (13)$$

where the magnetic-dipol operator is

$$\vec{M} = \sqrt{\frac{3}{4\pi}} \sum_{m,\tau} \left[(g_s^\tau - g_l^\tau) \overrightarrow{s_m^\tau} - g_e^\tau \overrightarrow{j_m^\tau} \right]. \quad (14)$$

Here g_s^τ and g_l^τ are the spin and the orbital gyromagnetic ratios of nucleons, respectively. By using the wave function (4) and by means of (9) and (10), transition matrix elements of 1^+ states from ground state to excited states can be expressed as

$$M_i = \sqrt{\frac{3}{4\pi}} \frac{\sum_{,\tau} \left[\frac{1}{2}(g_s^\tau - g_l^\tau) \overrightarrow{F_i^\tau} - g_e^\tau \overrightarrow{J_i^\tau} \right]}{\sqrt{Y(\omega_i)}} \quad (15)$$

where

$$\vec{J}_i^\tau = 2\sum_i{}^{\tau} \frac{\varepsilon_\mu j_\mu^2}{\varepsilon_\mu^2 - \omega_i^2}. \quad (16)$$

Here j_μ denote the single-particle matrix elements of the angular momentum operator.

Let us now generalize the sum rule in Eq. (1) for transitions between the ground and excited states which have different form. Let us suppose that shape of the excited state levels $|k\rangle$ have different deformation from the ground state. After this, the quantities corresponding to excited states which have different form from the ground state are denoted by ~(*tilda*) over themselves. Also, by taking the fact that the excited level wave function $|i\rangle = Q_i^+|0\rangle$ in the ground state bases form a complete set into consideration, we obtain the generalized sum rule of Eq. (1) for different forms as follows:

$$S(\delta_i, \delta_k) = \sum_{k>0} \omega_k \left| \sum_{i>0} M_i \langle i | k \rangle \right|^2 \quad (17)$$

$$\langle i | k \rangle = \left(\psi_\mu^i \psi_\mu^k - \varphi_\mu^i \varphi_\mu^k \right). \quad (18)$$

Here δ_i and δ_k are quadrupole deformation parameters characterizing the forms of the ground and excited states. The sum rules are successfully calculated in spherical nuclei. However, in the deformed nuclei, since the levels of the nucleus have high density, computing eigenvalues ω_i from Eq. (7) is numerically quite difficult. Hence, when computing transition matrix elements M_i and the sum rules corresponding to them may occur considerable errors. In [7], the solution methods of this problem are given and by exploiting mathematical properties of β-transition matrix elements, even β-decomposition sum rule is analitically calculated. Later, the method developed in [7] is successfully applied to electromagnetic transitions in [8]. In this study, we calculate this method which is put forward in [7] by applying to the sum rule given in [15] that we have generalized for transitions having different form.

For the sum rule (17), by exploiting the equations (7)-(12), we obtain:

$$S = \frac{3}{16\pi} \sum_{\mu\nu} d_\mu d_\nu . \Omega_{\mu\nu} \quad (19)$$

where

$$d_\mu = \sum_i M_i w_\mu^i = 2\chi\sigma_\mu L_\mu \sum_i \frac{\omega_i}{\left(\varepsilon_\mu^2 - \omega_i^2\right)} \frac{F(\omega_i)}{D'(\omega_i)} \quad (20)$$

DOLDURUCUNUN TİPİNDƏN VƏ MİQDARINDAN ASILI OLARAQ LAZIMİ TƏYİNATLI ELEKTRİK KEÇİRİCİLİ POLİMER KOMPOZİSİYALARIN İŞLƏNMƏSİ

A.M. RƏHİMOV, İ.İ. HƏSƏNOV, P.M. ƏHMƏDOV, Ç.A. ƏLİYEV, J.Ş. MEHTİYEV
«Neftin, qazın geotexnoloji problemləri və kimya ETİ»

Məqalədə göstərilən elektrik keçiricili kompozisiyalar yüksək və alçaq elektrik moduluna malik olduqlarından onlardan kipcəklərin və bərk, qaz və maye halında olan yanacaq maddələrin nəqli üçün tutumların hazırlanmasında istifadə oluna bilərlər. Bu materiallar yaranan elektrik yüklərinin ani boşalmasını təmin etməyə qadirdirlər.

Elektrik keçiricili polimer kompozisiyalar kompozisiya materialların yeni növlərindən olmaqla geniş funksiyalılığa görə çox əhəmiyyətli materiallardan biridir. Bir çox tədqiqatçılar artıq kompozisiya materialların sıralarının sürətlə genişlənməsini nəzərə alaraq onların asanlıqla ədəbiyyatlardan tapılmasını təmin etmək məqsədilə, yeni qruplaşdırma prinsiplərini təklif edirlər.[1].

Elektrik keçiricili polimerlərin və ya kompozisiyaların işlənməsi yarımkeçiricilərin, antistatik və s. məqsədlə müxtəlif sahələrdə istifadə oluna bilən materialların alınmasına imkan yaradır. Bu sahədə geniş işlər görən alimlərdən Balldcin, Norman, Qul, Saqalayevin işlərini misal gətirmək olar. Azərbaycan Dövlət Neft Akademiyasının əməkdaşları bu sahədə müəyyən əhəmiyyəti kəsb edən elmi monoqrafiya və əsərlər dərc etmişlər.[2;5].

Bir çox sahələri əhatə edə bilən elektrik keçiricili polimer kompozisiyaların yaradılması önəmli məsələlərdən biridir.

Müəyyən edilmşdir ki, elektrik yüklərinin yaranmaması üçün elektrik keçiricili polimer kompozisiyasının xüsusi həcmi elektrik müqaviməti 10^6 Om·m çox olmamalıdır. İstehsal olunan materialların elektrik keçiriciliyi göstərilən qiymətdə olarsa statiki elektrik yüklərindən qorunmaq üçün əlavə tədbirlərin görülməsinə ehtiyac qalmır.

Bu məqsədlə bir sıra polimer əsaslı metal və qrafit dolduruculu, elektrik keçiricili polimer materialların təhlilini nəzərdən keçirək. (cəd.1)

Cədvəl1.

Elektrik keçiricili polimer kompozisiya materiallarının tərkib hissələri, küt.%-lə

Elektrik Keçiricili kompozi-siya material-ları	Polimer	Qrafit	Terman Trasit	Mis tozu	Disul-fid mo-libden	Xüsusi həjmi elektrik müqavi mət	İşçi tempe-raturu, ^{0}S	Təz-yiq Mpa	Sürtünmə əmsalı		Mən bə
									Yağlı	yağsız	
ATM-2	50	5	45	-	-	10^6	110	40-50	0,02	0,12	7
EPK-7	70	20	-	-	10	10^3	50-60	15-20	0,015	0,16	3
Epoksid + Qrafit	40	60	-	-	-	10^{-3}	200-250	60-70	0,07	0,17	1
F F+Ju	30	30	-	40	-	10^{-3}	200-250	60-70	-	0,07-0,01	9

Elastikliyyət modulu böyük olan fenolfomaldehid və epoksid qatranların əsasında yaradılan elektrikkeçiricili polimer kompozisiyaları kipcək materialları kimi yüksək təzyiq və temperatur şəraitində işləyən avadanlıqların, hidroqurğuların və s, vakuum şəraitində işləyən qurğularda kipliyin uzun müddət təmin edici olmasına imkan verir. Termoplastik kütlə kapron əsasında yaradılmış ATM-2 qaz-kompressor qurğusunda kipcək materialı kimi çox yaxşı nəticələr vermişdir.[6].

Cədvəldə göstərilən elektrik keçiricili polimer kompozisiyalar müxtəlif üsullarla alınmışdır. ATM-2 kompoisiya materialı fasiləsiz işləyən iki rotorlu qarışdırıcıda alınır. Əvvəl kapron əriyir sonra doldurucu ilə qarışaraq qarışdırıcı başlığından çubuq şəklində çıxır və soyuduqdan sonra bıçaqlı qranulyatorda xırdalanır.

EPK-7 materialı isə polimerzasiya və ya da ATM-2 materialı kimi hazırlana bilər [8]. Digər epoksid və fenolformaldehid qatranları əsasında mexaniki qarışdırma ilə hazırlanır.

Yüksək dolduruculu kompozisiya materiallarında doludurucu müxtəlif dispersiyalı hissəciklərdən istifadə edilməsi materialın yüksək sıxlığını təmin edir, yəni iri hissəciklər arasında yaranan boşluqlar xırda hissəciklərlə dolur və alınan məmulun monolitliyini təmin edir.

Epoksid əsaslı kompozisiya materiallarında 100 küt.%-kaolinin olması qrafitin kritik konsentrasiyasını 40-50 küt.%-ə endirir, nətijcdə materialın nümunələrində alınan göstəricilərin fərqini azaldır [4]..

Cədvəl 1-də verilənlərə görə həmin elektrik keçiricili polimer kompozisiyaların müxtəlif doldurulma qiymətlərində həcmi xüsusi elektrik müqavimətinin qiymətlərini reqresiya düsturuna görə müəyyən etmək olar. Məsələn, ATM-2 materialı üçün aşağıdakı kimi göstərilir.

$$\rho_v = a \cdot 10^{13} e - bf \qquad (1)$$

burada *a* və *b* sabit kəmiyyəilərdir, *f* - doldurucunun miqdarı küt %, 10^{13} kapronun həcmi xüsusi elektrik müqavimətidir

ATM-2 üçün $\rho_v = 0.318 \cdot 10^{13} e^{-0.5534}$

Beləliklə, elektrik keçiricili kompozisiya materiallar üçün γ-nin müxtəlif qiymətlərində ρ_v-nin qymətini təyin etməklə materialın antistatik xassəsini müəyyən etmiş oluruq.

Doldurucunun tipini və miqdarının ümumi mahiyyətini göstərmək üçün [7] elmi məqalədən verilmiş riyazi modeldən istifadə etmək olar.

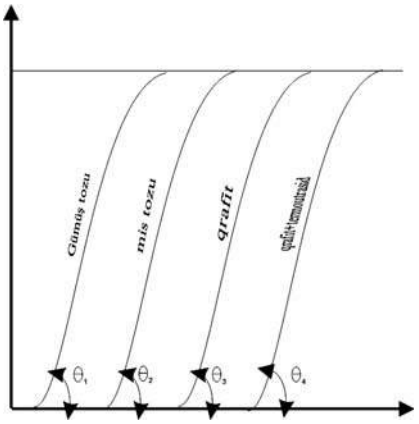

Şəkil 1. Elektrik keçiricili polimer kompozisiaylarının dold urucudan asılı olaraq seçilmə ardıcıllığı.

Şəkildən görünür ki, doldurucudan asılı olaraq elektrik keçiricili polimer əsaslı kompozisiyalarda xüsusi həcmi elektrik müqavimətinin istismar şəraitini nəzərə almaqla 10^6 Om·m şərtini ödəməsi üçün nə kimi dolduruculardan istifadə olunması üçün tövsiyyə xarakterli riyazi modeldən istifadə etməklə onların elektrik keçiriciliyinin və ya möhkəmlilik göstəricilərinin proqnozlaşdırılmasını tərtib etmək olar.

Bu cür yeni elektrik keçiricili polimer kompozisiyaların yaradılması müxtəlif sahələrdə onların geniş tətbiqini təmin etməklə yanaşı, ekoloji problemlərin həllini də təmin etmək olar. Məsələn, partlayıcı maddələrin, yanacaq məhsullarının saxlanması və nəql olunması üçün tutumların, konistrlərin, qabların hazırlanmasında, yarım keçirici kimi və sairə istifadə olunmasıdır.

θ-nün qiyməti aşağıdakı düsturdan hər bir kompozisiya üçün tapıla bilər.[7].

$$\text{tg} = \frac{\varphi_H}{x_2 - x_1}$$

Ümumiyyətlə elektrik keçiricili polimer kompozisiyalarının elektrik keçiricilərini ölçülməsin istilik keçirmə kimi aparılır. Ümumi qanunauyğunluqlardan müəyyən meylliklərinin olması yerli elektrik deşmə halı ilə izah edilir ki, bunun da səbəbləri çox müxtəlifdir.

Beləliklə, baxılan elektrik keçiricili polimer kompozisiylar yüksək və alçaq elastiklik moduluna malik olduqlarından onların kipcəklərin və bərk, qaz və maye halında olan yanacaq maddələrin nəqli üçün tullantıların hazırlanmasında istifadə oluna bilərlər. Bu materiallar yaranan elektrik yüklərinin ani boşalmasını təmin etməyə qadirdirlər.

[1] *A.M.Rəhimov, İ.İ.Həsənov, P.M.Əhmədov*. Neft avadanlıqlarında yeni kipcək materialları. ADNA ETİ, Elmi əsərlər IV jild, Bakı-2003, s 245-249.

[2] *B.E.Qul, L.Z.Şenfil*. Elektroprovodyaşşnu polimernıye kompozisii. Moskva. İzd. «Ximiya» 1984, 240 s. (rusca)

[3] *A.M. Raqimov*. Eksperimentalno - teoretiçeskiye osnovı razrabotki metodov pererabotki i rejimov izqotovleniya detaley iz elektroprovodnıx kompozisionnıx plastiçeskix mass. Avtoreferat, dokt. Dis. Baku, 1996. (rusca).

[4] *A.M. Berlyand*, Namizədlik.diss. Taşkent, Taşkentskiy politexniçeskiy institut,1972.(rusca).

[5] *A.M.Rəhimov*. Elektrik keçiricili polimer kompozisiyalarının elektrik xassələrinin tədqiqi. Elmi əsərlər ADNA.Bakı, 1997, №3 s 68-71.

[6] *N.M. Bıstrov i dr*. «İssledovaniye iznosostoykosti ATM-2 primenitelno k salnikam porşnevıx kompressorov», «Ximiçeskoye i neftyanoye maşinostroenie», №9, 1971,s 67.(rusca)

[7] *A.A.Babaeva, A.M.Raqimov*. Matematiçeskiye modeli dlya proqnozirovaniya elektriçeskix i proqnostnıy svoystv polimernıx materialov. Uçenıye zapiski. AQNA Baku 1995, №4, s 75-79. (rusca)

[8] Gnüiklopediya polimerov 1 tom M, 1972, s 278. (rusca).

[9] *T.İ. Şahtaxtinski, P.M. Əhmədov*, Mis Alüminium sürtünmə jütünün elektrikkeçirməsi haqqında ADNA, NQGP və ETİ, Elmi əsərlər, Bakı 2001, s.181-184

A.M.Rahimov, P.M.Ahmadov, I.I.Hasanov, Ch.A.Aliyev, G.Sh.Mehtiyev

THE USE OF DIRECT APPOINTING POLIMER COMPOSITIONS WITH ELECTRIC CONDUCTION DEPENDING ON THE TYPE AND QUANTITY OF FILLER

The polymer compositions with electric conduction pointing in the article have high and low module of electricity and they can be used stuffing-box for conduction of hard gas and liquid, fuel substances and preparing of reservoirs. These materials can provide momentary relaxation of electric loadings.

Received: 08.01.04

$$\Omega_{\mu\nu} = \sum_k \omega_k g_\mu^k g_\nu^k \qquad (21)$$

$$g_\mu = \psi_\mu + \varphi_\mu \ , \ w_\mu = \psi_\mu - \varphi_\mu \ .$$

Here, the sums with respect to *i* and *k* contain all positive and negative forces of the Eq. (7). Since ω_i are the zeros of the function $D(\omega_i)$, the basic theorem of the theory of residues [8] now allow us to write the expression for d_μ in the form of the contour integral:

$$d_\mu = 2\chi\sigma_\mu L_\mu \sum_i \oint_{L_i} \frac{zF(z)}{\left(\varepsilon_\mu^2 - z^2\right)D(z)} dz \qquad (22)$$

The contour L_i in the complex plane are shown in Fig. 1 and contain first-order singularities of the integrands at $z = \pm\omega_i$ which are the zeros of the corresponding function $D(z)$.

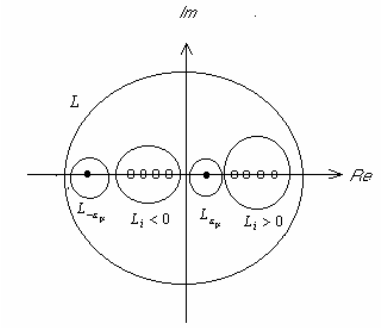

Fig. 1. The contour of integration in the complex plane for (20)

However, it is well-known from analysis that, outside L_i, the integrand in Eq. (22) have simple poles at $z = \pm\varepsilon_\mu$ and the corresponding residues can be evaluated easily. Since the sum of all residues of the an analytic function is equal to zero, we have

$$\oint_L = \sum_i \frac{\omega_i F\left(\omega_i^2\right)}{\left(\varepsilon_\mu^2 - \omega_i^2\right)D'(\omega_i)} + \mathrm{Re}\, z\left(f, -\varepsilon_\mu\right) + \mathrm{Re}\, z\left(f, +\varepsilon_\mu\right) = 0 \qquad (23)$$

Using Cauchy theorem, we find

$$d_\mu = -\oint_{L_\mu} \frac{zF(z)}{\left(\varepsilon_\mu^2 - z^2\right)D(z)} dz = 2\sigma_\mu L_\mu \ . \qquad (24)$$

After laborious calculations, we show that $\Omega_{\mu\neq\nu} = 0$, hence the Eq. (21) becomes

$$\Omega_{\mu\nu} = 2\widetilde{\varepsilon}_\mu \delta_{\mu\nu} \ . \qquad (25)$$

Finally, by exploiting (19), (22) and (23) formulas, we derived very simple formula for the generalized expression of the sum rule (17):

$$S(\delta_i, \delta_k) = \frac{3}{2\pi} \sum_{\mu,\tau} \widetilde{\varepsilon}_\mu^\tau [(g_s^\tau - g_l^\tau) s_\mu^\tau - g_e^\tau j_\mu^\tau]^2 \qquad (26)$$

where s_μ^τ and $\widetilde{\varepsilon}_\mu$ are the single particle matrix elements of the spin operator in the ground state base and two-quasi particle energies corresponding to the form of excited states which are calculated in different base. According to this, when $\delta_i = \delta_k$, the formula (24) is transformed into the known sum rule expression [6] for magnetic dipole transitions. For the spin transitions, the sum rule becomes

$$S_\sigma(\delta_i, \delta_k) = 2\sum_{\mu,\tau} \widetilde{\varepsilon}_\mu^\tau \sigma_\mu^{\tau\,2} L_\mu^{\tau\,2} \ . \qquad (27)$$

Numerical calculations are performed in a wide interval of the deformation parameter for the nucleus ^{140}Ce in the deformed Woods-Saxon potential [10]. The calculations are performed by using the sum rule (26) for the spin taransitions. When calculating the spin transitions using the sum rule (26), the quadrupole deformation parameter δ_0 =0.09 given in [11] from an experimental data of the ground state is taken and the deformation parameter of excited levels is changed in the 0.05 and 0.3 interval. As shown in Fig. 2., while the difference between the forms of the transition levels increases, the transition probability or the numerical values of the sum rule S declines sharply.

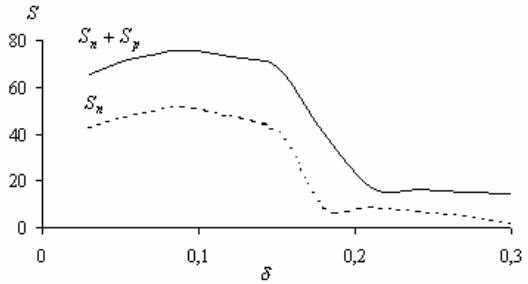

Fig. 2. The change in the sum rule (25) with respect to δ for the spin transitions (in MeV)

Consequently, the known energy weighted sum rule for the magnetic dipole transitions is generalized for transitions to levels, which have different forms from the ground state. Later, by using the theory of residue and contour integrals, analytical expressions is obtained for these sum rules. In numerical calculations, in the case of the spin transition operator, while the form of the nucleus changes, the numerical values of the energy-weighted sum rule decline sharply.

[1] *V.G.Solovyov*. Theory of Complex Nuclei. Pergamon Press, New York,1976.
[2] *D.J.Rowe.* Nuclear Collective Motion, Methuen, London,1970.
[3] *A.Richter*. Prog..Part.Nucl.Phys,34, 1995, 261.
[4] *A. Petrovichi, K.W.Scimid and Amand Faessler*. Nucl.Phys.A605, 1996, 290.
[5] *E.Ye.Berlovich, Yu.N.Novikov*. Phys.Letts. 19, 1965, 668.

[6] *S.I.Gabrakov, A.A.Kuliev, N.I.Pyatov, D.I.Salamov and H.Schulz*, Nucl.Phys.A.182, 1972, 625
[7] *A.A.Kuliev, D.I.Salamov and S.K.Balayev*. Bulletin of Academy of Sciences of the USSR,Ser.Phys. 53, 1989, 2140
[8] *H.Erbil, M.Gerçeklioğlu, M.Ilhan and A.A.Kuliev*. Mathematical and Computational Applications, 1997, 2, 1.
[9] *A.G. Sveshnicov et al.* The Theory of Functions of a Complex Variable [in Russian], Nauka, Moskow, 1967.
[10] *M. Cerkasski et al*. Phys.Letters B70, 1977, 9.
[11] *E.Guliyev, A.A.Kuliev, P.von Neumann-Cosel, Ö.Yavas*. Nuclear Physics A690, 2001, 255c

Received:

SÜRÜŞƏN KONTAKTLI CƏRƏYANQƏBULEDİCİLƏRDƏ HƏRƏKƏT ZAMANI YARANAN TEMPERATURUN HESABLANMASI

P.M. ƏHMƏDOV
«Neftin, qazın geotexnoloji problemləri və kimya ETİ»

Məqalədə sürüşən kontaktlı cərəyanqəbuledicilərdə hərəkət zamanı yaranan temperaturun hesablanması aparılmışdır.Məlum olmuşdur ki, cərəyanqəbuledicilərdə hərəkət zamanı yaranan temperatur doğrudan da hesablamadan alınan temperaturdan yüksək olmur. Bu da təklif etdiyimiz polimer+metal əsaslı elektrik keçiricili kompozisiya materiallarından fasiləsiz iş rejimində işlədilən cərəyanqəbuledicilərinin hazırlanmasına imkan yaradır.

Sənayenin müxtəlif sahələrində son zamanlar cərəyanqəbuledicilərdən geniş istifadə olunur. Cərəyanqəbuledicilər [1] əsasən sərnişin nəqliyyatında, təmir və quraşdırma sexlərində, yeraltı tunellərdə, dağ-mədən şaxtalarında və s. başqa yerlərdə tətbiq olunurlar. Bunlardan ən maraqlısı sərnişin nəqliyyatında işlədilən cərəyanqəbuledicilərdir. Bu cərəyanqəbuledicilər [2] açıq hava şəraitində işlədildiyindən onlar atmosferdəki bir sıra təsirlərə istiyə, yağışa,qara və şaxtaya məruz qalırlar. İstiliyin artması, yağış, qar, soyuq və şaxtalı hava şəraiti cərəyanqəbuledicilərin işinə öz mənfi təsirini göstərir.

Bunları nəzərə alaraq, cərəyanqəbulediciyə qoyulan tələblərdən biri də onun hərəkət zamanı yaranan temperatura [7] dözümlülüyüdür. Məlumdur ki, temperaturun artması ilə məmulatların tərkibində struktur dəyişməsi müşahidə olunur, bu da onların əvvəlki formalarının dəyişməsinə səbəb olur və bununla onların tətbiq olunduğu sahələr də fasiləli iş şəraiti yaranır.

Cərəyanqəbuledicidə yaranan temperatur əsasən elektrik cərəyanının və sürtünmənin hesabına yaranır. Elektrikin cərəyanqəbuledicidə yaratdığı temperatur (ətraf mühitin temperaturu da nəzərə alınmaqla) QOST 12058 – 72 üzrə ayrıd edilir. Yuxarıda deyildiyi kimi temperaturun artması cərəyanqəbuledicinin struktur dəyişməsi ilə onun yeyilməsinin artmasına və hətta dağılmasına səbəb olur. Buna görə də kontakt sahələrində yaranan temperaturun hesablanması cərəyanqəbulediciyə qoyulan əsas tələblərdən biridir.

Hərəkət zamanı cərəyanqəbuledicidə yaranan ümumi temperatur aşağıdaki kimi hesablanır [3].

$$V_{üm} = V_{el} + V_{sət} + V_{qığ} \qquad (1)$$

burada: V_{el} - elektrik enercisinin yaratdığı istiliyin həjmi temperaturudur; $V_{sət}$ – sürtünmə və kontakt müqavimətindən yaran temperatur; V_{qig} – temperatur alışması; V_{et} - elektrik jərəyanının yaratdığı temperatur axını aşağıdakı yolla tapılır.

$$V_{el} = \frac{4J^2\rho}{\pi^2 d^3 \sigma' \cdot 10^2} \qquad (2)$$

burada: J- jərəyanın gücü A ; d – naqilin diametri m; σ'- konveksiyanın istilik ölçmə əmsalı $vt/(m^2 \cdot °j)$.

$$V_{el} = 0,00887\left[\frac{J^{2\rho}}{\lambda d^3}\left(\frac{dT_0 \gamma_f}{g}\right)^{0,25}\right]^{0,8} \qquad (3)$$

burada ; λ_f - havanın istilikkeçirmə əmsalı $vt/(m^2 \cdot °j)$; γ- havanın kinematik özlülük əmsalı m^2/s; T_0 – havanın temperaturu $°C$; g- sərbəst düşmə təcili m/s^2.

Səthdə yaranan temperatur həm sürtünmədən və həm də elektrikdən yaranır. Ona görə də [3]

$$V_{sət} = \frac{0,942 q_0 \alpha_{tp1}}{\lambda_1}\sqrt{\frac{\alpha_1 l_1}{\pi v}} \qquad (4)$$

burada; q_0- kontakt səthində friksion sürtünmə və elektrik hesabına yaranan istilik axınıdır.

$$q_0 = \frac{1}{A_0}\left[fN\upsilon + I^2\left(\frac{\rho\sqrt{HB}}{\sqrt{\pi N}} + \frac{\sigma\, HB}{N}\right)\right] \qquad (5)$$

burada; σ - kontaktda təbəqənin yaratdığı nisbi müqavimət; α_{tp1}- istilik axınının paylanma əmsalı olub 0,75 - 0,90; aralığında dəyişdiyindən 0,85 qəbul edilir; λ_1; α_1 – naqilin istilikkeçirmə və temperaturkeçirmə əmsalıdır ; l_1- naqil ilə cərəyanqəbuledicinin əlaqə (kontakt) səthinin uzunluğudur.

Temperaturun yaratdığı alışma (qığılcım) [3,5] işində yazıldığı üsulla təyin edilir.

$$V_{qığ} = 1,707\,\frac{fN\upsilon d_{or}}{A_r\lambda\left[4 + \left(\pi\,\frac{\upsilon d_{or}}{\alpha}\right)^{1/2}\right]} \qquad (6)$$

burada; d_{or} – kontaktda yaranan ləkənin orta diametridir.

Bunları nəzərə alaraq naqil (mf-85) mis, cərəyanqəbuledici isə 40% mis; 30% fenolformaldehid; 30% isə qrafit ovuntusundan hazırlanmışdır. A_a=0,5·10^{-3}m^2; A_r=1,1·10^{-8}m^2; f=0,12; ρ=1,75·10^{-6}Om·sm; σ=10^{-3}om·sm^2; N=150H; HB 118…123; $İ$=500A; v=50m/s; l_1=0,12m; l_2=0,00417m; $\lambda_1=\lambda_2$=398vt/(m.°C); a=0,111·10^{-3}m^2/s; d_{or}=10^{-6}m; məlum qiymətləri (2), (3), (4), (5), və (6)- da nəzərə alsaq onda (1)-dən V=417,5 °C alınır.

Aparılmış hesablamalar göstərir ki, doğrudan da maksimum yarana biləcək temperatur QOST 12058-82

üzrə göstərilmiş həcmi temperaturdan yüksəkdir. Ona görə də hesablama və ya sınaq aparılan zaman mütləq bu temperatur nəzərə alınmalıdır [3, 4]. Cərəyanqəbuledicidə temperaturun elektrik cərəyanı ilə sürtün-mədən yarandığını nəzərə alsaq onda görərik cərəyanqəbuledicinin mis naqilə sıxılması ikili xarakter daşıyır. Birincisi mis naqilə yaxşı sıxılmış cərəyanqəbuledici elektrik itkisinə yol verməməklə kontakt müqavimətini [9, 10] azaldır bu da onun fasiləsiz iş rejimi yaratmağına müsbət təsir göstərir. İkinci tərəfdən sıxılma cərəyanqəbuledicinin mexaniki yeyilməsinin artmasına [6] səbəb olur. Müxtəlif materiallardan hazırlanmış cərəyanqəbuledicilərin keçirici müqavimətlərinin sıxılmadan asılılıq qrafiki şəkil-1 də göstərilmişdir.

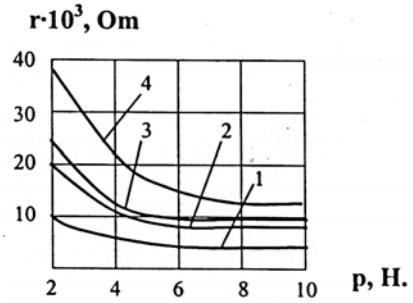

Şəkil 1. Jərəyanqəbulediji üçün sıxılmadan müqavimətin asıllığı.
1. Mis.
2. 40% - mis; 30% - f.f.; 30% qrafit.
3. Metalkirəmit.
4. Kömür.

Elektrik cərəyanının itməməsinin və yeyilmənin minimum həddə endirilməsi üçün sıxılmanın (55-150) H arasında götürülməsi [8] məsləhət görülür.

Temperaturun artmasına təsir göstərən amillərdən biridə trolleybusun sürətidir. Sürət artdıqca [5] məlumdur ki, sürtünən cisimlərin hər birinin temperaturu artır. Misin yaxşı istilikkeçirmə qabiliyyətini nəzərə alaraq aparılan sınaq zamanı müşahidə edilmişdir ki, cərəyanqəbuledicinin səthində yaranan temperaturun artmaması onun fasiləsiz iş rejimi yaratmağına müsbət təsir göstərir.

Cərəyanqəğuledicidə yaranan temperaturun artmamasına səbəb onun tərkibində 40%-ə qədər misin olması ilə bərabər onun açıq hava şəraitində işləməsidir. Bununla bərabər məlumdur ki, dayanacaqlarda nəqliyyatın saxlandığı müddət də temperaturun düşməsi müşahidə olunur.

Aparılan bir çox araşdırmalar və sınaqlar zamanı məlum olmuşdur ki, bu materiallar içərisində özünü ən etibarlı element kimi tərkibi 40-% mis; 30%-fenolformaldehid və 30%- qrafit tozu olan cərəyanqəbuledici göstərmişdir. Sınaq zamanı cərəyanqəbuledicinin maksimum temperatura dözümlülüyü öyrənilmişdir.Bu cərəyanqəbuledici başqa məmulatlarla birlikdə yüksək gərginlik və temperatur şəraitində işləyən elektrik avadanlıqlarında da tətbiq oluna bilər.

Beləliklə təklif etdiyimiz polimer+metal əsaslı elektrik keçiricili kompozisiya materiallarının istismar şəraitini tam mənası ilə nəzərə alan hesablamaların nəticələri təcrübə nəticələri ilə sübuta yetirilmişdir.

[1] *A.N. Trafimov*. Kontaktnıe vstavki tokosğemnikov trolleybusov, M., 141 s.
[2] *P.M. Əhmədov*. Elektrik keçirijili plastik kütlələrin tətbiqinin bir sahəsi haqqında, Azərbayjan Dövlət Neft Akademiyasının 80 illiyinə həsr olunmuş «Quyuda işləyən neft avadanlıqlarının etibarlılığı və effektivliyi» mövzusunda elmi-texniki konfransın materialları, BAKU-2000, səh. 35-37.
[3] *V.V. Alisin, B.M. Astaşkeviç, G.D. Braun i dr.* «Trenie, iznaşivanie i smazka» Spravoçnik. V 2-x kniqax. Kn. 2. «Maşinostraenie» M., 1978, 439 s.
[4] *İ.A. Beləev*. Tokopriemniki glektropodvicnoqo sostava. M., Transport, 1970, 160 s.
[5] *A.Q. Qinzburq, A.M. Maxanğko, A.V. Çiçinadze*. Rasçet sredney temperaturı skolğzəöheqo kontakta parı kontaktnoy provod-tokosğemnıe plastinı pantoqrafa. V sb., Trenie i iznos friküionnıx materialov. M., Nauka, 1977, -S. 20-26.
[6] *A.V. Çiçinadze, A.M. Maxanğko*. Metodika provedeniə ispıtaniy materialov na trenie i iznos s proxocdeniem glektriçeskoqo toka çerez skolğzəhiy kontakt. M., Nauka, 1974, -S.79-85.
[7] *A.V. Çiçinadze, A.M. Maxanğko, A.S. Paştala*. Metodika opredeleniə glektrofriküionnoy teplostoykosti materialov. V sb.; Teplovaə dinamika i modelirovanie vneşnoqo treniə. M., Nauka, 1975, -S. 97-101.
[8] *E.M. Pokusaev, V.Q. Baranovskiy, İ.S. Malevanıy*. İnstruküiə po ustroystvu i gkspluataüiy trolleybusa. Vilğnös, 1965, 191 s.
[9] *T.İ. Şahtaxtinski, P.M. Əhmədov*. Mis-alüminium sürtünmə jütünün elektrik keçirməsi haqqında. Azərbayjan Dövlət Neft Akademiyası. «Neftin, qazın geotexnoloci problemləri və kimya» Elmi-Tedqiqat İnstitutu. ELMİ ƏSƏRLƏR. 2-ji jild. Bakı-2001. səh. 181-184.
[10] D.N. Qarkunov. Tribotexnika. M. Maşinostroenie, 1989, 328 s.

П.М. Ахмедов

РАСЧЕТ ТЕМПЕРАТУРЫ, ВОЗНИКАЮЩЕЙ ВО ВРЕМЯ ДВИЖЕНИЯ В ТОКОСЬЕМНИКАХ СО СКОЛЬЗЯЩИМИ КОНТАКТАМИ

В статье приводятся результаты расчета температуры, возникающей во время движения в токосъемниках со скользящими контактами. Выявлено, что полученная расчетным путем температура, возникающая в токосъемниках во время скольжения не превышает приведенные в опубликованной литературе действительные значения температуры. Полученные результаты позволяют соз-

давать токосъемники из предлагаемого электропроводящего композиционного материала: полимер + металл, в условиях эксплуатации в беспрерывном режиме.

P.M. Akhmedov

CALCULATION OF THE TEMPERATURE ARISINIG DURING MOVEMENT IN SLIP RINGS WITH SLIDING CONTACTS

In article results of calculation of the temperature arising during movement in slip rings with sliding contacts are exposed. It is revealed that, the temperature received by settlement way arising in slip rings during sliding does not exceed the valid values of temperature resulted in the published literature. The received results allow to create slip rings from offered electroconductive composite material: polymer+metal, under operating conditions in a conditions mode.

Received: 25.03.04

THE INFLUENCE OF THERMAL ANNEALING ON PHOTOSENSITIVITY OF $TlInSe_2$ SINGLE CRYSTALS

V.D. RUSTAMOV
Gyanja State University
Khatai ave., 187, AZ 2000, Gyanja, Azerbaijan

The paper is devoted to results of study of influence of thermal annealing on spectral photosensitivity of $TlInSe_2$ single crystals. The crystals $TlInSe_2$ have positive temperature coefficient of photosensitivity in an interval 77÷300 K and above. The thermal annealing consist in endurance of photosensitive elements at 475 K within 24 hours and subsequent cooling up to temperature of liquid nitrogen. As a result of thermal annealing the photosensitivity of various samples raised 1630÷3330 times at 77 K and 35÷100 times at 300 K.

The crystals $TlInSe_2$ are the typical representatives of ternary semiconductor compounds of $A^{III}B^{III}C^{VI}_2$ groups, being materials with good photosensitivity and distinguished by stability of the performance capabilities. In particular, the compound $TlInSe_2$ is the physical analogue of quasione-dimensional materials, the study which promotes finding - out of essence much important phenomena in physics of the condensed matters [1].

Semiconductor behaviour of electroconductivity of compound $TlInSe_2$ and their high photosensitivity for the first time are established in [2, 3].

The actuality of research of $TlInSe_2$ crystals and application of them as the photosensitive element of photodetectors are obvious, with the following reasons:

- high photosensitivity;
- simple and accessible way of reception of crystals;
- high adaptability to manufacture, thanking cleavability on planes of cleavage;
- the opportunity of isovalent replacement of components within the frame of the given structural type, opens the large prospects of selection of the mixed crystals allowing purposefully to vary the performance capabilities of detectors over a wide range.

The photosensitive elements are made as rectangular plates with two reciprocally parallel by mirror sides of natural chip. The sizes of samples are about (1÷3) x (2÷9) x (0,05÷1) mm^3. As measuring electrodes are used, mainly, welded in a flow of the heated up inert gas by the condenser category of nickel wire with a diameter ~ 0,1 mm, and also sprayed in vacuum, indium lags. The performance capabilities of active elements are determined at meanings of voltage, which not exceeding 10÷20 V in /001/ crystallographic direction. Current-voltage characteristics within the limits of the specified working voltage, for all investigated samples at various temperatures in darkness and at illumination light of appropriate length of the wave, have appeared linear.

The creation of photodetectors is preceded by detailed definitions of the performance capabilities of photosensitive elements on the basis of $TlInSe_2$ single crystals and also parametrical dependence of the performance capabilities.

Initial item of all researches became the definition of the performance capabilities of photosensitive elements on the basis of $TlInSe_2$ single crystals in stationary conditions.
Stationary conditions are considered as:

- ohmic contacts;
- the photon flux is constant and is distributed in regular intervals on a surface;
- the fixed meanings of temperature and other parametrical conditions;
- ligth intensity from a linear site lumineus - current characteristics (LCC);

In fig. 1. is presented the curve of spectral distribution of stationary photoconductivity given to equal number photons at 77 and 300 K for five samples of photosensitive elements with various parameters. Intensity of the electrical field $E \cong$ 20÷30 V/sm is enclosed in the direction parallel axis /001/, and monochromatic light are directed perpendicularly to the plane (110).

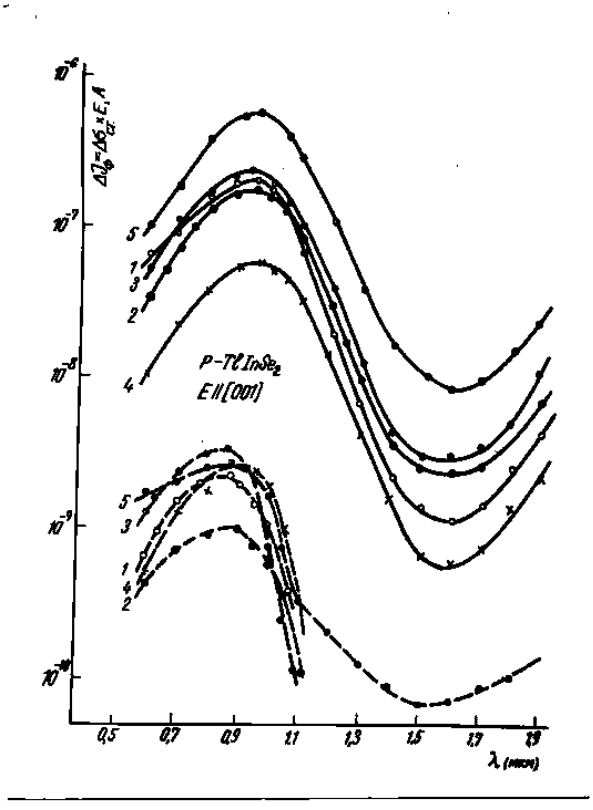

Fig.1. Spectral dependence of photodetectors at 77 K (dotted line) and 300 K (firm line).

As following from the fig. 1. spectral sensitivity with increase of temperature increases sharply. The ratio of values of stationary photoconductivity on spectral maxima at the appropriate temperatures makes 20 ÷ 750.

As a rule, the known semiconductor photodetectors have negative temperature coefficient of photocurrent (TCI_{ph}). For example, sulfide-cadmic photoresistors, have the least

negative value TCI_{ph} = $-10^{-3} \div 4.10^{-3}$ degree^{-1} [4]. Unlike known, TCI_{ph} for active elements on the basis of $TlInSe_2$ single crystals is positive in the temperature interval 77÷300 K and above. For example, for an active element of №1 temperature coefficient, average value, makes 0,46 degree^{-1}.

As it is already mentioned above, the increase of temperature is one of the factors increasing sensitivity of photodetectors on the basis of $TlInSe_2$ crystals. The carried out researches have revealed that the spectral sensitivity of photodetectors substantially can also be increased by preliminary thermal annealing of photosensitive elements. In fig. 2 the results of influence of thermal annealing on spectral photosensitivity of $TlInSe_2$ crystals are shown.

The thermal annealing thus consist in endurance of photosensitive elements at 475 K within 24 hours and subsequent cooling up to temperature of liquid nitrogen (77 K). As the spectral sensitivity of photodetectors follows from the diagrams, given in the fig. 2, at a maximum of photoconductivity (calculated from area LCC, where $\alpha = 1$), $k = J^{мак}_{ph}/I \cdot V$, in consequence of the mentioned above thermal annealing increased: for the sample № 7 3330 times at 77 K and 100 times at 300 K, and for the sample № 8, 1630 times at 77 K and 35 times at 300 K.

LCC at the noted temperatures both up to, and after heat treatment carried power-dependence $J_{ph} \sim I^{\alpha}$ with a parameter of degree $\alpha = 0{,}5 \div 1$. And with thermal annealing is observed the contiguity to the linear recombination case ($\alpha \rightarrow 1$).

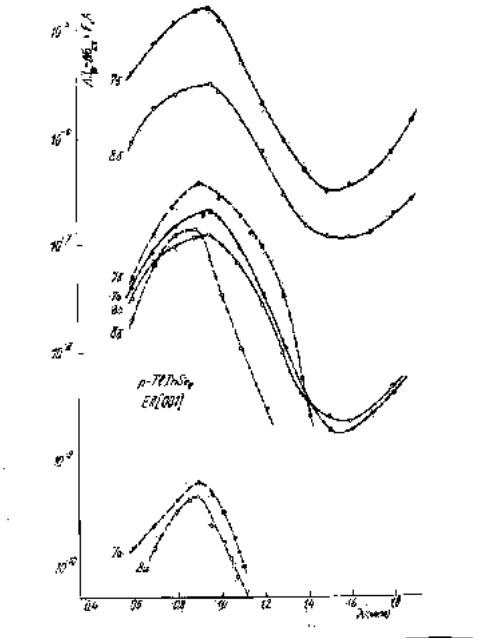

Fig. 2. Influence of preliminary thermal processing on spectral sensitivity of photodetectors with a photosensitive element on the basis p- $TlInSe_2$ at 77 K (dotted line) and 300K (firm line). (Samples № 7*a* and № 8*a*, as the same as in the fig.. 1 up to thermal processing, and samples № 7*b* and № 8*b* after thermal processing).

[1] *V.A. Aliyev, M.A. Aldzhanov, S.N. Aliyev*. JETP Lett., 1987, v.45, N 9, pp.534-536.

[2] *G.D. Guseinov, A.M. Ramazanzade, E.M. Kerimova, M.Z. Ismailov*. Physica Status Solidi, 1967, v.22, N 2, pp.k117-k122.

[3] *G.D. Guseinov, E.M. Mooser, E.M. Kerimova, R.S. Gamidov, I.V. Alekseev, M.Z. Ismailov*. Physica Status Solidi, 1969, v.34, N 1, pp.33-44.

[4] *S.M. Sze*. Physics of Semiconductor Devices. v.2, Toronto-Singapore, 1981, p.344.

V.D. Rüstəmov

TERMİK EMALIN $TlInSe_2$ MONOKRİSTALLARININ FOTOHƏSSASLIĞINA TƏSİRİ

Məqalə $TlInSe_2$ monokristallarının spektral fotohəssaslığına termik emalın təsirinə həsr olunmuşdur. Bu kristallarda 77÷300K intervalında və bundan yuxarı temperaturlarda fotohəssaslığın temperatur əmsalı müsbət işarəlidir. Termik emalın mahiyyəti ondan ibarətdir ki, fotohəssas elementlər 475K temperaturda 24 saat saxlandıqdan sonra tədricən maye azot temperaturuna qədər soyudulur. Termik emal nəticəsində müxtəlif nümunələrin fotohəssaslığı 77K temperaturunda 1630÷3330 dəfə, 300K temperaturunda isə 35÷100 dəfə artır.

В.Д. Рустамов

ВЛИЯНИЕ ТЕРМИЧЕСКОЙ ОБРАБОТКИ НА ФОТОЧУВСТВИТЕЛЬНОСТЬ МОНОКРИСТАЛЛОВ $TlInSe_2$

Статья посвящена результатам изучения влияния термической обработки на спектральную фоточувствительность монокристаллов $TlInSe_2$. Кристаллы $TlInSe_2$ обладают положительным температурным коэффициентом фоточувствительности в интервале 77÷300 К и выше. Термическая обработка заключалась в выдержке фоточувствительных элементов при 475 К в течение 24 часов и последующем охлаждении до температуры жидкого азота. В результате термической обработки фоточувствительность различных образцов повышалась в 1630÷3330 раз при 77 К и в 35÷100 раз при 300 К.

Received: 22.06.04

HIGH SENSITIVE ULTRA-VIOLET PHOTO DETECTOR AND INTERMEDIATE TYPE EXCITONS IN SEMITRANSPARENT METAL-A^3B^6 SEMICONDUCTOR BARRIER STRUCTURES

O.Z. ALEKPEROV, A.I. NADJAFOV
Institute of Physics, Azerbaijan National Academy of Sciences,
Javid av. 33, Az-1143, Baku, Azerbaijan

Photoelectric spectrums of Shottky barriers on InSe, GaSe and GaS layered crystals are investigated from band edge of corresponding crystals up to ultra-violet (6.5eV) quantum energies. Spectral dependence of photo-resistors and barrier structures are essentially different, especially in the region of intermediate type excitons. It is shown that InSe-Au Shottky barrier structure is high sensitive photo detector ($10^6 - 10^7 V/Wt$) in ultra-violet region.

1.INTRODUCTION

Semiconductor materials are used widely in problems of detection of electromagnetic radiation with different quantum energies- from far infrared (FIR) up to γ-radiation regions.

The most of semiconductor photo detector devices operate on the base of the conductivity change $\delta\sigma$ of the material under the radiation. For different regions of quantum energies $\hbar\omega$ the mechanisms of interaction of radiation with carriers in semiconductor, and as a consequence the change of conductivity, is due to different mechanisms.

For FIR these mechanisms are the shallow impurity photo ionization, free carriers heating and, for small and zero gap semiconductors, increase of free carrier concentration due to interband absorption.

For near IR and visible regions the interband absorption is the main mechanism ($Hg_xCd_{1-x}Te$- and PbSnSe type semiconductors in IR and InSb, InSe, GaAs, GaSe ZnSe CdSe CdS and so on in visible regions).

With increasing of the quantum energy from the visible to ultra violet (UV) region the interband absorption still remains the main mechanism of photo conductivity (PC). But with increasing of the energy gap- E_g of semiconductor the efficiency of PC is decreased because the increase of carriers effective mass takes place. As a result the mobility $\mu_i = e\,\tau_p / m_i^*$ (τ_p- carriers elastic scattering time) and lifetime τ_i of photo-excited carriers decrease take place ($\delta\sigma \approx \sum_i e_i \mu_i \delta n_i, \delta n_i = G\tau_i$ where G – the rate of carriers generation).

There is another more valuable reason for decreasing of PC efficiency with increasing of quantum energy. This is the decrease of the radiation penetration length $J(x) = J_0 \exp(-\alpha x)$, ($x_p \approx \alpha^{-1}$) inside of semiconductor as a result of absorption coefficient (α) increase with quantum energy. For example at UV energies $\varepsilon > 4E_g$ for the most of above indicated semiconductors $\alpha \geq 10^7 cm^{-1}$ and penetration α^{-1} is about of a few tens $\overset{o}{A}$. This means that all radiation would be absorbed at the surface of semiconductor. But from scattering of carriers point of view the situation is different inside and on the surface of semiconductor. The existing of 3 types of surface states causes the decrease of PC at small penetration length. For this reason in classic semiconductors the PC efficiency falls to zero at UV region.

As against this the absence of surface states is characteristic for layered semiconductors (LS), because all bindings between atoms are directed inside of layered packets, and forces between layers are very weak- Van-der-Wals ones.

2.PHOTO ELECTRIC SPECTRUMS OF A^3B^6 LAYERED CRYSTALS AND THEIR SHOTTKY BARRIERS

We have investigated PC of some LS (InSe, GaSe and GaS) from band edge up to UV (6.5 eV). The results showed that at some quantum energies (2.4eV; 2.9 eV in InSe and 3.5; 3.9eV inGaSe) PC is decreased. The more detailed investigations have proved the existence of deep interband excitonic states in the region where PC decreases [1]. This excitons are characterized with small Bohr radius ($r_B \sim 10\mathring{A}$) and higher binding energies ($\varepsilon_b \sim 100meV$) than the band edge Wannier-Mott excitons (about $10 - 14meV$ in these semiconductors). They are so called intermediate type excitons (ITE) which were widely investigated in alkaline-haloid crystals [2]. So the decrease of PC in the indicated region is due to the excitation of carriers from the higher effective masses bands, which are immediately captured to each other forming ITE. Being the highly binding carriers pair they can not broken up to free carries and do not give the contribution to the PC in indicated PC decreasing region. At higher energies (4-6.5eV) the PC efficiency of these layered semiconductors increases again, reaching the values much more than band edge PC. So these semiconductors are high sensitive photo detectors in UV region. But the full of PC in near UV as a result of binding of photo-excited carriers in ITE restricts the application of these photo detectors. To avoid this we have prepared the semitransparent metal (Au with 200-300A thickness) and LS Shottky barrier structures. The PC spectra of

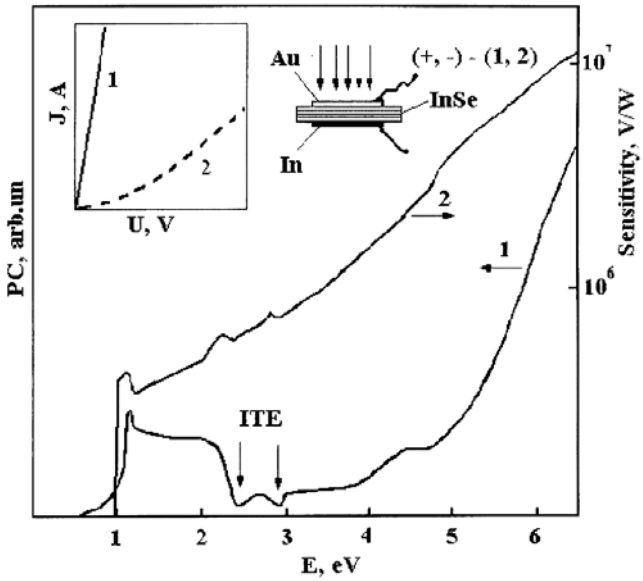

Fig.1. Photo conductivity and sensitivity spectral dependencies of Au-InSe-In barrier Shottky structure for two directions of applied electric field. The I-V – characteristics of the structure are shown in inset.

this device for two directions of applied electric field as well I-V characteristics are shown in figure1. As seen from curve 2 there is not PC decrease for barrier structure in the region where for semiconductor the PC full takes place. In opposite direction of the applied field the spectral characteristic of PC is similar to that of InSe photo resistor (curve1) [1]. The absence of the PC decreasing region is due to ionization of ITE in the electric field of the barrier, which according to our estimation is about $10^5 - 10^6 V/cm$. Decreasing of PC in opposite direction of applied electric field proves this fact (curve1). Note that the higher PC value in the UV than that in near band gap region can not be explained by perfect surface of LS only. So, in this case the UV PC would has the value as band gap one, at the best. Our comparative photo-Hall effect and photo excited carriers life-time experiments at near band gap and UV regions testifies that in the UV region photo signal is mainly due to the excitation of the holes with smaller effective masses from the deeper hole bands than band gap carriers. The same results as indicated in fig1 were obtained for GaSe and GaS Shottky barriers with ITE energy positions at 3.5-3.9eV and 4.1-4.5eV correspondingly. So we established that the main reasons of high effectiveness photo detectors of LS InSe and GaSe in UV region of radiation are: higher mobility ($\mu = e\,\tau_p / m^*$) of photo excited carriers, perfect condition of surface of LS and higher life time of photo-excited carriers τ_i. These devises are high sensitive ($10^6 - 10^7 V/Wt$ with noises smaller than 0.1 mkV) photo detectors.

[1] O.Z. Alekperov, M.O. Godjaev, M.Z.Zarbaliev and R.A. Suleimanov, Solid State Communications, 77, 65 (1991).
[2] *F.Bassani and G. Pastory* Parvachini, Electronic states and optical transitions in solids, Sidney, Pergamon Press, 1975, 391p.